



Universidade do Minho
Escola de Engenharia

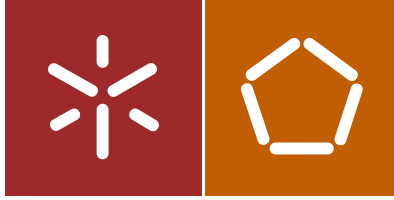
Zahra Abdollahnejad

Development of Foam One-Part Geopolymers

Zahra Abdollahnejad | Development of Foam One-Part Geopolymers

UMinho | 2016

July 2016



Universidade do Minho
Escola de Engenharia

Zahra Abdollahnejad

Development of Foam One-Part Geopolymers

Doctoral Thesis
Civil Engineering, Material

Work performed under the supervision of
Associate Professor Dr. José Luís Barroso de Aguiar

Co-Supervisor
Dr. Fernando Pacheco Torgal

July 2016

STATEMENT OF INTEGRITY

I hereby declare having conducted my thesis with integrity. I confirm that I have not used plagiarism or any form of falsification of results in the process of the thesis elaboration.

I further declare that I have fully acknowledged the Code of Ethical Conduct of the University of Minho.

University of Minho, _____

Full name: Zahara Abdollahnejad _____

Signature: _____

Acknowledgments

This thesis would not have been possible without the support of many people. Foremost, I would like to express my sincere gratitude to my supervisors Prof. Jose Barroso Aguiar for the continuous support of my PhD study and Investigator Pacheco-Torgal for his patience, motivation, enthusiasm, and immense knowledge. Their guidance helped me alot throughout writing this thesis. I could not have imagined having a better advisors and mentors for my PhD study.

The author wishes to express her love and gratitude to her beloved father and mother; for their understanding and endless love, through the duration of her studies.

Last but not the least; I would like to thank my supportive friend Mohammad Mastali throughout my PhD programme.

Resumo

A produção de cimento Portland normal (CPN) o mais importante constituinte do betão requer uma elevada produção de energia com a consequente libertação para a atmosfera de dióxido de carbono e outros gases responsáveis por efeito de estufa (GEE). As preocupações ambientais relacionadas com as elevadas emissões de CO₂ geradas durante a produção do CPN motivaram investigações para o desenvolvimento de novos materiais ligantes eco-eficientes. Os geopolímeros são ligantes alternativos ao CPN obtidos a partir de aluminossilicatos e activadores alcalinos. A geopolimerização é um processo químico complexo que envolve a dissolução dos aluminossilicatos, o seu transporte, orientação e policondensação de produtos de reação. Contudo são reconhecidas algumas limitações aos geopolímeros correntes, bicomponentes (contendo soluções alcalinas e silicatos solúveis). A utilização de soluções alcalinas agressivas dificulta a aplicação dos geopolímeros. A utilização de silicato de sódio é responsável por uma elevada pegada carbónica dos geopolímeros. A durabilidade destes materiais é ainda tema controverso. Por exemplo os geopolímeros correntes (bicomponentes) estão associados à formação substancial de eflorescências pelo facto das soluções alcalinas e silicatos solúveis não reagirem totalmente durante o processo de geopolimerização. Este fenómeno é responsável por um aumento da permeabilidade dos geopolímeros e por uma redução da sua durabilidade. Consequentemente é necessário estudar novas e melhores misturas geopoliméricas. A descoberta dos geopolímeros monofásicos é considerada um importante acontecimento em termos de geopolímeros de baixas emissões de carbono aos quais basta juntar água, exactamente como sucede com o CPN. Contudo até ao presente momento estes novos ligantes tem estado associados a baixos valores de resistência à compressão. Alguns autores até referem uma perda de resistência ao longo do tempo em geopolímeros monofásicos à base de lamas vermelhas calcinadas e hidróxido de sódio. A presente tese pretende desenvolver novas misturas de geopolímeros monofásicos com um desempenho suficiente para poderem ser utilizadas pela indústria da construção. Na mesma foram estudadas as propriedades mecânicas e a durabilidade das novas misturas. Analisou-se a aplicabilidade de um modelo numérico para a previsão da resistência à compressão das novas misturas. Efetuou-se a caracterização dos produtos de reação através da análise da microestrutura e da espectroscopia de infravermelhos. Estudou-se a possibilidade da utilização dos geopolímeros monofásicos na produção de argamassas porosas leves com condutibilidade térmica melhorada. O seu desempenho foi comparado com o desempenho de argamassas porosas leves obtidas de geopolímeros correntes (bicomponentes) em termos de propriedades, custo e potencial de aquecimento global.

Abstract

The production of ordinary Portland cement (OPC) as the essential constituent of concrete requires considerable energy, releasing a significant amount of carbon dioxide and other greenhouse gases (GHGs) into atmosphere. Environmental concerns regarding the high CO₂ emissions related to the production of OPC led to research efforts on the development of eco-efficient alternative binders. Geopolymers constitute promising inorganic binders alternative to OPC which are based on aluminosilicates by-products and alkali activators. The geopolymerization is a complex chemical process evolving dissolution of raw materials, transportation, orientation and polycondensation of the reaction products. However, there are still many drawbacks associated with traditional two part geopolymer mixes (containing alkaline species and soluble silicates). The caustic alkaline solutions make the handling and application of geopolymers difficult. The use of sodium silicate is responsible for a high carbon footprint of two part geopolymers. The durability of these binders is also subject of some controversy. For instance, current two part geopolymeric mixes can suffer from a high amount of efflorescence originated by the fact that alkaline or soluble silicates that are added during processing cannot be totally consumed during geopolymerisation. This phenomenon is responsible for an increase in geopolymer permeability and reduced durability. Therefore, the study of new and improved geopolymer mixes is needed. The discovery of one-part geopolymers is considered as a key event on the evolution of low carbon dioxide geopolymer technology in the “just add water” concept as it happens with OPC. However so far they were associated with very low compressive strength. Some authors even report a compressive strength decrease with time for one-part geopolymers based on calcined red mud and sodium hydroxide blends. The present thesis aimed to develop one part geopolymer mixtures with acceptable performance to be of some use for the construction industry. The mechanical properties and the durability performance of the new one-part geopolymer mixtures were studied. A numerical model to predict the compressive strength of one part-geopolymers was suggested. Hydration products results assessed with SEM/EDS and FTIR spectra were presented. The use of one part geopolymers for production of lightweight foam mortars with the improved thermal performance was studied. Comparisons to foam two part geopolymer mortars were made concerning properties, cost and global warming potential assessment.

Contents	Page
CHAPTER 1-Introduction	
1.1 Justification	1
1.2 Objectives	2
1.3 Publications	3
1.3.1. International Journal Papers	3
1.3.2. Conference Papers	4
1.3.3. Book Chapters	4
1.4 Thesis structure	5
CHAPTER 2-Literature review on two part geopolymers	
2.1 Two part geopolymers	7
2.1.1 Alkali-activated binder	7
2.2 Limitation of durability of geopolymer	13
2.2.1 Resistance to acid attack	14
2.2.2 Alkali-silica reaction (ASR)	16
2.2.3 Corrosion of steel reinforcement	18
2.2.4 Resistance to high temperatures	20
2.2.5 Efflorescences	21
2.3 One part geopolymers	25
2.4 Conclusions	26
CHAPTER 3-Experimental	
3. Experimental	29
3.1 Materials	29
3.1.1 Ordinary Portland Cement (OPC)	29
3.1.2 Superplasticizer (SP)	29
3.1.3 Fly ash	29
3.1.4 Sand	30
3.1.5 Kaolin	30
3.1.6 Alkali activators	31
3.1.6.1 Sodium hydroxide	32
3.1.6.2 Sodium silicate	32
3.1.7 Foam agents	32

3.1.7.1 Hydrogen peroxide	33
3.1.7.2 Sodium perborate	33
3.1.7.3 Aluminum powder	33
3.4 Executed tests	33
3.4.1 Water absorption by immersion	33
3.4.2 Capillarity water absorption	34
3.4.3 Compressive strength	34
3.4.4 Chloride diffusion	34
3.4.5 Carbonation resistance	35
3.4.6 Resistance to acid attack	35
3.4.7 Bulk density	36
3.4.8 Thermal conductivity	36
3.4.9 XRD	37
3.4.10 SEM/EDS	37
3.2.11 FTIR	38
CHAPTER 4- Mix design, properties and durability	
4.1 Mechanical properties	40
4.1.1 Mix design	40
4.1.2 Results and discussions	42
4.2. Compressive strength model	57
4.3 Microstructure	57
4.3.1 SEM	58
4.3.2 EDS analysis	58
4.4 FTIR	58
4.5 Mix proportioning	60
4.5.1 Compressive strength.	60
4.6 Durability	61
4.6.1 Efflorescences	61
4.6.2 Water absorption by immersion	61
4.6.3 Capillarity water absorption	62
4.6.4 Chloride diffusion	63
4.6.5 Carbonation resistance	64
4.6.6 Resistance to acid attack	65

4.7 Conclusions	66
-----------------	----

CHAPTER 5 – Performance of foam geopolymers: Two part versus one part

5.1 Introduction	69
5.2 Two part foam geopolymers	70
5.2.1 Properties	70
5.2.2 Cost analysis	84
5.3 One part foam geopolymers	88
5.3.1 Properties	88
5.3.2 Cost analysis	98
5.3.3 Global warming potential	100
5.4 Conclusions	100

CHAPTER 6-Conclusions and suggestions for further investigations

6.1 Conclusions and suggestions for further investigations	103
--	-----

Figures Index	Page
Fig. 2.1 Summary of CO ₂ -e for Grade 40 concrete mixtures with OPC and geopolymer binders	10
Fig. 2.2 Alkali-activated concrete after 10 months curing. (A) Reactive aggregate. (G) Alkali-silica gel	17
Fig 2.3 Ratios of the expansion relative to the limit proposed in the standard used for ASR test, for Portland cement and alkali-activated slag mixtures (Cyr and Pouhet,2014)	19
Fig. 2.4 Transverse sections of carbonated alkali-activated slag concretes after 1000 h of exposure to a 1% CO ₂ environment, with the extent of carbonation revealed by a phenolphthalein indicator. Samples are 76.2 mm in diameter	20
Fig. 2.5 Geopolymer structure model	22
Fig. 2.6 Alkali-activated mine waste mortars specimens after water immersion	23
Fig 2.7 High efflorescence after 50 days of partially-immersed Alkali activated fly ash	24
Fig 2.8 Efflorescence of the dense geopolymer TRSF0 and the foamed geopolymer TRSF2 specimens stored for times with the bottom in contact with water	25
Fig 2.9 Compressive strengths of red mud-based one-part geopolymers produced with different activator doses as a function of the time of curing (Ke et al., 2015)	26
Fig. 3.1 Kaolin particle diameter obtained with and without a defloculation agent	30
Fig. 3.2 DTA/TGA curves for kaolin	31
Fig. 3.3 Alambeta device	36
Fig. 3.4 Machine used to obtain XRD results	37
Fig. 3.5 Machine used to take SEM images	38
Fig. 3.6 Device employed to obtain FTIR spectra	38
Fig. 4.1 Compressive strength: Phase A	43
Fig. 4.2 Compressive strength: Phase B	44
Fig. 4.3 Compressive strength: Phase C	44
Fig. 4.4 Compressive strength: Phase D	45
Fig. 4.5 Experimental and predicted compressive strength of mixtures a) 30 OPC_58.3 FA_7.7 CH_4 CS, b) 26 OPC_58.3 FA_7.7 CH_8 CS and c) 18 OPC_58.3 FA_7.7 CH_16CS	54
Fig. 4.6 Plots for determining k and n in a) 30 OPC_58.3 FA_7.7 CH_4 CS, b) 26 OPC_58.3 FA_7.7 CH_8 CS and c) 18 OPC_58.3 FA_7.7 CH_16CS	55
Fig. 4.7 Compressive strength a) 30 OPC_58.3 FA_7.7 CH_4 CS, b) 26 OPC_58.3 FA_7.7 CH_8 CS and c) 18 OPC_58.3 FA_7.7 CH_16CS in logarithmic scale	56
Fig. 4.8 SEM micrograph of interfacial transition zone	57
Fig. 4.9 SEM micrograph of hybrid alkaline cement mortar	57
Fig. 4.10 FTIR spectra	59

Fig. 4.11 Compressive strength	61
Fig. 4.12 Water absorption by immersion	62
Fig. 4.13 Water absorption capillarity coefficient	63
Fig. 4.14 Chloride diffusion coefficient	63
Fig. 4.15 Carbonation depth	64
Fig. 4.16 Weight loss of specimens due to acid attack	65
Fig. 5.1 Water absorption by immersion according to activator/binder ratio and sodium silicate/sodium hydroxide mass ratio: a) Activator/binder ratio=1; b) Activator/binder ratio=0.8; Activator/binder ratio=0.6	72
Fig. 5.2 Density according to activator/binder ratio and sodium silicate/sodium hydroxide mass ratio: a) Activator/binder ratio=1; b) Activator/binder ratio=0.8; Activator/binder ratio=0.6	73
Fig. 5.3 Thermal conductivity according to activator/binder ratio and sodium silicate/sodium hydroxide mass ratio: a) Activator/binder ratio=1; b) Activator/binder ratio=0.8; Activator/binder ratio=0.6	75
Fig. 5.4 Thermal conductivity versus density: a) Hydrogen peroxide based geopolymers; b) Sodium perborate based geopolymers; c) both	76
Fig. 5.5 Compressive strength according to activator/binder ratio and sodium silicate/sodium hydroxide mass ratio: a) Activator/binder ratio=1; b) Activator/binder ratio=0.8; Activator/binder ratio=0.6	78
Fig. 5.6 Compressive strength versus density: a) Hydrogen peroxide based geopolymers; b) Sodium perborate based geopolymers; c) both	79
Fig. 5.7 SEM mix FGA	80
Fig. 5.8 SEM mix FGB	81
Fig. 5.9 SEM mix FGC	82
Fig. 5.10 IR bands of foam geopolymers: a) FGA; b) FGB; c) FGC	84
Fig. 5.11 Cost according to activator/binder ratio and sodium silicate/sodium hydroxide mass ratio: a) Activator/binder ratio=1; b) Activator/binder ratio=0.8; Activator/binder ratio=0.6	85
Fig. 5.12 Cost to thermal resistance ratio	86
Fig. 5.13 Cost to thermal resistance ratio a) Activator/binder ratio=1; b) Activator/binder ratio=0.8; Activator/binder ratio=0.6	87
Fig. 5.14 XRD patterns of: a) 100 OPC (1.5% AL); b) 30 OPC_58.3 FA_4 CS_7.7 CH (0.5% AL); c) 30 OPC_58.3 FA_4 CS_7.7 CH (5% H ₂ O ₂); d) 30 OPC_58.3 FA_4 CS_7.7 CH (3.5% H ₂ O ₂); M-Mullite; Q-Quartz; C- Calcite; CA-Calcite silicate oxide	89
Fig. 5.15 SEM images of: a) 30 OPC_58.3 FA_4 CS_7.7 CH (3.5% H ₂ O ₂); b) 30 OPC_58.3 FA_4 CS_7.7 CH (5% H ₂ O ₂); c) 30 OPC_58.3 FA_4 CS_7.7 CH (0.5% AL); d) 100 OPC (1.5% AL);	90
Fig. 5.16 Compressive strength	91
Fig. 5.17 Water absorption	93
Fig. 5.18 Bulk density	95
Fig. 5.19 Thermal conductivity	97
Fig. 5.20 Cost of one-part geopolymer mixtures: Gray bars) Materials cost; Red bars) Materials cost for a carbon cost in scenario 1; Gree bars) Materials cost for a carbon cost in scenario 2	99

Fig. 5.21 Cost to thermal resistance ratio	99
Fig. 5.22 Global warming potential to thermal resistance ratio	100

Tables Index	Page
Table 2.1 Bibliographic history of some important alkali-activated cement/geopolymer	8
Table 3.1 Chemical composition of the Portland cement	29
Table 3.2 Chemical composition and physical properties of the fly ash	30
Table 3.3 Characteristics of the sand	30
Table 4.1 Mix proportions used in phase A	40
Table 4.2 Mix proportions used in phase B	41
Table 4.3 Mix proportions used in phase C	41
Table 4.4 Phase C-Volumetric ratios	41
Table 4.5 Mix proportions used in phase D	42
Table 4.6 Phase D-Weight ratios	42
Table 4.7 Composition of one part geopolymer mixes used for modeling compressive strength	46
Table 4.8 Constant, exponent and equation of compressive strength evolution for one part geopolymers	53
Table 4.9 Phase D-Weight ratios	58
Table 4.10 EDS Atomic ratio analysis	58
Table 4.11 Mix composition [Kg/m ³]	60
Table 4.12 Resistance to chloride penetration	64
Table 5.1 EDS atomic ratios	70
Table 5.2 EDS atomic ratios	77
Table 5.3 Content of geopolymer samples used for FTIR	83
Table 5.4 Cost of the materials (euro/kg)	85
Table 5.5 Composition of one-part geopolymer mixtures	88
Table 5.6 EDS atomic ratios	89
Table 5.7 Costs of the materials (euro/kg)	98

Abbreviations and acronyms

OPC – Ordinary Portland cement

FA- Fly ash

SP- Superplasticizer

DTA- Differential thermal analysis

TGA- Thermo gravimetric analysis

SEM- Scanning Electron Microscopy

FEG- Field Emission Gun

EDS- Energy Dispersive Spectroscopy

ITZ- Interfacial transition zone

FTIR- Fourier transform infrared spectroscopy

CSH- Calcium silicate hydrates

Na-C-S-H- Sodium calcium silicate hydrates

Na-A-S-H - Sodium aluminum silicate hydrates

K-A-S-H - Potassium aluminum silicate hydrates

1. Introduction

This section presents a brief introduction and justifications on foam one-part geopolymer mortars. Then, the main objectives and finally published papers in this thesis are discussed.

1.1 Justifications

The increasing worldwide demand for energy is a major cause of unsustainable development on our Planet. Between 2007 and 2030, energy demand will have risen around 40%, reaching a total of 16.8 billion tonnes of equivalent petroleum-TEP (Pacheco-Torgal & Jalali, 2011). The rise in energy consumption has two main causes, the increase in world population and the fact that there are an increasing number of people with access to electricity. In fact, currently, there are 1.5 billion people that still have no access to electricity (UN, 2010). Besides, since the urban human population will almost double, increasing from approximately 3.4 billion in 2009 to 6.4 billion in 2050 (WHO, 2014), this will dramatically increase electricity demand. Since buildings consume throughout their life cycle, more than 40% of all energy produced (OECD, 2003), this subsector has a high potential for reducing carbon dioxide emissions. The European Union has been producing legislation in the field of building's energy performance, which was materialised in the form of the European Energy Performance of Buildings Directive 2002/91/EC (EPBD), which in turn, has been recast in the form of the 2010/ 31/ EU by the European Parliament on 19 May 2010. One of the new aspects of the EPBD that reflects an ambitious agenda on the reduction of the energy consumption is the introduction of the concept of nearly zero-energy building (Pacheco-Torgal, Cabeza, Mistretta, Kaklauskas, & Granqvist, 2013). The use of thermal insulation materials constitutes the most effective way of mitigating heat loss in buildings, thus reducing heat energy needs, and therefore contributing to the nearly zero energy target. These materials are very important for the building material industry and represent a 21 billion € market share (Pacheco-Torgal, 2014). However, most current insulation materials are associated with negative impacts in terms of toxicity. Polystyrene, for example contains anti-oxidant additives and ignition retardants, additionally, its production involves the generation of benzene and chlorofluorocarbons. On the other hand, polyurethane is obtained from isocyanates, which are widely known for their tragic association with the Bhopal disaster. Besides, they release toxic fumes when subjected to fire (PachecoTorgal, Jalali, & Fucic, 2012). In terms of legislation, the European Union recently approved the Regulation (EU) 305/2011 (2011) related to the Construction Products.

Regulation that will replace the current Directive 89/106/CEE, already amended by Directive 1993/68/EEC, known as the Construction Products Directive. In the last years, several papers were published on foam alkali-activated cements with enhanced thermal conductivity (Feng et al., 2015; Hlaváček, Šmilauer, Škvára, Kopecký, & Šulc, 2015; Sanjayan, Nazari, Chen, & Nguyen, 2015; Zhang, Provis, Reid, & Wang, 2014). However, cost analysis was oddly avoided. Those authors strangely mentioned that low-cost alkali-activated cements materials could be produced.

The discovery of one-part alkali-activated cements is considered a key event on the evolution of low-carbon alkali-activated cements technology in the “just add water” concept. Contrary to ordinary Portland cement (OPC)-based materials, alkali-activated cements use caustic activators that makes the handling and application of alkali-activated cements very difficult. That is why the alkali-activated cements based on the OPC concept of just add water to a powder are an important research line. However, investigations made so far on one-part alkali-activated cements show that these materials are associated with very low compressive strength (Koloušek et al., 2007; Peng, Wan, Shen, & Xiao, 2014). Some authors even report a compressive strength decrease with time for one-part alkali-activated cements based on calcined red mud and sodium hydroxide blends (Ke, Bernal, Ye, Provis, & Yang, 2015). Since supply chain risks can limit the alkali-activated cements technology’s wider adoption, (Van Deventer, Provis, & Duxson, 2012) the use of minor volumes of OPC can help overcome this problem. Yang and Lee (2013) and Yang, Lee, Song, and Gong (2014) studied foam-ground granulated blast-furnace slag concrete produced with three alkali activators: Ca(OH)_2 plus $\text{Mg(NO}_3)_2$, Ca(OH)_2 plus 6.5% Na_2SiO_3 , and 2.5% Ca(OH)_2 plus Na_2SiO_3 . These authors concluded that a unit binder content of approximately 400 kg/m^3 is required to achieve the minimum quality requirements specified by the Korean Industrial Standard for floor heating systems.

1.2 Objectives

Developing a new composition of geopolymer to produce a mortar with higher level of efficiency and sustainability, is the main objective of this study. This aim can be decomposed into the following specific objectives:

1. Developing mix composition of one-part geopolymers;
2. Obtaining mechanical properties of one-part geopolymer;
3. Microstructure study on the hydration products of one-part geopolymers;

4. Development of an analytical model to predict the compressive strength of one-part geopolymers;
5. Assessment of durability performance of one-part geopolymers;
6. Development of mix compositions related to one-part foam geopolymers;
7. Study the cost-efficiency performance of foam one-part geopolymers;
8. Comparative study on the cost analysis of one-part geopolymers and two-part geopolymers;
9. Compare the global warming potential of one-part foam geopolymers and two-part foam geopolymers

1.3 Publications

1.3.1 International Journal Papers

1. **Abdollahnejad, Z.**, Nazari, A., Pacheco-Torgal, F., Sanjayan, J., Aguiar, J. Numerical modelling of the compressive strength of one-part geopolymers. *Construction and Building Materials*. 2015; Submitted.
2. **Abdollahnejad, Z.**, Miraldo, S., Pacheco-Torgal, F., Aguiar, J., Cost-efficient one-part geopolymers with low global warming potential for floor heating systems applications, *Construction and Building Materials*. 2015; Submitted.
3. **Abdollahnejad, Z.**, Pacheco-Torgal, F., Félix, T., Tahri, W. Aguiar, J., Mix design, properties and cost analysis of fly ash-based geopolymer foam, *Construction and Building Materials*. 2015; 80, 18-30.
4. Tahri, W., **Abdollahnejad, Z.**, Mendes, J., Pacheco-Torgal, F., Barroso de Aguiar, J., “Fly Ash Geopolymeric Mortar for Coating of Ordinary Portland Cement Concrete Exposed to Harsh Chemical Environments. *Advanced Materials Research*. 2015; (accepted)
5. **Abdollahnejad, Z.**, Pacheco-Torgal, F., Aguiar, J., Jesus, C., Durability performance of fly ash based one-part geopolymer mortars, *Key Engineering Materials*, 2014; 634, 113-120.
6. **Abdollahnejad, Z.**, Hlavacek, P., Pacheco-Torgal, F., Aguiar, J., Compressive strength and microstructure of hybrid alkaline cements, *Materials Research Ibero-American Journal of Materials*. 2014; 17, Issue 4, 829- 837.
7. Mastali M., **Abdollahnejad M.**, Ghasemi Naghibdehi., M., Sharbatdar, M.K., Numerical Evaluations of Functionally Graded RC Slabs, *Chinese Journal of Engineering*. 2014.

8. Pacheco-Torgal, F., Ding, Y., Miraldo, S., **Abdollahnejad, Z.**, Labricha. J.A., Are geopolymers more suitable than Portland cement to produce high volume recycled aggregate HPC?, *Construction and Building Material*. 2012; 36, 1048-1052.

9. Pacheco-Torgal, F., **Abdollahnejad, Z.**, Miraldo, S., Baklouti, S., Ding, Y., An overview on the potential of geopolymer for concrete infrastructure rehabilitation, *Construction and Building Materials*.2012; 36, 1053-1058.

10. Pacheco-Torgal, F., **Abdollahnejad, Z.**, Camoes, A.F., Jamshidi, M, Ding, Y., Durability of alkali activated binders: A clear advantage over Portland cement or an unproven issue, *Construction and Building Materials*. 2012; 30, 400-405.

1.3.2 Conference Papers

1. **Z. Abdollahnejad**, A. Nazari, F. Pacheco-Torgal, J. Sanjayan, J.L Barroso Aguiar, 2015, “Prediction of the compressive strength of one-part geopolymers with the JMAK model”, ICEUBI2015, Covilha, Portugal.

2. **Z. Abdollahnejad**, F. Pacheco-Torgal, J.L Barroso Aguiar, 2015, “Development of Foam One-Part Geopolymers with Enhanced Thermal Insulation Performance and Low Global Warming Potential”, ICPIC 2015, Singapore.

3. W. Tahri, **Z. Abdollahnejad**, J. Mendes, F. Pacheco-Torgal, José Barroso de Aguiar, 2015, “Fly Ash Geopolymeric Mortar for Coating of Ordinary Portland Cement Concrete Exposed to Harsh Chemical Environments”, ICPIC 2015, Singapore.

4. **Z. Abdollahnejad**, T. Félix, F. Pacheco Torgal, J.Barroso de Aguiar, 2015, “Preliminary experimental investigation on one-part geopolymer mixes”, European Mortar Summit 2015, Lisbon, Portugal.

5. **Z. Abdollahnejad**, C. Jesus, F. Pacheco Torgal, J. L Barroso Aguiar, 2013, “One-part geopolymer mixes versus Ordinary Portland Cement (OPC): Durability assessment”, Braga, Portugal.

6. **Z. Abdollahnejad**, P. Hlavacek, F. Pacheco Torgal, J. L Barroso Aguiar, 2012, “Preliminary experimental investigation on one-part geopolymer mixes”, Coimbra, Portugal.

1.3.3 Book Chapters

1. Pacheco-Torgal, F., Ding, Y., Miraldo, S., **Abdollahnejad, Z.**, Labricha. J.A., Handbook of recycled concrete and demolition waste, Part 3, “The sustainability of concrete using recycled

aggregate (RAs) for high performance concrete”, Woodhead Publishing series in Civil and Structural Engineering. 2013; 17, 424-438.

2. Pacheco-Torgal, F.; **Abdollahnejad, Z.**; Camoes, A.F., Jamshidi, M, Ding, Y. (2016) Some durability shortcomings of geopolymers. In Handbook of low carbon concrete (Eds) Nazari, A.; Sanjayan, J., Elsevier, Waltham, US (in progress)

1.4 Structure and content of the thesis

This thesis is composed by six chapters. Its content can be summarized as follows:

Chapter 1 presents the justification of this thesis along with its objectives. It also presents a list of publications in which the author of thesis participated during her PhD works.

Chapter 2 reviews the state of the art of current two part geopolymers. Including some of its durability shortcomings namely the important problem of efflorescences that has received little attention by geopolymer researchers. This chapter also includes a brief review on one part geopolymers.

Chapter 3 has a characterization of the materials used during the experimental work of this thesis along with a description of the tests.

Chapter 4 addresses the study of the mix design of the one-part geopolymers. It also analyzes the mechanical properties and the durability of the new binders. Its hydration products are characterized and a model to predict the compressive strength is developed.

Chapter 5 concerns the study of the mix design of one-part foam geopolymers. Its properties, cost efficiency and global warming impact its compared with the one of current two-part geopolymers.

Chapter 6 presents the general conclusions of thesis along with suggestion for further investigation on the field of one part geopolymers.

CHAPTER TWO

Literature Review

2.1 Two part geopolymers

In this part, the review of the relevant literature will be discussed. Presenting an overview of what has been done in previous researches.

2.1.1 Alkali-activated binder

Research works carried out so far in developing alkali-activated binders show that this new material is likely to have enormous potential to become an alternative to Portland cement. The German cement chemist and engineer Kuhl made the first experiences on this field in 1908 (Provis and Deventer, 2014). The bibliographic history of some important alkali-activated cement/geopolymer related events is presented in Table 2.1 although this table does not mention the contribution of Kuhl works.

Alkali activated concrete have been receiving increased attention, due to the need of reducing greenhouse gas emissions generated by Portland cement and to the need of new binders with enhanced durability performance (Duxon et al., 2007; Pacheco-Torgal et al., 2008b).

Research works carried out so far in the development of alkali-activated cements showed that much has already been investigated and also that an environmental friendly alternative to Portland cement is rising (Pacheco-Torgal et. al., 2008c; Li et. al., 2010; Davidovits et al., 1990).

Davidovits et al. (1990) was the first author to address the carbon dioxide emissions of these binders stating that they generate just 0.184 tons of CO₂ per ton of binder. Duxson et al. (2009) do not confirm these numbers; they stated that although the CO₂ emissions generated during the production of Na₂O are very high, still the production of alkali-activated binders is associated to a level of carbon dioxide emissions lower than the emissions generated in the production of OPC. According to those authors, the reductions can go from 50% to 100%.

Table 2.1 Bibliographic history of some important alkali-activated cement/geopolymer related events (Li et al., 2010).

Author	Year	Event
Feret	1939	Slags used for cement.
Purdon	1940	Alkali–slag combinations.
Glukhovsky	1959	Theoretical basis and development of alkaline cements.
Glukhovsky	1965	First called “alkaline cements”.
Davidovits	1979	“Geopolymer” term.
Malinowski	1979	Ancient aqueducts characterized.
Forss	1983	F-cement (slag–alkali–superplasticizer).
Langton and Roy	1984	Ancient building materials characterized.
Davidovits and Sawyer	1985	Patent of “Pyrament” cement.
Krivenko	1986	DSc thesis, $R_2O-RO-SiO_2-H_2O$.
Malolepsy and Petri	1986	Activation of synthetic melilite slags.
Malek et al.	1986	Slag cement-low level radioactive wastes forms.
Davidovits	1987	Ancient and modern concretes compared.
Deja and Malolepsy	1989	Resistance to chlorides shown.
Kaushal et al.	1989	Adiabatic cured nuclear wastes forms from alkaline mixtures.
Roy and Langton	1989	Ancient concretes analogs.
Majundar et al.	1989	$C_{12}A_7$ –slag activation.
Talling and Brandstetr	1989	Alkali-activated slag.
Wu et al.	1990	Activation of slag cement.
Roy et al.	1991	Rapid setting alkali-activated cements.
Roy and Silsbee	1992	Alkali-activated cements: an overview.
Palomo and Glasser	1992	CBC with metakaolin.
Roy and Malek	1993	Slag cement.
Glukhovsky	1994	Ancient, modern and future concretes.
Krivenko	1994	Alkaline cements.
Wang and Scivener	1995	Slag and alkali-activated microstructure.
Shi	1996	Strength, pore structure and permeability of alkali-activated slag.
Fernández-Jiménez and Puertas	1997	Kinetic studies of alkali-activated slag cements.
Katz	1998	Microstructure of alkali-activated fly ash.
Davidovits	1999	Chemistry of geopolymeric systems, technology.
Roy	1999	Opportunities and challenges of alkali-activated cements.
Palomo	1999	Alkali-activated fly ash — a cement for the future.
Gong and Yang	2000	Alkali-activated red mud–slag cement.
Puertas	2000	Alkali-activated fly ash/slag cement.
Bakharev	2001–2002	Alkali-activated slag concrete.
Palomo and Palacios	2003	Immobilization of hazardous wastes.
Grutzeck	2004	Zeolite formation.
Sun	2006	Sialite technology.
Duxson	2007	Geopolymer technology: the current state of the art.
Hajimohammadi, Provis and Deventer	2008	One-part geopolymer.
Provis and Deventer	2009	Geopolymers: structure, processing, properties and industrial applications.

Note: According to Pacheco-Torgal (2014) this table should have credited the “one-part geopolymer” concept to Kolousek et al (2007) because their paper was submitted to review process in March 19 of 2007 and published online in 27 of July of 2007 while the paper of Hajimohammadi et al. (mentioned in the table) was submitted to review process on April 28 of 2008 and accepted by September 23 and published only by October 29 of 2008.

Duxson and Van Deventer (2009) mention an independent study made by Zeobond Pty. Ltd. in which a low emissions Portland cement (0.67 ton/ton) and alkali-activated binders were compared, reporting that the latter had 80% lower CO₂ emissions. Weil et al. (2009) mentioned that the sodium hydroxide and the sodium silicate are responsible for the majority of CO₂ emissions in alkali-activated binders. These authors compared Portland cement concrete and alkali-activated concrete with similar durability reporting that the latter have 70% lower CO₂ emissions, which confirmed the aforementioned reductions. McLellan et al. (2011) reported 44% to 64% reduction in greenhouse gas emissions of alkali-activated binders when compared to OPC.

Habert et al. (2011) carried out a detailed environmental evaluation of alkali activated binders using the Life Cycle Assessment methodology confirming that they have a lower impact on global warming than OPC, but on the other side they have a higher environmental impact regarding other categories. More recently Turner and Collins (2013) showed that the CO₂ footprint of a 40 MPa geopolymer concrete was approximately just 9% less than comparable concrete containing 100% OPC binder (328 kg/m³). Being that the major part was due to sodium silicate (Fig. 2.1).

The high cost of alkali-activated binders is one of the major factors, which remain a severe disadvantage over Portland cement (Habert et al., 2011). Therefore, investigations about the replacement of water glass by sodic wastes are needed (Laldji et al., 2007). Currently alkali-activated binders only becomes economic competitive for high performance structural purposes, because the cost of alkali-activated concretes is located midway between OPC concretes and high performance concretes. Since the average concrete class production lies between C25/30 and C30/37 and only 11% of the ready-mixed concrete production is above the strength class C35/45 (ERMCO, 2011), this means that alkali-activated binders are targeting a small market share.

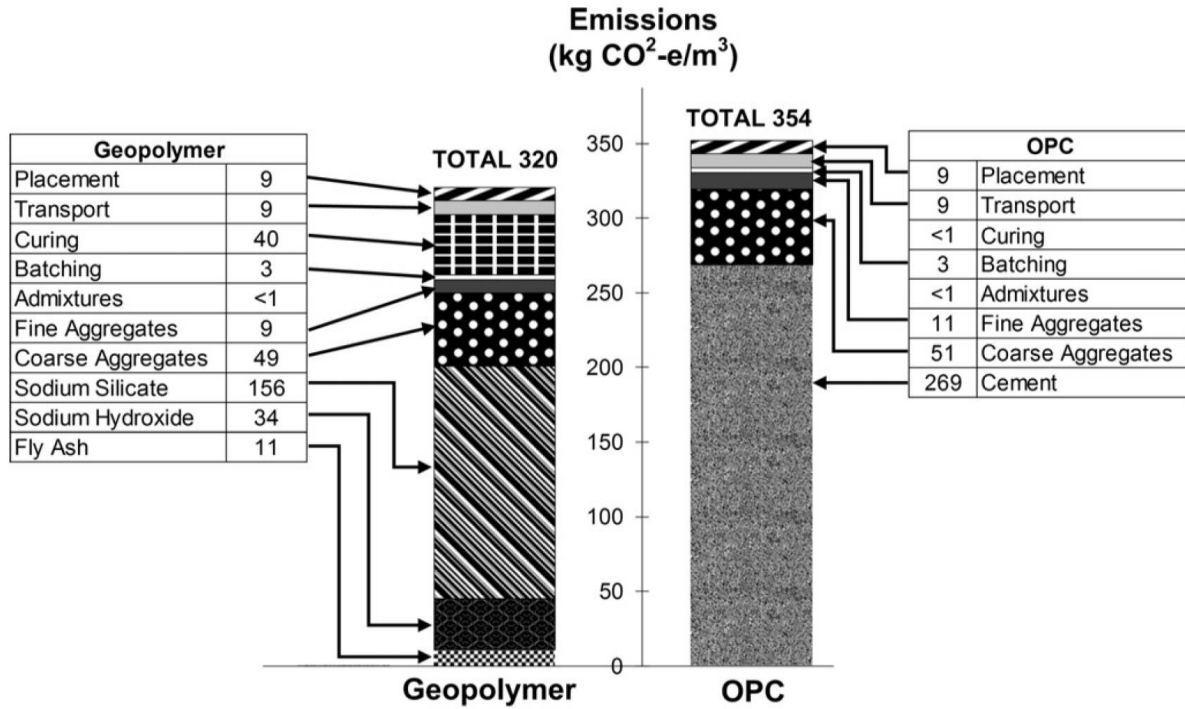


Fig 2.1. Summary of CO₂-emission for Grade 40 concrete mixtures with OPC and geopolymer binders (Turner and Collins, 2013)

Therefore, in the short term the above cited disadvantage means that the study of alkali-activated applications should focus on high cost materials such as, commercial concrete repair mortars. Pacheco-Torgal (2008a and 2009) showed that alkali-activated mortars could be as much as 7 times cheaper than current commercial repair mortars thus pointing available alternative for alkali-activated binders. These materials are still at the beginning stages of development and hence need further research work in order to become technically and economically viable construction materials.

Alkali activated materials is the broadest classification encompassing any binder derived by the reaction of an alkali metal source with a solid silicate powder while geopolymers is a subset of alkali activated materials where the binding phase is almost exclusively aluminosilicate and highly coordinated (Provis and Deventer, 2014).

Research in this field has been published as “alkali-activated” binders, the term “geopolymer” is the generally accepted name for this technology. Investigations in the field of geopolymers had an exponential increase after the research results of Davidovits who developed and patented

binders obtained from the alkali-activation of metakaolin, having named it with the term “geopolymer” in 1978. For the chemical designation of the geopolymer. Davidovits suggests the name “polysialates”, in which sialate is an abbreviation for aluminosilicate oxide. The sialate network is composed of tetrahedral anions $[\text{SiO}_4]^{4-}$ and $[\text{AlO}_4]^{5-}$ sharing the oxygen, which need positive ions such as (Na^+ , K^+ , Li^+ , Ca^{++} , Na^+ , Ba^{++} , NH_4^+ , H_3O^+) to compensate the electric charge of Al^{3+} in tetrahedral coordination (after dehydroxilation the aluminum changes from coordination 6 (octahedral) to coordination 4 (tetrahedral)).

The polysialate has the following empiric formulae:



in which: n is the degree of polymerization, z is 1, 2 or 3, and M is an alkalication, such as potassium or sodium, generating different types of poly(sialates). According to Davidovits, geopolymers are polymers because they transform, polymerize and harden at low temperature.

But they are also geopolymers, because they are inorganic, hard and stable at high temperature and also non inflammable. Over the last years several authors have reported research in a large number of aspects related to geopolymers such as: dependence of the nature of source materials (alkali-activated binders synthesized from calcined sources show a higher compressive strength than from raw materials) (Provis, 2009; Bakharev, 2005), immobilization of toxic metals (Barbosa et al., 2000; Vance et al., 2009; Vinsova et al., 2007), reaction mechanisms and hydration products (Provis et al., 2009; Bakharev, 2005; MacKenzi et al., 2005; Fernandez-Jimenez et al., 2005b), the role of calcium in geopolymerization (Weng et al., 2005; Yip et al., 2003; Yip et al., 2005) the development of lightweight building materials (Buchwald et al., 2005), durability issues (Hwai-Chung and Peijang, 2005; Provis et al., 2008; Kani et al., 2011) and even LCA (Weil et al., 2009; Habert et al., 2011).

According to those authors (Glukhovsky, 1981), an increase in the compressive strength of 4 MPa would require 24 h hydrothermal treatment at 100 °C. The use of a much more intensive treatment (140 °C) would increase compressive strength of 12-20 MPa. Some authors recently investigated

these materials having reported a 28 days curing compressive strength of 27 MPa by using fly ash and 30% OPC (Abdollahnejad et al., 2014).

So far investigations related to the geopolymerization of concentration and determination work are scarce (Lampris et al., 2009; Allahverdi and Najafi Kani, 2009), nevertheless, it seems that this binder has potential features to reuse recycled aggregates for the production of HPC. For the same water/binder ratio several authors reported that geopolymers present a higher mechanical strength than Portland cement.

Wang in 1991 states a case of a geopolymeric concrete with 125 MPa compression strength. Other authors (Davidovits, 1994a) declare having obtained a 20 MPa strength just after 4 h increasing to 70–100 MPa after 28 days curing. Fernandez-Jimenez et al. (2005a) studied mortars ($w/b = 0.51$) activated with NaOH and waterglass reporting 100 MPa for compressive strength. Fernandez-Jimenez and Palomo in 2005a used slag/fly ashes mixtures activated with NaOH and waterglass ($w/b = 0.35$) announcing a 90 MPa compressive strength just after 20 h. Bakharev in 2005 studied fly ash pastes activated with NaOH and waterglass ($w/b = 0.3$) stating a 60 MPa compressive strength just after 2 days. Other authors (Pacheco-Torgal et al., 2007) report a compressive strength higher than 30 MPa after only one day, reaching almost 70 MPa after 28 days curing and 90 MPa at 90 days curing. In conventional concrete, the aggregates form a rigid skeleton of granular elements, which are responsible for compressive strength, in geopolymers most of the compressive strength is related to the matrix characteristics, therefore, this material does not rely in well-proportioned aggregate mixtures. This makes geopolymer concrete more suitable to reuse recycled aggregates.

These materials have another advantage over Portland cement concrete that is particularly interesting in the case of reusing contaminated recycled aggregates, a high immobilization capacity. According to Hermann et al. in 1999 the use of alkali-activated binders is a good way to immobilize a wide range of harmful constituents such as toxic metals, hydrocarbonates and even nuclear wastes in a final product with high durability and costing much less than the current vitrification process (Hermann et al., 1999). In 2007, Vinsova et al. refer that alkali-activated

binders show a good performance in the immobilization of lead, cadmium and chromium, being less effective for immobilization of arsenic.

Lancellotti et al. (2010) showed that metakaolin based geopolymers binders are able to immobilize toxic metals present in fly ash due to the incineration of municipal solid wastes. Immobilization of a municipal solid waste incineration residue using geopolymers was recently reported (Galiano, et al., 2010). Other authors (Hermann et al., 1999; Vinsova et al., 2007; Lancellotti, et al., 2010; Galiano, et al., 2010; Pacheco-Torgal, et al., 2010; Garcia-Lodeiro, et al., 2007; Fu, et al., 2011; Zhang, et al., 2011) showed that geopolymeric binders can be used for the reuse of mine wastes. Besides geopolymeric concretes are associated to lower CO₂ emissions than Portland cement concretes (Duxson, et al., 2007; Weil, et al., 2009; Habert, et al., 2011). This is a crucial advantage because Portland cement represents almost 80% of the total CO₂ emissions of concrete, which in turn are about 6–7% of the Planet's total CO₂ emissions (Shi, et al., 2011; Pacheco-Torgal, et al., 2012b).

With a view to the large-scale adaptation of alkalin cement technology the world over, in 2007 a RILEM technical committee (TC 224 – AAM) began to compile and summarize experiences in connection with prime materials, cements, concretes, structures, output, test procedures, durability, envisaged use and so on. The ultimate aim is to develop basic recommendations for specifications designed to bring these cements to a market where they can compete on a level playing field with Portland cements.

2.2 Limitation of durability of geopolymer

Besides the durability of alkali-activated binder is a subject of some controversy, while Duxson et al. (2009) state this is the most important determining the success of these new materials and other authors mention that the fact that samples from the former Soviet Union that have been exposed to service conditions for in excess of 30 years showing little degradation means that geopolymers do therefore appear to stand the test of time (Pacheco-Torgal F et al., 2012b).

However, since those materials were of the (Si + Ca) type that conclusion cannot be extended to geopolymers defined as “alkali alumino silicate gel, with aluminium and silicon linked in a tetrahedral gel framework” (Weil M et al., 2009). On the other side Juenger et al. (2011) argue

that “the key unsolved question in the development and application of alkali activation technology is the issue of durability” and more recently Van Deventer et al. (2012) recognized that “whether geopolymer concretes are durable remains the major obstacle to recognition in standards for structural concrete”.

Geopolymers as the alkali-activated binder have some properties which have advantages and disadvantages. Recently the following geopolymer properties were concerned by researchers which include:

1. Resistance to acid attack;
2. Alkali-silica reaction (ASR);
3. Corrosion of steel reinforcement;
4. Resistance to high temperatures;
5. Efflorescence;

2.2.1 Resistance to acid attack

Concerning the resistance to acid attack, geopolymer performance is far better than that of Portland cement concretes because it does not contain $\text{Ca}(\text{OH})_2$, a soluble hydration product that constitutes the “Achilles’ heel” of Portland cement concrete. Calcium hydroxide contributes slightly to the strength and impermeability of the paste, because it reduces the total pore volume by converting some of the liquid water into solid form. In this respect it is much less important than the C-S-H, however. CH is the most soluble of the hydration products, and thus is a weak link in cement and concrete from a durability point of view. If the paste is exposed to fresh water, the CH will leach out (dissolve), increasing the porosity and thus making the paste more vulnerable to further leaching and chemical attack.

Davidovits et al. (1990) reported mass losses of 6% and 7% for geopolymeric binders immersed in 5% concentration hydrochloric and sulfuric acids during 4 weeks. For the same conditions he also observed that Portland cement based concretes suffered mass losses between 78% and 95%. Other authors (Gourley and Johnson, 2005) mentioned that a Portland cement concrete with a service life of 50 years lost 25% of its mass after 80 immersions cycles in a sulfuric acid solution ($\text{pH} = 1$) while a geopolymeric concrete required 1400 immersions cycles to lose the same mass, thus meaning a service life of 900 years.

More recently Pacheco-Torgal et al. (2010) mentioned an average mass loss of just 2.6% after being submitted to the attack of (sulfuric, hydrochloric and nitric) acids during 28 days, while the mass loss for Portland cement concretes is more than twice that value.

Several authors reported that chemical resistance is one of the major advantages of alkali-activated binders over Portland cement. In 1981, Glukhovskiy used alkali-activated slag mortars noticing that they showed increase tensile strength even after being immersed in lactic and hydrochloric acid solutions ($\text{pH} = 3$). Jiang (1997) studied the exposure of alkali-activated slag mortars during six months in 5% acid solution concentration, reporting that for citric acid changes were low, for nitric and hydrochloric acid changes were moderate although severe changes were noticed when sulphuric acid was used.

Davidovits et al. (1990) reported mass losses of 6% and 7% for alkali-activated binders immersed in 5% concentration hydrochloric and sulphuric acids during 4 weeks. For the same conditions, he also reported that Portland cement based concretes suffered mass losses between 78% and 95% (1999 a), Palomo et al. studied metakaolin mixtures activated with NaOH and water-glass when submitted to sulphuric acid ($\text{pH} = 3$), sea water ported a minor flexural strength decrease from 7 to 28 days immersion, between 28 and 56 days flexural strength rises, decreasing again from 56 to 90 days and rising from that day forward. They reported that the behavior was similar to the several acid solutions. According to these authors, unreacted sodium particles are not in the structure of the hardened material, remaining in a soluble condition thus when in contact with a solution they are leached increasing the binder porosity and lowering mechanical strength. On the other hand, strength increase after 3 months indicates that the reaction process is still evolving, with the formation of zeolitic precipitates thus lowering porosity and increasing strength.

Shi and Stegmann (2000) compared the acid resistance of several binders; alkali-activated slags (AASs), OPC binders, fly ash/lime binders (FAL) and high alumina cement (AC), when immersed in nitric ($\text{pH} = 3$) and acetic ($\text{pH} = 3$ and 5) acid solutions. They reported that OPC binders presented higher mass losses than AAS and FAL binders while AC pastes were completely dissolved. According to these authors, OPC pastes are more porous than AAS but less porous than

FAL pastes, so chemical attack is more influenced by the nature of hydration products than from porosity. They also reported that low pH acids are responsible for the highest chemical attack.

Bakharev et al. (2002) also compared OPC and alkali-activated slag concrete resistance to sulphat attack, reporting that the former showed a lower strength reduction, that could be explained due to the binder structure chemical differences. Bakharev et al. (2002) studied OPC and slag concretes activated with NaOH and water glass, immersed in an acetic acid solution (pH = 4) during one year. They reported a 33% strength loss for the former and 47% for OPC concretes.

They claim that the strength loss is influenced by Ca content, 64% for OPC concretes and just 39% for alkali-activated slag concretes. Besides slag compounds have lower Ca/Si molar ratio and are more stable in acid medium. As for OPC concrete calcium compounds, possess high Ca/Si molar ratios and react with acetic acid forming acetic calcium compounds which is very soluble.

2.2.2 Alkali-silica reaction (ASR)

The chance of ASR may take place in alkali-activated binders is an unknown subject. For OPC binders, however, the knowledge of ASR has been intensively studied; therefore, some explanations could be also applied to understand the possibility of ASR when alkali-activated binders are used. ASR was reported by the first time by Stanton (1940) and needs the simultaneous action of three elements in order to occur: (a) enough amorphous silica, (b) alkali ions and (c) water (Sims and Brown, 1998).

The ASR begins when the reactive silica from the aggregates is attacked by the alkaline ions from cement forming an alkali-silica gel, which attracts water and starts to expand. The gel expansion leads to internal cracking, what have been confirmed by others (Wood and Johnson, 1993) reporting 4 MPa pressures. Those internal tensions are higher than OPC concrete tensile strength, thus leading to cracking. However, some authors believe that ASR is not just a reaction between alkaline ions and amorphous silica but also requires the presence of Ca²⁺ ions (Davies, 1998). In 1991, Davidovits compared alkali-activated binders and OPC binders when submitted to the ASTM C227 mortar-bar test, reporting a shrinkage behavior in the first case and a serious expansion for the OPC binder. Other authors (Fernandez-Jimenez and Puertas, 2002) reported

some expansion behavior for alkali-activated binders although smaller than for OPC binders. However, Puertas (1995) believe ASR could occur for alkali-activated slag binders containing reactive opala aggregates. Bakharev et al. (2001) compared the expansion of OPC and alkali-activated binders reporting that the first ones had higher expansion. This is clear from the microstructure analysis (Fig. 2.2).

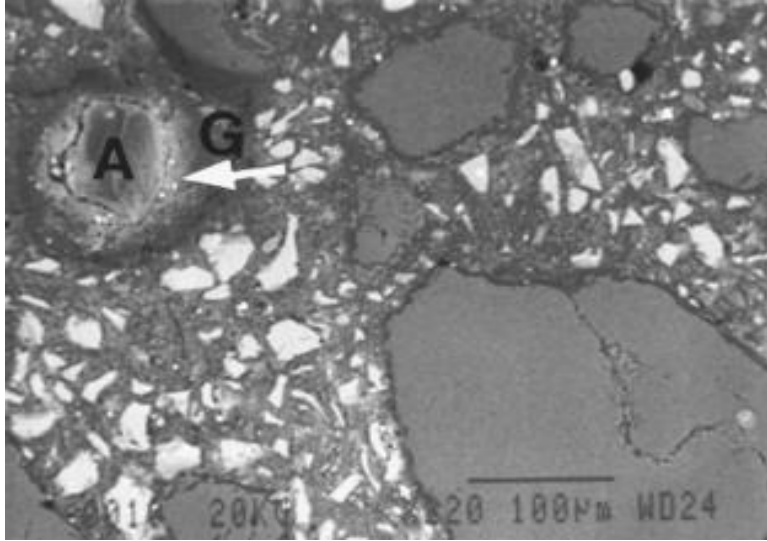


Fig 2.2. Alkali-activated concrete after 10 months curing. (A) Reactive aggregate. (G) Alkali-silica gel (Puertas F et al., 2009).

García-Lodeiro et al. (2007) showed that alkali-activated fly ash is less susceptible to generate expansion by alkali-silica reaction than OPC. They also showed that the calcium plays an essential role in the expansive nature of the gels. Recent investigations (Puertas et al., 2009) show that siliceous aggregates are more prone to ASR than calcareous aggregates in alkali-activated mixtures. Cyr and Pouhet (2014) reviewed the work of several authors concerning the expansion due to ASR (Fig. 2.3) noticing that some mixtures show an expansion above the limit proposed in the standard used for ASR tests. Therefore the study of ASR, in alkali-activated binders is not a closed subject, at least for the geopolymer mixtures containing calcium.

2.2.3 Corrosion of steel reinforcement

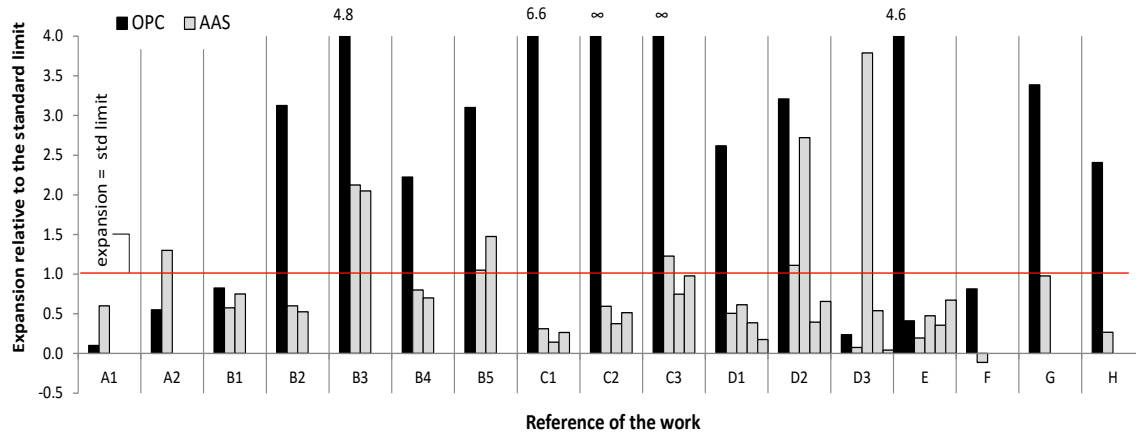
The corrosion of steel reinforcement is one of the causes that influences the structural capability of concrete elements. As concrete attack depends on its high volume and therefore is not of great

concern, an attack to the steel reinforced bars is a serious threat eased by the fact that steel bars are very near of concrete surface and are very corrosion sensitive. In OPC binders, steel bars are protected by a passive layer, due to the high alkalinity of calcium hydroxide. The steel bars corrosion may happen if pH decreases thus destroying the passive layer, due to carbonation phenomenon or chloride ingress. The steel corrosion occurs due to an electrochemical action, when metals of different nature are in electrical contact in the presence of water and oxygen. The process consists in the anodic dissolution of iron when the positively charged iron ions pass into the solution and the excess of negatively charged electrons goes to steel through the cathode, where they are absorbed by the electrolyte constituents to form hydroxyl ions. These in turn combine with the iron ions to form ferric hydroxide, which then converts to rust. The volume increase associated with the formation of the corrosion products will lead to cracking and spalling of the concrete cover.

For alkali-activated binders the literature is small about its capability to prevent reinforced steel corrosion. Torgal et.al investigated on the chloride diffusion, which clearly showed alkali-activated binders are able to prevent the ingress of harmful elements that could start steel corrosion.

Roy et al. (2000) compared chloride diffusion for OPC and alkali-activated binders reporting that the former presented almost half of the diffusion values of the OPC binders. Saraswathy et al. (2003) studied alkali-activated fly ash mixtures reporting a steel corrosion resistance similar to the one of OPC binders.

Miranda et al. (2005) even demonstrated that alkali-activated fly ash binders have superior pH conditions than OPC binders. They reported that pH decreased with hydration reaction development, however an alkaline condition remained even after 5 years, since carbonation phenomenon did not take place.



	Reference	Temperature	Age of test	Explanation of the different AAS mixtures
A1, A2	Bakharev et al. (2001)	38°C	1 year	A1: non-reactive aggregate A2: reactive aggregate
B1 to B5	Gifford and Gillott (1996)	38°C	1 year	B1: non-reactive aggregate B2: reactive (ASR) aggregate S1 B3: reactive (ASR) aggregate S2 B4: reactive (ASR) aggregate V B5: reactive (ASR) aggregate B AAS activated with Na ₂ CO ₃ or Na ₂ SiO ₃
C1 to C3	Chen et al. (2002)	38°C	180 days	C1, C2 and C3: 2, 3.5 and 5% alkalis, respectively AAS activated with waterglass, NaOH, Na ₂ CO ₃ or Na ₂ SO ₄
D1 to D3	Metso (1982)	40°C	70 days	D1, D2 and D3: 3, 8 and 15% of opal, respectively Two types of slag, activated with 1.5 or 2.4% Na
E	Al-Otaibi (2007)	60°C	1 year	AAS activated with sodium silicate or sodium metasilicate, with Na ₂ O content of 4 or 6% Two OPC references: doped and non-doped in alkalis
F	Fernandez-Jimenez A, Palomo A., Puertas F. (1999)	80°C	16 days	
G	Puertas et al. (2009)	80°C	14 days	
H	Wang et al. (2010)	80°C	14 days	

Fig 2. 3 Ratios of the expansion relative to the limit proposed in the standard used for ASR test, for Portland cement and alkali-activated slag mixtures (Cyr and Pouhet, 2014)

Aperador et al. (2009) mention that alkali-activated slag concrete is associated to poor carbonation resistance a major cause for corrosion of steel reinforcement. Bernal et al. (2010) shows that the activation of granulated blast furnace slag (GBFS)–metakaolin (MK) blends have low carbonation resistance. The same authors (Bernal et al., 2010) found that alkali-activated slag concretes present some susceptibility to carbonation, which depends on the binder content (Fig. 2.4).

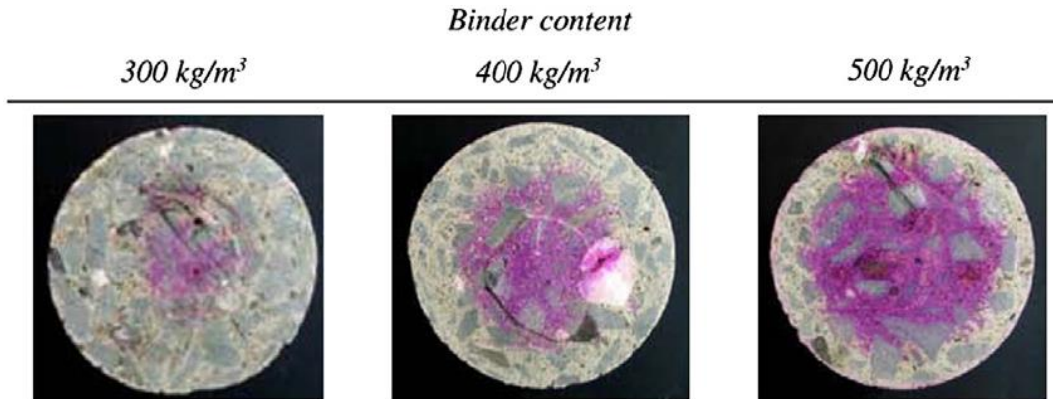


Fig 2.4. Transverse sections of carbonated alkali-activated slag concretes after 1000 h of exposure to a 1% CO₂ environment, with the extent of carbonation revealed by a phenolphthalein indicator.

Samples are 76.2 mm in diameter (Bernal et al., 2010).

Lloyd et al. (2010) show that geopolymer cement is prone to alkali leaching. This leads to a reduction in the pH and could cause steel corrosion.

They also mention that the presence of calcium is crucial for having “durable steel-reinforced concrete” which is a setback for Si–Al geopolymers. Further research about reinforced steel corrosion is therefore needed, concerning alkalinity stability with curing time, as well as about chloride diffusion and carbonation resistance.

2.2.4 Resistance to high temperatures and to fire

Concretes based on Portland cement show a weak performance when subjected to a thermal treatment and when the temperature rises above 300 °C they begin to disintegrate. As the alkali-activated binders show a high stability when submitted to high temperatures even around 1000 °C (Pawlasova et al., 2007). Other authors (Bortnovsky et al., 2007) studied the activation of metakaolin and shale wastes reporting a high mechanical performance after a thermal phase. The

specimens show some slight strength loss between 600 °C and 1000 °C, however in some cases they show a strength increase at 1200 °C. Kong et al. (2008) studied alkali-activated metakaolin binders observing that the residual strength after a thermal phase up to 800 °C is influenced by the Si/Al ratio. The higher residual strength was obtained by the mixtures with a Si/Al ratio between 1.5 and 1.7.

Krivenko and Guziy (2007) found that alkali-activated binders show a high performance in the resistance to fire, thus suggesting that this material is suitable for use in works with a high fire risk like tunnels and tall buildings. Perná et al. (2007) confirmed that alkali-activated binders can be used as a 120 min anti-fire material in accordance with related standards of the Czech Republic. The anti-fire material must show a temperature lower than 120 °C in the opposite side of the fire action.

Temuujin et al. (2011) used alkali-activated binders as steel coatings stating that they maintained high structural integrity even after being submitted to a heat treatment by a gas torch. Zhao and Sanjayan (2011) compared the performance of OPC concrete and alkali activated concrete under the standard curve fire test mentioning that only the former exhibit spalling behavior. The internal pore structure of the latter allows a quick escape of the water vapor resulting in lower internal pore pressure.

2.2.5 Efflorescences

Very few authors have investigated this serious limitation of geopolymers. Davidovits never mentioned and a search on the website of Geopolymer Institute show no paper about efflorescences. Also a search on Scopus about the words “geopolymers” and “efflorescences” show that only in 2007 was published the first paper where this problem is mentioned.

Nevertheless, geopolymers suffer from severe efflorescence (Pacheco-Torgal and Jalali, 2010) because the bond between the sodium ions (Na^+) and the aluminosilicate structure is weak which explains the leaching behavior (Skvara et al., 2008). According to those authors it is the presence of water that weakens the bond of sodium in the aluminosilicate polymers, a behavior that is confirmed by the geopolymer structure model (Fig. 2.5).

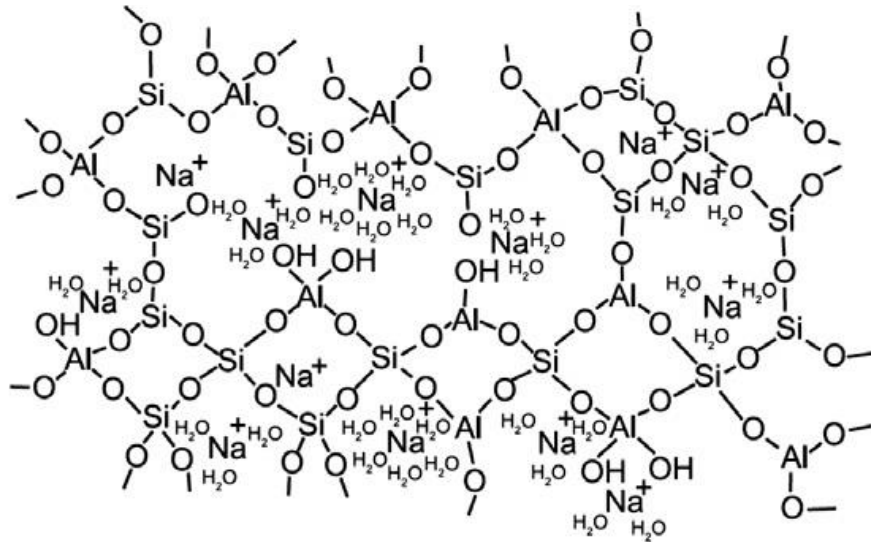


Fig 2.5. Geopolymer structure model (Skvara et al., 2008).

The subject of efflorescences in alkali-activated binders is relatively new, since very few authors have addressed this problem.

Pacheco-Torgal and Jalali (2010) also found that sodium efflorescences are higher in alkali-activated binders based aluminosilicate prime materials calcined at a temperature range below the dehydroxylation temperature with the addition of sodium carbonate as a source of sodium cations (Fig. 2.6).

Temuujin et al. (2009) refer that although ambient cured fly ash alkali-activated binders exhibited efflorescences and that phenomena do not occur when the same alkali-activated binders are cured at elevated temperature which means the leach ate of sodium could be a sign of insufficient geopolymerisation.



Fig 2.6. Alkali-activated mine waste mortars specimens after water immersion: Above mortars based on plain mine waste mud calcined at 950 °C for 2 h; Below mortars based on mine waste mud calcined at different temperatures with sodium carbonate (Pacheco-Torgal and Jalali, 2010)

Van Deventer et al. (2010) recognized that current two part geopolymers suffer from severe efflorescence which is originated by the fact that “alkaline and/or soluble silicates that are added during processing cannot be totally consumed during geopolymerisation”. Kani et al. (2011) showed that efflorescences can be reduced either by the addition of alumina-rich admixtures or by hydrothermal curing at temperatures of 65°C or higher. These authors found that the use of 8% of calcium aluminate cement greatly reduces the mobility of alkalis leading to minimum efflorescences (this cement has 28% of CaO).

Recently Skvara et al. (2012) showed that Na, K is bounded only weakly in the nanostructure of the geopolymer (N, K)–A–S–H gel and is therefore leachable almost completely. This confirms that efflorescences is a worrying limitation of two part geopolymers when exposed to water or environments with RH above 30% (Fig. 2.7).

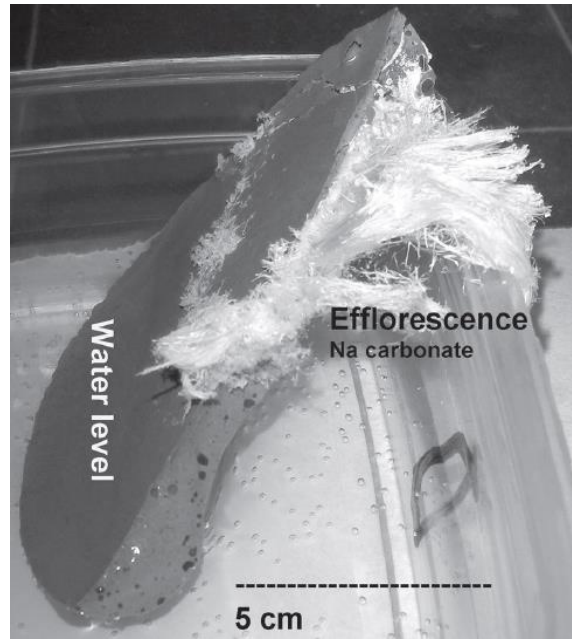


Fig 2.7. High efflorescence after 50 days of partially-immersed Alkali activated fly ash

Zhang et al. (2014) also confirmed the presence of efflorescences in fly ash based geopolymers (Fig.2.8). Those authors recommended the use of hydrothermal treatments of geopolymers in order to reduce efflorescences formation. However this not only increases the cost of geopolymers but also increases its carbon dioxide footprint.

There are many drawbacks associated with traditional two part mixes for the synthesis of geopolymers. The caustic alkaline solutions needed to form the geopolymers make the handling and application of geopolymers difficult. In addition, workability is generally poor and not easily adjustable due to a sticky and thick mortar that is generated during processing. The system is also sensitive to the ratio of alkaline and soluble silicate, which is difficult to control in practice.

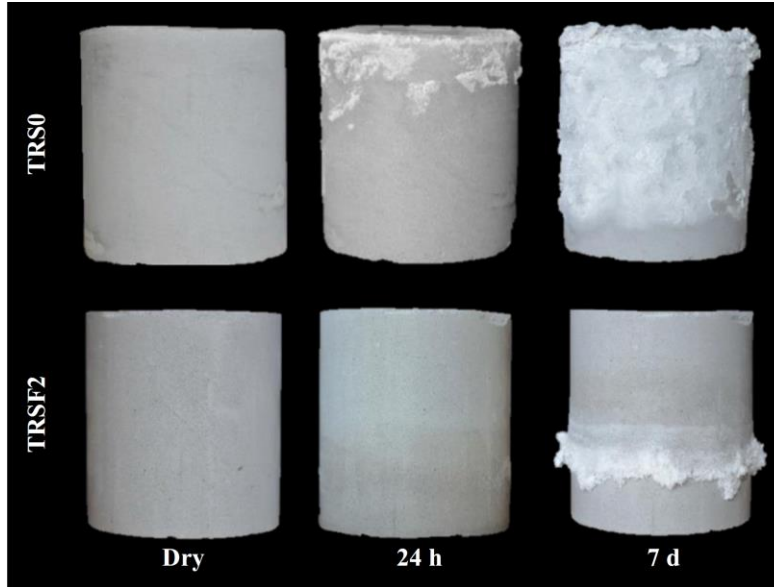


Fig 2.8. Efflorescence of the dense geopolymer TRSF0 and the foamed geopolymer TRSF2 specimens stored for times with the bottom in contact with water (Zhang et al., 2014)

Additionally, using hydrothermal curing has serious limitations for on-site concrete placement operations. Most importantly, the alkaline soluble silicate that are added during processing cannot be totally consumed during geopolymerisation, even with curing at a raised temperature, due to the existence of dissolution equilibrium of raw aluminosilicate materials in alkaline silicate solutions. This causes severe efflorescences of the final geopolymer products and high permeability and water absorption due to the movement of alkali together with water to the geopolymer surfaces. This means that this subject merits further investigations.

2.3 One part geopolymers

One-part geopolymers represent a key event on geopolymer technology having been described by the first time in 2007 (Kolousek et al., 2007; Shi et al., 2011). The present invention provides an alternative to the conventional two part mixes and advantageously alleviates one or more of the disadvantages of prior part. The discovery of one-part geopolymers is considered as an important phenomena in the evolution of low carbon geopolymer technology in the “just add water” concept. However they were associated with low compressive strength (Koulosek et al., 2007). Recent investigations (Peng et al., 2015) confirm that one-part geopolymers show low mechanical strength. These authors noticed that the one part geopolymer mixtures show an increased reduced

compressive strength after being immersed in water. This reduction being dependent on the kaolin thermal treatment. Higher calcination temperatures being responsible for higher compressive losses. Other authors (Ke et al., 2015) even reported a compressive strength decrease for one-part geopolymers based on calcined red mud and sodium hydroxide blends just after the first week of curing (Fig. 2.9). These limitations mean that further investigations are needed concerning the development of new and improved one part geopolymers.

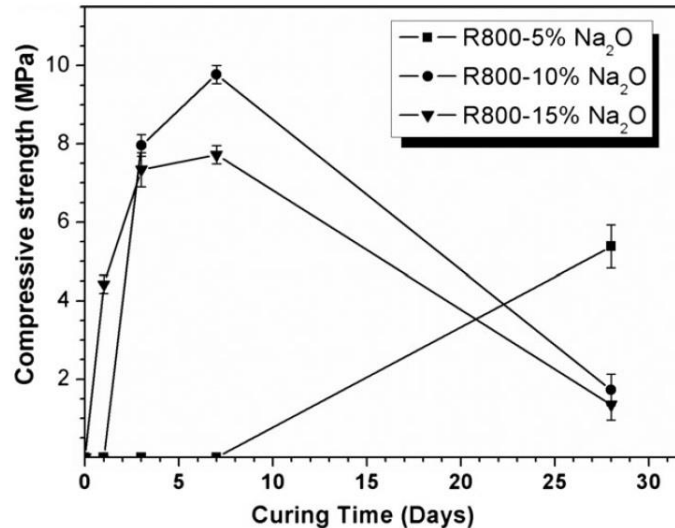


Fig. 2.9 Compressive strengths of red mud-based one-part geopolymers produced with different activator doses as a function of the time of curing (Ke et al., 2015)

2.4 Conclusions

Research on alkali-activated binders shows a broadest potential due to low CO₂ emissions. These materials can be taken into account as an alternative to Portland cement, although various investigations need to be performed on the characteristics of these new materials. Many authors confirmed the reduction of CO₂ emission when the alkali activated binder in compared to Portland cement, which leads to lower impact on global warming than OPC. Geopolymer is a subset of alkali activated materials with mostly binding phase of aluminosilicate and highly coordinated. New investigations are needed on the use of sodic wastes to replace sodium silicate in order to reduce the cost of this material; The new binders present higher chemical resistance, however it seems that depends more on the low content of soluble calcium compounds than their low permeability; although these binders contain a high level of alkali elements, they do not appear to be associated with the occurrence of ASR, which may be because the majority of alkali elements

are associated with other reaction products. However, that explanation forgets the crucial role played by calcium in the ASR development meaning that although it is rather natural the absence of ASR in free calcium alkali-activated binders, that problem must be taken under consideration when calcium based binders were used. As the capability to keep an alkaline environment through time, which is crucial to maintain reinforced steel safe from corrosion, the current studies are not enough to prove it, as a matter of fact their resistance to carbonation is lower than OPC binders and recent investigation show that it is difficult to synthesize a low-Ca geopolymer capable of preserving the steel reinforcement passivation film; the use of calcium in alkali-activated binders is indispensable to keep a high pH but at the same time could be the responsible for triggering ASR; Contrary to standard OPC binders alkali-activated binders show a high stability when submitted to high temperatures which dependent on the Si/Al ratio. The investigations on the fire behavior of alkali-activated binders show that these materials are specially recommended for works with a high fire risk like tunnels and tall buildings; Alkali-activated binders are prone to the formation of efflorescences however this disadvantage can be greatly reduced when using hydrothermal curing treatments or calcium aluminate admixtures. Nevertheless, hydrothermal curing has limited applications for on situ concrete placement operations and the use of a calcium-based admixture raises issues about its acid resistance. Furthermore, alkali-activated binders containing calcium-based admixture have a higher global warming impact than alkali-activated Si-Al mixtures. There are many drawbacks associated with the application of traditional two part mixes for the synthesis of geopolymers. One-part geopolymers 'just add water concept' represent a key event on geopolymer technology. The present invention provides an alternative to the conventional two part mixes and advantageously alleviates one or more of the disadvantages of prior part.

CHAPTER THREE
Experimental Tests

3. Experimental tests

In this chapter, the used materials will be explained in details and the mechanical tests which is going to be carry out, will be presented. Following the mechanical test the durability tests and microstructure analysis will also be performed which is going to be presented. In the first step of this study, evaluation of the characteristics of aluminosilicate materials like fly ash, kaolin and other will be carried out.

3.1 Materials

The composition of dry mix in this study was kaolin, fly ash, ordinary Portland cement (OPC), sodium hydroxide, calcium hydroxide ($\text{Ca}(\text{OH})_2$), water and superplasticizer. The mixtures under investigation are based on the one described in the international patent authorized by Zheng et.al. in 2007.

3.1.1 Ordinary Portland Cement (OPC)

The OPC is of type I 42.5 R class with clinker content between 95-100%, a specific weight of 3.15 g/cm^3 and a Blaine fineness of $3842 \text{ cm}^2/\text{g}$ (Table 3.1).

Table 3.1 Chemical composition of the Portland cement

Loss on ignition %	Cl %	SO ₃ %	CaO Reactive %	SiO ₂ %	Fe ₂ O ₃ %	MgO %	Al ₂ O ₃ %
1.7	0.01	2.83	63.1	20.9	3.40	2.71	5.03

3.1.2 Superplasticizer (SP)

The superplasticizer (SP) used was polycarboxylate. The SP was used to maintain a uniform consistency between the different mixes.

3.1.3 Fly ash

Private Portuguese Company has provided fly ash. The chemical composition of the fly ash complies with the minimum requirements indicated in EN-450-1:2005 for being used as a partial replacement of cement in concrete. Based on this standard the fly ash was categorized in class B and group N for the loss of ignition and fineness, respectively. It has a specific weight of 2.42 g/cm^3 and the chemical composition is shown in Table 3.2.

Table 3.2 Chemical composition and physical properties of the fly ash (%)

Retained on No. 325 sieve	SiO ₂	Al ₂ O ₃ +Fe ₂ O ₃ +SiO ₂	CaO	MgO	SO ₃	K ₂ O	P ₂ O ₅	I.A. _{28D}	I.D. _{90D}	Total alkalis
15	40.8	89.8	2.36	1.9	0.12	3.34	1.92	79	99	0.25

3.1.4 Sand

The characteristics of the sand are shown in Table 3.3. The used sand can be categorized as fine sand.

Table 3.3 Characteristics of the sand

Max dimension (mm)	Fine content (%)	Density (kg/m ³)	Water absorption (%)
2.0	≤3	2660	0.2

3.1.5 Kaolin

The kaolin has a BET surface area of 21 m²/g and its particle size is shown in Fig. 3.1. This is crucial information as this parameter influences the dihydroxylation temperature of kaolin.

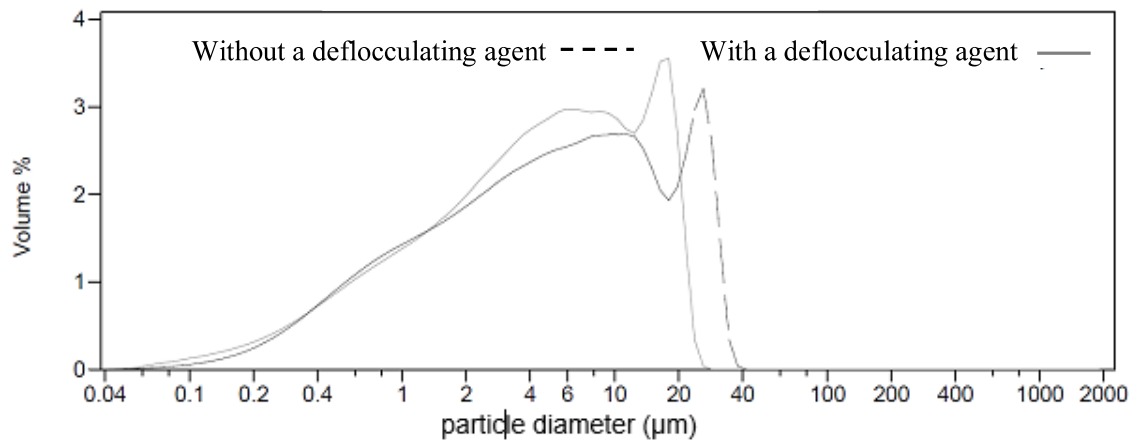


Fig. 3.1 Kaolin particle diameter obtained with and without a deflocculating agent

The DTA/TGA curves for kaolin are presented in Fig. 3.2.

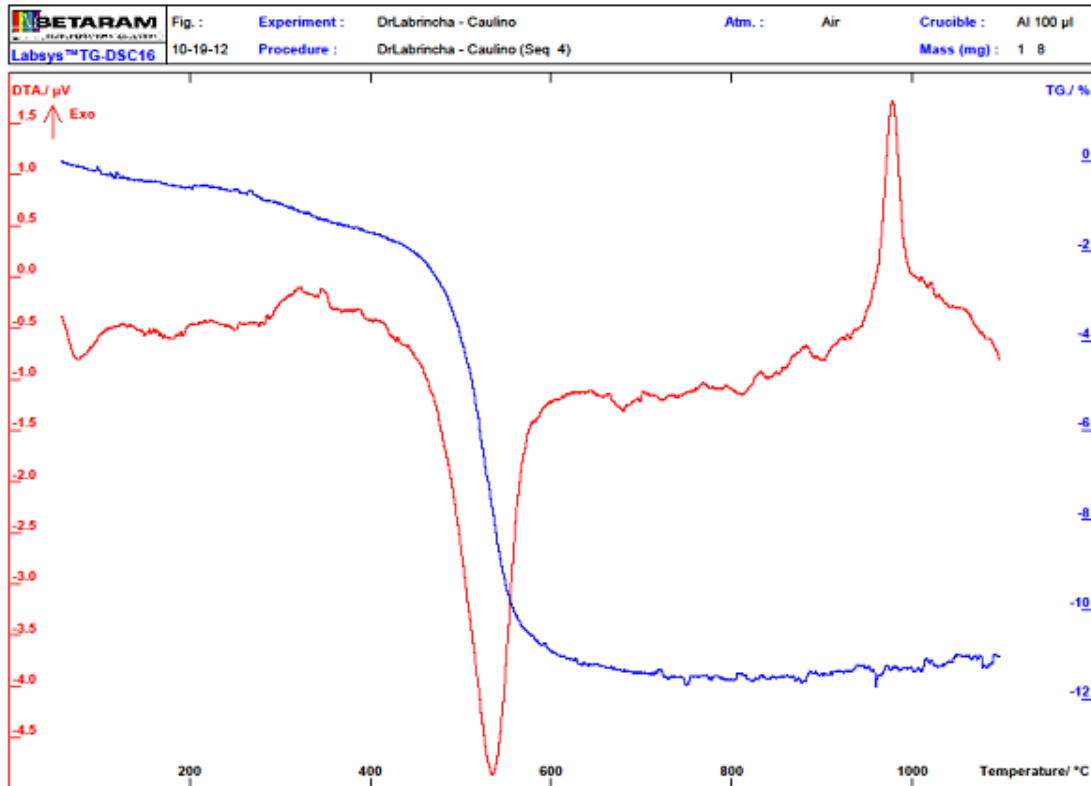


Fig. 3.2 DTA/TGA curves for kaolin

A well-defined endothermic DTA peak and sharp weight loss in the TGA curve appears between 550 °C and 600 °C. This loss results from the transition to the amorphous and more reactive metakaolin phase.

A mixture of kaolin and sodium hydroxide was calcined in a furnace at 650 °C during 140 minutes. The cooled mixture was grinded into powder. The used temperature and duration were based on the international patent.

3.1.6 Alkali activators

The alkaline liquid could be used to react with the silice (Si) and the aluminum (Al) in a source material of natural minerals or in by-product materials such as fly ash and rice-husk ash to produce binders (Davidovits, 1994). The alkaline activation of materials can be defined as a chemical process that provides a rapid change of some specific structures, partial or totally amorphous, into compact cemented frameworks (Fernandez and Palomo, 2003). The most used alkaline activators are a mixture of sodium or potassium hydroxide (NaOH, KOH) with sodium

water glass ($n\text{SiO}_2\text{Na}_2\text{O}$) or potassium water glass ($n\text{SiO}_2\text{K}_2\text{O}$) (Davidovits, 1994; Palomo et al., 1999; Vijaya Rangan, 2008). Thus, the activator solution consists of a hydroxide donor solution in water, typically sodium hydroxide or potassium hydroxide, and an additional source of amorphous silica, typically sodium silicate, as needed to approach the desired Silica: Alumina ratio.

3.1.6.1 Sodium hydroxide

Sodium hydroxide (NaOH), also known as lye and caustic soda, is an inorganic compound. It is a white solid and highly caustic metallic base and alkali salt. Sodium hydroxide in some particular applications is prepared solutions within water, ethanol and methanol (Material Safety Data Sheet, 2015). Dissolution of solid sodium hydroxide in water is a highly exothermic reaction which a large amount of heat liberated, posing a threat to safety through the possibility of splashing. The resulting solution is usually colorless and odorless with slippery feeling upon contact in common with other alkalis. Sodium hydroxide (12 M) was used.

3.1.6.2 Sodium silicate

Sodium silicate is known as water glass or liquid glass. These materials are available in aqueous solution and in solid form. In this research aqueous solution was used. Sodium silicate is readily soluble in water, producing an alkaline solution. It is one of a number of related compounds, which include sodium orthosilicate, Na_4SiO_4 , sodium pyrosilicate, $\text{Na}_6\text{Si}_2\text{O}_7$, and others. All the components are glassy, colorless and soluble in water (Greenwood, et al., 1997).

3.1.7 Foam agents

A blowing agent is a substance which is capable of producing a cellular structure via a foaming process in a variety of materials that undergo hardening or phase transition, such as polymers, plastics, and metals. They are typically applied when the blown material is in a liquid stage. The cellular structure in a matrix reduces density, increasing thermal and acoustic insulation, while increasing relative stiffness of the original polymer (IUPAC Compendium of Chemical Terminology, 2006).

3.1.7.1 Hydrogen peroxide

Hydrogen peroxide is often described as being “water but with one more oxygen atom. A description which can give the incorrect impression that there is a great deal of similarity between the two compounds. Pure hydrogen peroxide will explode if heated to boiling, will cause serious contact burns to the skin and can set materials alight on contact. For these reasons

it is usually handled as a dilute solution (household grades are typically 3-6%). Its chemistry is dominated by the nature of its unstable peroxide bond (Hill, 2001).

3.1.7.2 Sodium perborate

Sodium perborate (PBS) is a white, odorless, water-soluble chemical compound with the chemical formula NaBO_3 . It crystallizes as the monohydrate, $\text{NaBO}_3 \cdot \text{H}_2\text{O}$, trihydrate, $\text{NaBO}_3 \cdot 3\text{H}_2\text{O}$ and tetrahydrate, $\text{NaBO}_3 \cdot 4\text{H}_2\text{O}$ (Boron, 1994).

3.1.7.3 Aluminum powder

Aluminium (Al) powder is utilized to create bubbles in cementitious composites. It was introduced by adding 0.05-1% Al-powder as the initiated materials of geopolymers to react with water in those materials and promote hydrogen gas inside specimens. Aluminium powder contains elemental Si (silica fume, FeSi or SiC) (Keawpapasson et al., 2014).

3.2 Executed tests

The tests used in this research consist of mechanical tests, durability tests and micro-structure analysis are presented in full details. Samples were cured at an ambient temperature for 28 days and then tested. The results were obtained from the average of three tested samples.

3.2.1 Water absorption by immersion

Tests were performed on $100 \times 100 \times 100 \text{ mm}^3$ specimens. All the specimens were kept in an ambient temperature for 28 days before being tested. The obtained results were obtained from the average of 3 tested specimens. The specimens were immersed in water at room temperature for 24 hours. First, the weight of the specimens while suspended by a thin wire and completely submerged in water is recorded as W_{im} (immersed weight). After that, the specimens were removed from water, and placed for 1 min on a wire mesh allowing water to drain, then visible surface water was removed with a damp cloth and weight was recorded as W_{sat} (saturated weight). All specimens were placed in a ventilated oven at $105 \text{ }^\circ\text{C}$ for not less than 24 hours and allowing that two successive weights, at intervals of 2 hours, showed an increment of loss not greater than 0,1% of the last previously determined weight of the specimen. The weight of the dried specimens was recorded as W_{dry} (oven-dry weight). Absorption coefficient is determined as following equation:

$$A(\%) = \frac{W_{sat} - W_{dry}}{W_{sat} - W_{im}} \times 100 \quad (1)$$

3.2.2 Capillarity water absorption

The water absorption by capillarity test was done according to EN 1015-18:2002 using three specimens with $100 \times 100 \times 100 \text{ mm}^3$. The tests were performed by using 28 days cured samples. After being dried in the oven at $105 \text{ }^\circ\text{C}$ during 60 hours and then cooled in 24 h to achieve a constant moisture level. Four sides of the specimens were then sealed by paraffin to avoid evaporative effect as well as to maintain uniaxial water flow during the test, and two opposite faces were left unsealed. Before the specimens were located in water, their initial weight was recorded. One face of the specimen was in contact with water. The sorptivity coefficient can be calculated by the following expression:

$$S = \left(\frac{Q}{A}\right) / \sqrt{t} \quad (2)$$

Where S is the sorptivity ($\text{cm/s}^{1/2}$), Q is the volume of water absorbed (cm^3), A is the surface area in contact with water (cm^2) and t is the time (s). S was obtained from the slope of linear relationship between Q/A and \sqrt{t} .

3.2.3 Compressive strength

Compressive strength was approached based on NP EN 195-1:2004. In this way, in order to obtain compressive strength, three cubic specimens with dimensions of $50 \times 50 \times 50 \text{ mm}^3$ were tested. The compressive load was applied to the cubic specimens with pace of 0.36 to 0.72 N/s. mm^2 . Selection of the speed rate was based on the duration of the test. If a test was feasible at a speed rate of 0.36 N/s. mm^2 in 30-90 seconds, the pace was considered acceptable; but, if this pace implied a longer time frame, the pace had to be increased up to 0.72 N/s. mm^2 . The specimens were cured 28 days before the test.

3.2.4 Chloride diffusion

The chloride ion diffusion coefficient was carried out following the specification LNEC 463. In this test the penetration depth of chloride ions through 50 mm thick cylindrical slices (100 mm nominal diameter) with 28 days of curing at an ambient temperature is assessed. The cylindrical slices with 50 mm thickness cut through using wet sawing. A potential electric difference of $30 \pm 0.2 \text{ V}$ is maintained across the specimens. One face is immersed in a solution with sodium chloride and sodium hydroxide, and the other in a sodium hydroxide solution. After the migration of chloride ions the penetration depth is measured by splitting the specimens. The surface of the split mortar is then spread with silver nitrate (NO_3Ag) solution and the penetration depth is measured by difference in the colour.

The chloride diffusion coefficient can be calculated using the following equation:

$$D_{nssm} = \frac{0.0239 (273+T)L}{(U-2)t} (x_d - 0.0238 \sqrt{\frac{(273+T)Lx_d}{U-2}}) \quad (3)$$

where D_{nssm} is non-steady-state migration coefficient, $\times 10^{-12} \text{ m}^2/\text{s}$; U : absolute value of the applied voltage (V); T : average value of the initial and final temperature in the anolyte solution ($^{\circ}\text{C}$); L : Thickness of the specimen (mm); X_d : Average value of the penetration depth (mm).

3.2.5 Carbonation resistance

The lateral surface of the three specimens were covered by paraffin before being placed in carbonation chamber box. The carbonation resistance test was performed with the following conditions of temperature, relative humidity (RH) and CO_2 concentration: 20°C , 55% and 4%, respectively. The specimens were taken out from the carbonation chamber and split in a tensile test. The split surfaces were cleaned and sprayed with a phenolphthalein pH indicator. The indicator used was a phenolphthalein 1% ethanol solution with 1 g phenolphthalein and 90 ml 95.0 V/V% ethanol diluted in water to 100 ml. In the noncarbonated part of the specimen, where the mortar was still highly alkaline, a purple-red colour was obtained. In the carbonated part of the specimen where the alkalinity of mortar is reduced, no coloration occurred. The average depth of the colourless phenolphthalein region was measured in twenty points, perpendicular to the two edges of the split face.

3.2.6 Resistance to acid attack

The resistance to acid attack was carried out using cubic specimens with $50 \times 50 \times 50 \text{ mm}^3$. Before being immersed in a solution containing 10% sulphuric acid (H_2SO_4) the weight of the water saturated specimens were assessed. The weights of specimens were assessed again after 7, 14, 28 and 56 days after immersion in the acid solution. The appearances of specimens were also observed.

3.2.7 Bulk density

Bulk density was assessed according to ASTM C373-78:2014 and calculated through given equations (4) and (5):

$$v = \frac{(M_{Sat} - M_{imm})}{\rho_w} \quad (4)$$

$$\rho_{Bulk} = \frac{M_{Dry}}{v} \quad (5)$$

where, M_{sat} , M_{imm} , and M_{Dry} are weight of specimens in case of saturation, immersion and dry, respectively. Additionally, ρ_w is representing water density.

3.2.8 Thermal conductivity

Thermal conductivity was assessed utilizing an Alambeta instrument developed at the Technical University of Liberec, Czech Republic (Fig 3.3). This computer controlled instrument, called ALAMBETA, works in the semi-automatic regime, calculates all measurement statistic parameters and exhibits the instrument auto diagnostics. These diagnostics include checking measurement precision and avoiding any faulty instrument operation. The instrument measures the behavior of heat flowing through the foam geopolymer mortars due to the different temperatures of the lower measuring body and the heated measuring head. During the measurements, the initial temperature of the samples and the relative humidity were in the range of 22 to 24°C and 55 to 65%, respectively. To investigate the effect of the temperature drop on the thermal properties of the samples, the temperature of the measuring head at first was 10 °C higher than the environmental temperature. During the second set of measurements, the measuring head was 40 °C higher than the base plate.



Fig 3.3 Alambeta device

3.2.9 XRD

To assess the crystalline structure of these mixtures, X-ray diffraction (XRD) analysis were employed. Powder X-ray diffraction (XRD) was implemented on a Bruker D8 Discover with Cu-K α radiation ($\lambda=1,54060\text{\AA}$) at 40 kV and 40 mA. Each sample was scanned from 5° to 70° at a speed of 0,4°/s. The analysis for phase identification was performed using analytical software EVA (Fig 3.4).

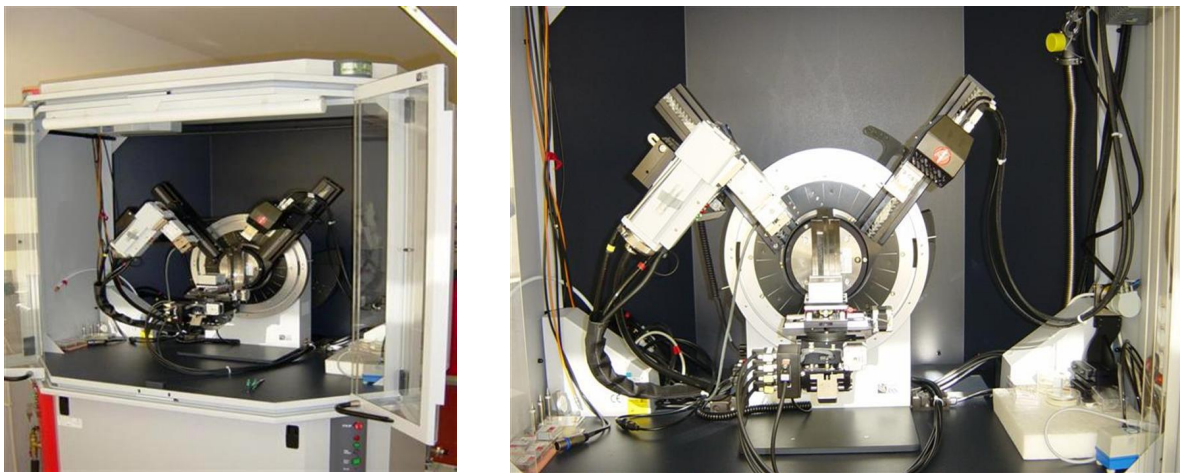


Fig 3.4 Machine used to obtain XRD results

3.2.10 SEM/EDS

For examination through scanning electron microscopy (SEM), the samples were covered with 40 nm film of Au-Pd (80-20 weight %); in a high resolution sputter coater, 208HR Cressington Company, coupled to a MTM-20 Cressington High Resolution Thickness Controller. Ultra-high resolution Field Emission Gun Scanning Electron Microscopy (FEG-SEM), NOVA 200 Nano SEM and FEI Company were also used. Backscattering Electron images were achieved through an acceleration voltage of 15 kV. Chemical analyses of samples were performed with the Energy Dispersive Spectroscopy (EDS) technique, using an EDAX Si (Li) detector with an acceleration voltage of 20 kV (Fig 3.5).



Fig 3.5. Machine used to take SEM images

3.2.11 FTIR

The FTIR spectra were acquired in the attenuated total reflectance mode (ATR), between 4000 and 550 cm^{-1} , using a Perkin Elmer FTIR Spectrum BX with an ATR PIKE MIRacle. Specimens for FTIR study were prepared by mixing 1 mg of sample in 100 mg of KBr as suggested by Zhang et al. (1996). Spectral analysis was performed over the range 4000–400 cm^{-1} at a resolution of 4 cm^{-1} (Fig 3.6).

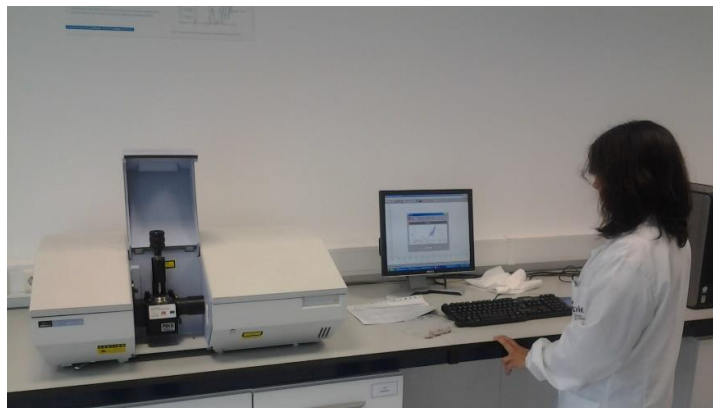


Fig 3.6. Device employed to obtain FTIR spectra

CHAPTER FOUR
Mechanical Properties, Microstructure and Durability

4.1 Mechanical properties

After obtaining suitable values of materials for mortar, different specimens will be made with different mixtures and the properties of the fresh and hardened mortar will be evaluated.

Mechanical properties and durability of hardened mortar will be assessed according to relevant standards such as ASTM and EN. Based on the results of the primary tests, new mixtures will be selected for assessment and the effect of constituent proportions will be evaluated.

The SEM observations on these mixtures are also presented. The mixtures under investigation were based on the ones described in the international patent authored by Zheng et al. (2007).

4.1.1 Mix design

Table 4.1 and 4.2 shows the mix proportion respectively used in phases A and B. In the mixes 7 up to 12, potassium hydroxide were used instead of sodium hydroxide.

Table 4.1 Mix proportions used in phase A

Mix	Calcined stuff**/Powder	Fly ash/ Powder	OPC/ Powder *	Ca(OH) ₂ / Powder	Water/ Powder	Sand/ Powder	SP/ OPC
1-A	4 %	32.5 %	30 %	33.5%	31%	-----	-----
2-A	4 %	58.3 %	30 %	7.7 %	26%	-----	-----
3-A	4 %	58.3 %	30 %	7.7 %	34%	-----	-----
4-A	4 %	32.5 %	30 %	33.5 %	52%	80%	-----
5-A	4 %	32.5 %	30 %	33.5 %	52%		-----
6-A	4 %	58.3 %	30 %	7.7 %	31%		-----
7-A	4 %	58.3 %	30 %	7.7 %	40%		-----
8-A	4 %	58.3 %	30 %	7.7 %	35%		0.8%
9-A	4 %	32.5 %	30 %	33.5 %	37%		1.3%
10-A	4 %	32.5 %	30 %	33.5 %	35%		2.5%
11-A	4 %	32.5 %	30 %	33.5 %	31%		2.4%
12-A	4 %	32.5 %	30 %	33.5 %	36%		1.5 %

*Powder: OPC + Fly ash + Ca(OH)₂ + Calcined stuff

**Calcined stuff has been prepared by mixing kaolin and sodium hydroxide with 2.5/1 ratio.

Table 4.2 Mix proportions used in phase B

Mix	Calcined stuff**/Powder	Fly ash/ Powder	OPC/ Powder *	Ca(OH) ₂ / Powder	Water/ Powder	Sand/ Powder	SP/ OPC
1-B	3.0%	33%	32.2%	33.5%	35%	80%	2.7%
2-B	3.0%	33%	32.2%	31.6%	35%		2.3%
3-B	4%	32%	30%	33.5%	35%		1.5
4-B	4%	32.5%	30%	33.5%	39%		1.5%
5-B	3.2%	60%	30%	6.8%	35%		1.0%
6-B	4%	32.5%	30%	33.5%	34%		1.0%
7-B	4%	58.3%	30%	7.7%	30%		0.5%
8-B	4%	32.5%	30%	33.5%	35%	85%	1%
9-B	4%	58.3%	30%	7.7%	35%		1%
10-B	4%	32.0%	30%	33.0%	30%		1%
11-B	5%	32.0%	40%	23.0%	35%		1%
12-B	5%	32.0%	30%	34.5%	35%		1%

*Powder: OPC + Fly ash + Ca(OH)₂ + Calcined stuff

*Calcined stuff has been prepared by mixing kaolin and sodium hydroxide with 2.5/1 ratio.

The initial phases were meant to find out the mixtures with the highest compressive strength. Phases C (Table 4.3 and 4.4) and D (Tables 4.5 and 4.6) were meant to evaluate the influence of aggregate and calcium hydroxide. Tests were performed on 50×50×50 mm³ mortar specimens according to ASTM C109.

Table 4.3 Mix proportions used in phase C

Mix	Calcined stuff**/Powder	Fly ash/ Powder	OPC/Powder *	Ca(OH) ₂ / Powder	Water/ Powder	Sand/ Powder	SP/ OPC
1-C	5 %	32.0%	40 %	23.0%	34%	80%	3%
2-C					34%		2%
3-C					29%		2%
4-C					30%		3%

*Powder: OPC + Fly ash + Ca(OH)₂ + Calcined stuff

*Calcined stuff has been prepared by mixing kaolin and sodium hydroxide with 2.5/1 ratio.

Table 4.4 Phase C-Volumetric ratios

Vs/Vp	Vw/Vp	Vsp/Vp
1	0.77	0.023
0.95	0.77	0.023
0.9	0.77	0.023
0.85	0.77	0.023

-Vs/Vp=Sand volume/powder volume

- V_w/V_p =Water volume/powder volume

- V_{sp}/V_p =Superplasticizer volume/powder volume

Table 4.5 Mix proportions used in phase D

Mix	Calcined stuff**/Powder	Fly ash/Powder	OPC/Powder *	Ca(OH) ₂ /Powder	Water/Powder	Sand/Powder	SP/OPC
1-D	5%	32.0 %	40 %	21.0%	29%	80%	2%
2-D				24.0 %			1%
3-D				27.0 %			1%
4-D				19.0%			4%

*Powder: OPC + Fly ash + Ca(OH)₂ + Calcined stuff

*Calcined stuff has been prepared by mixing kaolin and sodium hydroxide with 2.5/1 ratio.

Table 4.6 Phase D-Weight ratios

WCa/Wc	WCs/Wc	WFA/Wc	WSP/Wc
0.45	0.12	0.79	0.01
0.5	0.12	0.79	0.01
0.65	0.12	0.79	0.01
0.7	0.12	0.79	0.01

-Ca= Calcium hydroxide

-SP= Superplasticizer

-Cs= Calcined stuff

-FA=Fly ash

- C=Cement

4.1.2 Results and discussions

The obtained results from casted samples in part A, B, C, and D under compression will be evaluated in this section.

Fig. 4.1 shows the compressive strength of the mixtures tested in Phase A. The results show that the most promising mixture (8A) has a compressive strength around 27 MPa after 28 days curing.

This mixture also has the eco-efficient advantage of containing a high content of an industrial by-product. The mixture 2A shows a high compressive strength performance which is due to a low w/b ratio. The results also show that the curing days increase the compressive strength.

This is a behaviour that is not observed in two part alkali-activated cements in which the compressive strength just after one day can reach 50% to 70% of the compressive strength after 28 days curing (Pacheco-Torgal et al, 2007). However, while this behaviour is most evident for

mixture 8A, the one with the highest compressive strength at 14 days and at 28 days is not so evident for mixture 4A which as a lower fly ash content and a higher w/b. The use of a w/b=0.52 leads to compressive strength results below 12 MPa after 28 days curing which is a very modest performance unsuitable to be used in future applications. The mixture with the lowest 1 day compressive strength (6A) is of difficult explanation because it has the same composition of the mixture with the highest 28 days compressive strength with the exception of the w/b content which is lower.

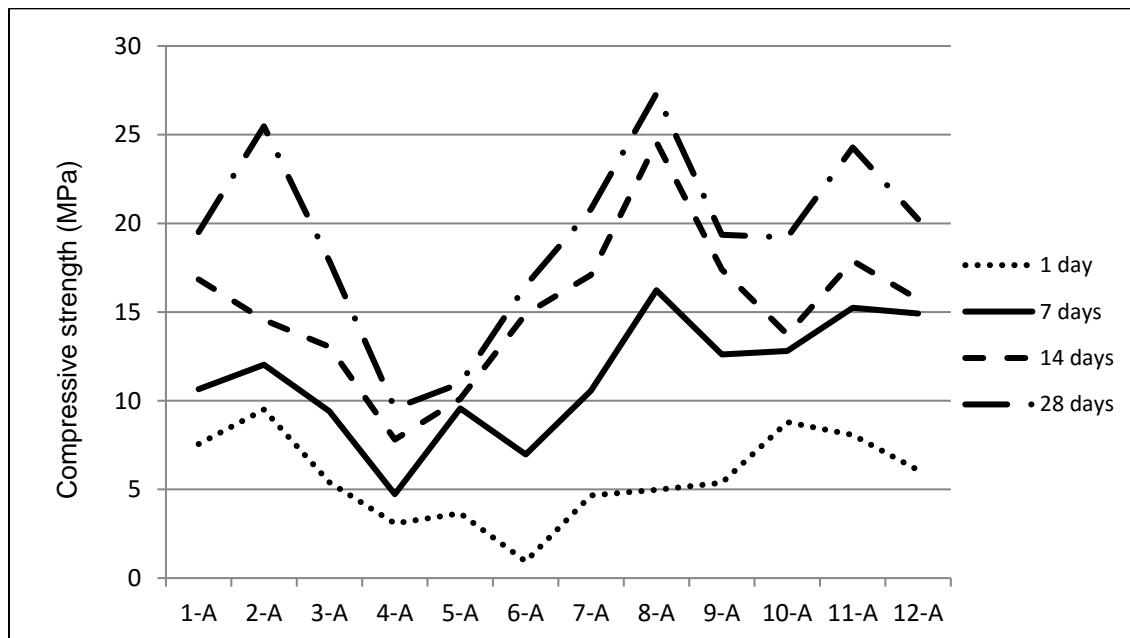


Fig. 4.1 Variation of compressive strength with composition and curing days (Phase A)

Mixtures based on calcined kaolin and sodium hydroxide revealed lower reactivity than the mixtures in which this last constituent was replaced by potassium hydroxide. This confirms the results obtained by other authors (Xu and Van Deventer, 2000; Diamond, 1976) who also found that geopolymers based on several alumino-silicate minerals had a high compressive strength in KOH than in NaOH. This fact is however independent of the extent of dissolution, being that those minerals show a higher dissolution when NaOH is used. Fig. 4.2 shows the compressive strength of the mixtures test in Phase B. The results indicate that a higher compressive strength mixture was obtained (11B) reaching 30 MPa after 28 days curing. Environmentally speaking since this mixture has more 10% OPC and more 15% of calcium hydroxide this mixture does seem as eco-efficient as the previous mixture 8A. An interesting behaviour can be observed when comparing the mixture 11B with mixture 10B.

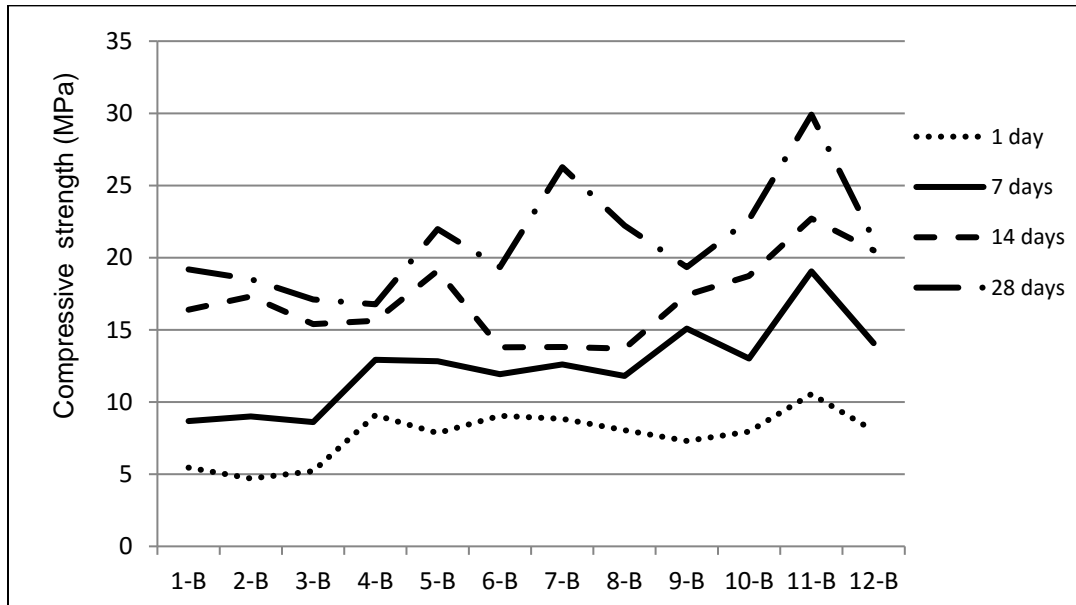


Fig. 4.2 Variation of compressive strength with composition and curing days (Phase B)

The differences between the two are the fact that mixture 10B includes less 10% of OPC but more 10% in calcium hydroxide and also has a low w/b. As a consequence its compressive strength after 28 days curing is almost 10 MPa apart from mixture 11B. And probably if the w/b was the same the compressive strength difference could be even higher. This shows the existence of very reactive constituents existing in OPC. Again the mixtures where sodium hydroxide was replaced by potassium hydroxide show a higher compressive strength. Fig. 4.3 shows the compressive strength of the mixtures tested in Phase C.

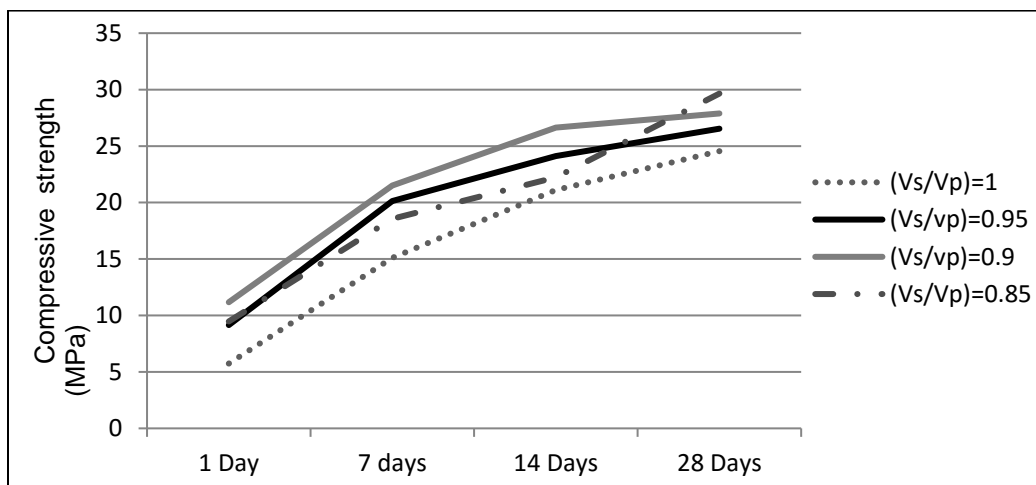


Fig. 4.3 Variation of compressive strength with the sand content and curing days (Mixture 11B)

In this phase the mixture 11B was used as reference in order to evaluate the compressive strength variation due to aggregate content. V_s relates to the volume of sand and V_p for the volume of powder (OPC, FA, Kaolin, Potassium hydroxide and $\text{Ca}(\text{OH})_2$). Increasing the sand content leads to lower compressive strength because the w/b ratio has also increased in order to maintain the workability. Fig. 4.4 shows the compressive strength of the mixtures tested in Phase D. In this phase the mixture 11B was used as reference in order to evaluate the compressive strength variation due to calcium hydroxide content. The calcium hydroxide is presented as a function of the Portland cement percentage.

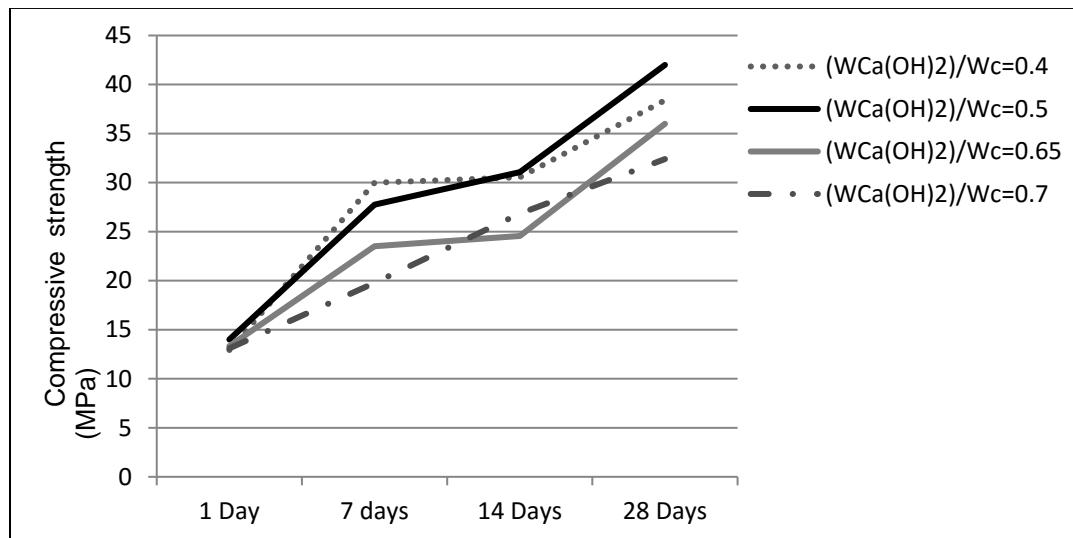


Fig. 4.4 Variation of compressive strength with the $\text{Ca}(\text{OH})_2$ content and curing days (Mixture 11B)

The results show that there is not a direct linear relationship between the calcium hydroxide content and the compressive strength. The use of calcium hydroxide as much as 50% of Portland cement leads to the highest compressive strength. Increasing the $\text{Ca}(\text{OH})_2$ percentage beyond that percentage can lead to a decrease in the compressive strength. Concerning the efflorescences no relevant presence was observed. This confirmed the observations included in the international related patent.

4.2 Compressive strength modelling

Arshad and Maaroufi (2015) recently applied the Johnson–Mehl–Avrami–Kolmogorov (JMAK) model to the kinetics of crystallization in amorphous materials. Therefore this section discloses results regarding the modelling the compressive strength of one part-geopolymers with the JMAK model.

Table 4.7 shows the compositions of the one part geopolymer mixtures used in the present study. After demoulding, the specimens were submitted for a thermal treatment during 24 h at different temperatures (40°C, 60°C and 80°C). The specimens were also placed in the chamber room, with relative humidity of 58 %, during the curing time.

Table 4.7- Composition of one part geopolymer mixes used for modeling compressive strength

Mix	OPC/Powder*	Fly ash/ Powder	Ca(OH) ₂ / Powder	Calcined stuff**/Powder	Sand/ Powder	SP/ OPC	Water/ Powder
OPC 30-FL 58.3-CH 7.7-CS 4	30%	58.3%	7.7%	4%	80%	0.08%	35%
OPC 26-FL 58.3-CH 7.7-CS 8	26%			8%			
OPC 18-FL 58.3-CH 7.7-CS 16	18%			16%			

*Powder: OPC + Fly ash + Ca(OH)₂ + Calcined stuff

**Calcined stuff has been prepared by mixing kaolin and sodium hydroxide with 2.5/1 ratio.

Figure 4.5 shows compressive strengths of one part geopolymers according to curing time. It also includes the predicted values according to the JMAK model. The equation of this model is as follows:

$$f(t) = 1 - \exp(-kt^n) \quad (1)$$

Where f(t) is degree of reaction, t is time of reaction, k is a constant and n is the exponent.

According to Fig. 4.5 the degree of reaction in cementitious systems is related directly to compressive strength. Therefore, Eq. (1) can be adopted for compressive strength of geopolymers as follows:

$$f_c = \alpha(1 - \exp(-kt^n)) \quad (2)$$

where f_c is the compressive strength and α is a constant. Eq. (1) is solved for degree of reaction varying between 0 and 1. In Eq. (2), f_c is greater than 1 and hence for our case where strengths are below 100MPa, we divide the strengths by 100. This normalized number can be included in the constant α . For specimens with higher strengths, one can divide them by a reference number. To determine k and n , Eq. (3) can be written in the following form:

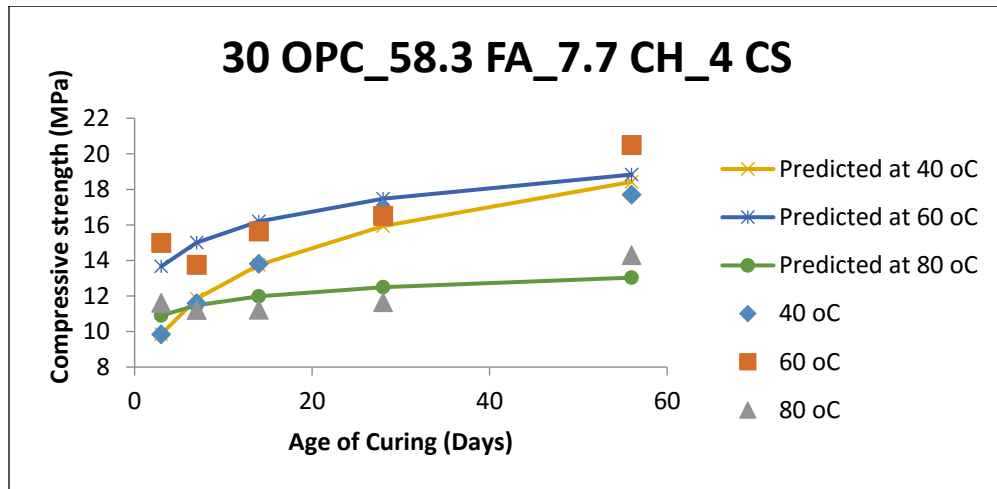
$$\ln(-\ln(1 - f_c)) = \ln(k) + n \ln(t) \quad (3)$$

k and n can be easily found from intercept and slope of the line plotted in the form of $\ln(1 - \ln(1 - f_c))$ versus $\ln t$ respectively. These lines for the whole considered geopolymeric systems considered in this study have been plotted in Fig. 4.5. Calculated k and n and their corresponding equations have been given in Table 4.8. The predicted compressive strengths for one part geopolymeric mixtures was presented in Fig. 4.6 The results are influenced not only by the one part geopolymer mixture but also by the temperature treatment.

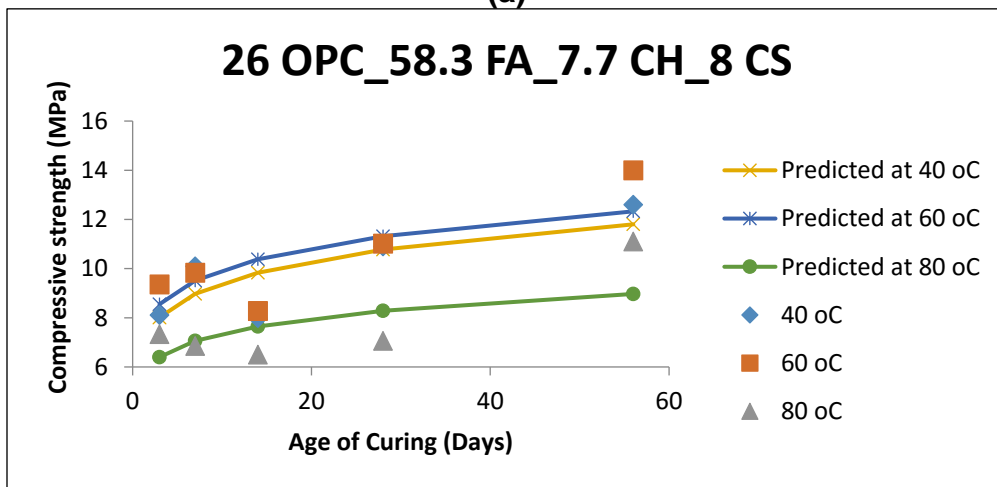
Compressive strength evolution vs. time plotted in logarithmic scale is presented in Fig. 4.7 The results are influenced not only by the one part geopolymer mixture but also by the temperature treatment. Traditional J shape diagrams were found only for 30-OPC-58.3FA_7.7CH_4CS treated at 40 °C.

Table 4.8 Constant, exponent and equation of compressive strength evolution for one part geopolymers

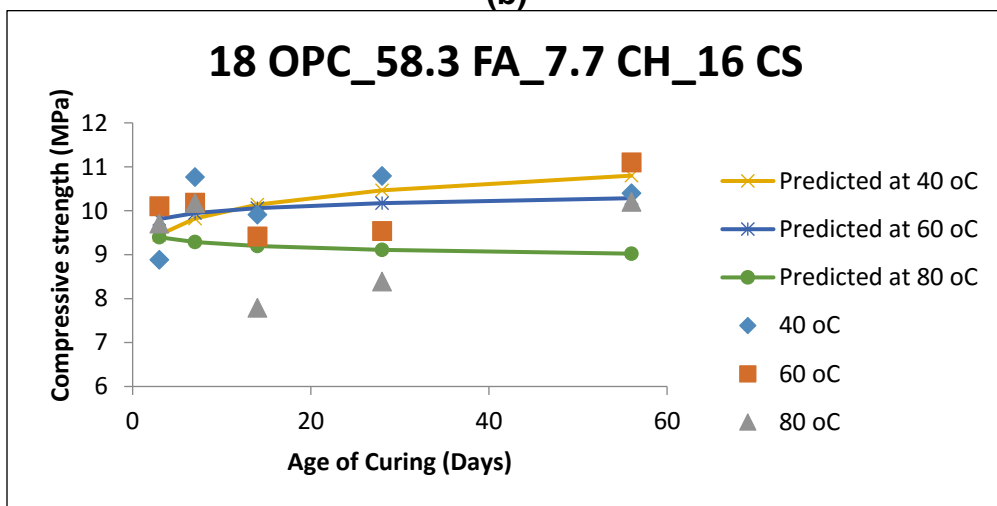
Curing temperature (°C)	30 OPC_58.3 FA_7.7 CH_4 CS			26 OPC_58.3 FA_7.7 CH_8 CS			26 OPC_58.3 FA_7.7 CH_16 CS		
	<i>k</i>	<i>n</i>	Equation	<i>k</i>	<i>n</i>	Equation	<i>k</i>	<i>n</i>	Equation
40	0.0805	0.2305	$f_c = 100[1 - e^{-0.0805t^{0.2305}}]$	0.0717	0.1393	$f_c = 100[1 - e^{-0.07178t^{0.1393}}]$	0.0942	0.0481	$f_c = 100[1 - e^{-0.0942t^{0.0481}}]$
60	0.1288	0.1198	$f_c = 100[1 - e^{-0.1288t^{0.1198}}]$	0.0773	0.1321	$f_c = 100[1 - e^{-0.0773t^{0.1321}}]$	0.1014	0.017	$f_c = 100[1 - e^{-0.1014t^{0.017}}]$
80	0.1075	0.0651	$f_c = 100[1 - e^{-0.1075t^{0.0651}}]$	0.0580	0.1201	$f_c = 100[1 - e^{-0.085t^{0.1201}}]$	0.1002	0.0145	$f_c = 100[1 - e^{-0.1002t^{-0.0145}}]$



(a)

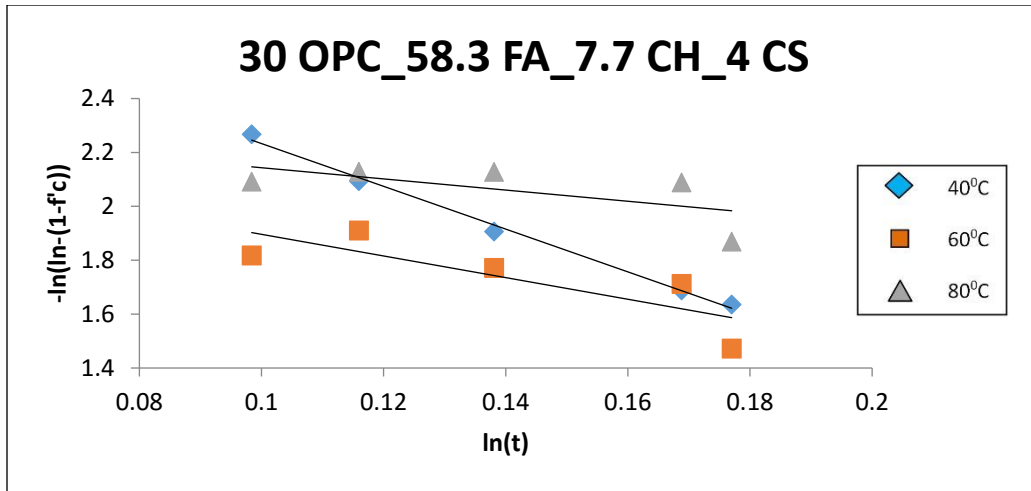


(b)

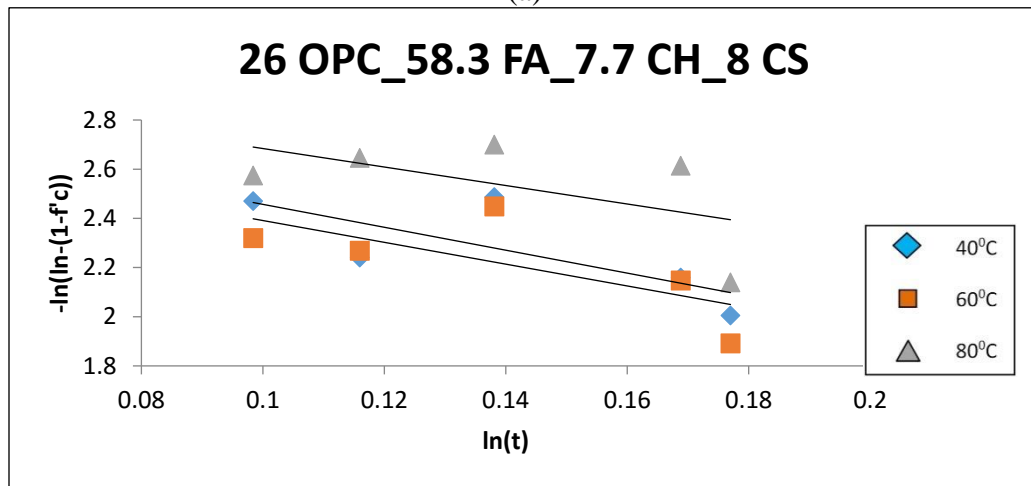


(c)

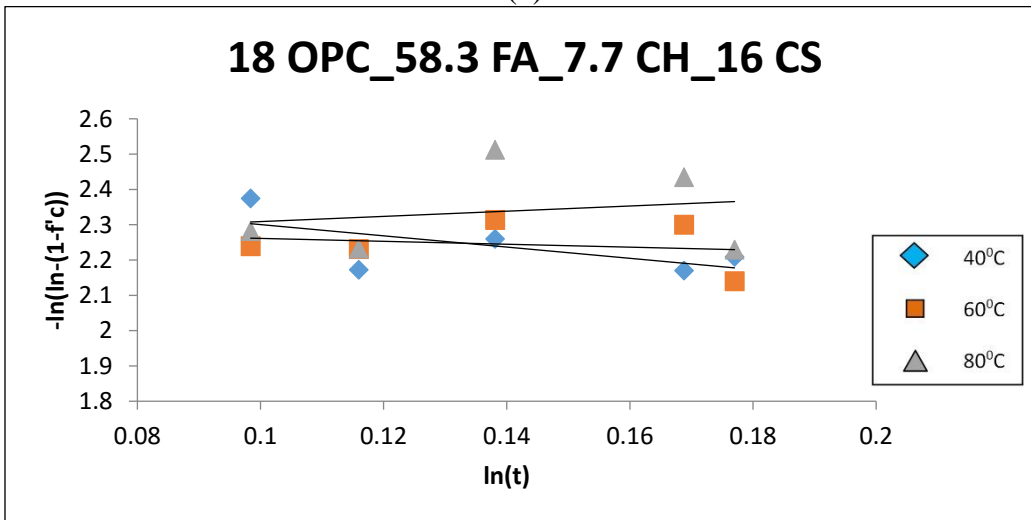
Figure 4.5. Experimental and predicted compressive strength of mixtures a) 30 OPC_58.3 FA_7.7 CH_4 CS, b) 26 OPC_58.3 FA_7.7 CH_8 CS and c) 18 OPC_58.3 FA_7.7 CH_16CS



(a)

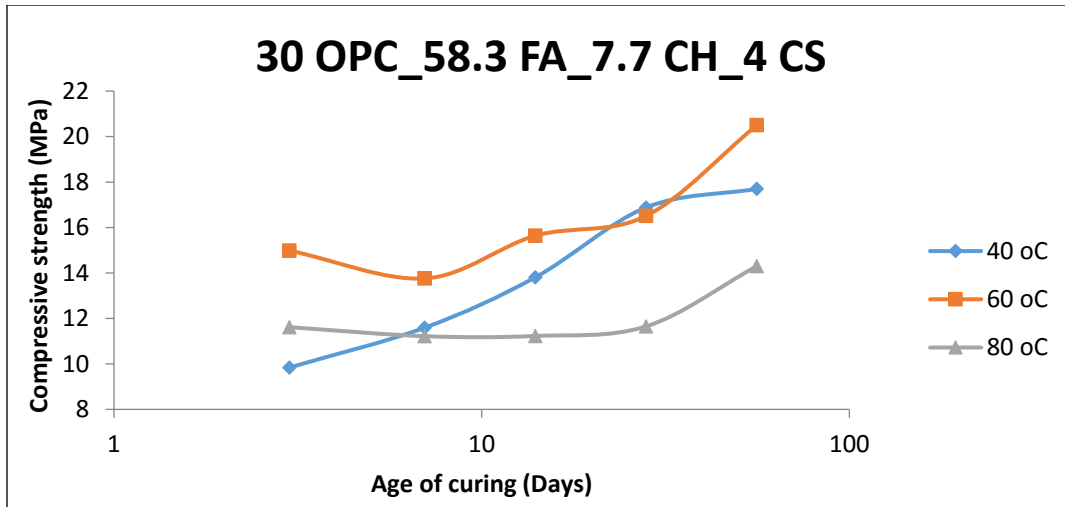


(b)

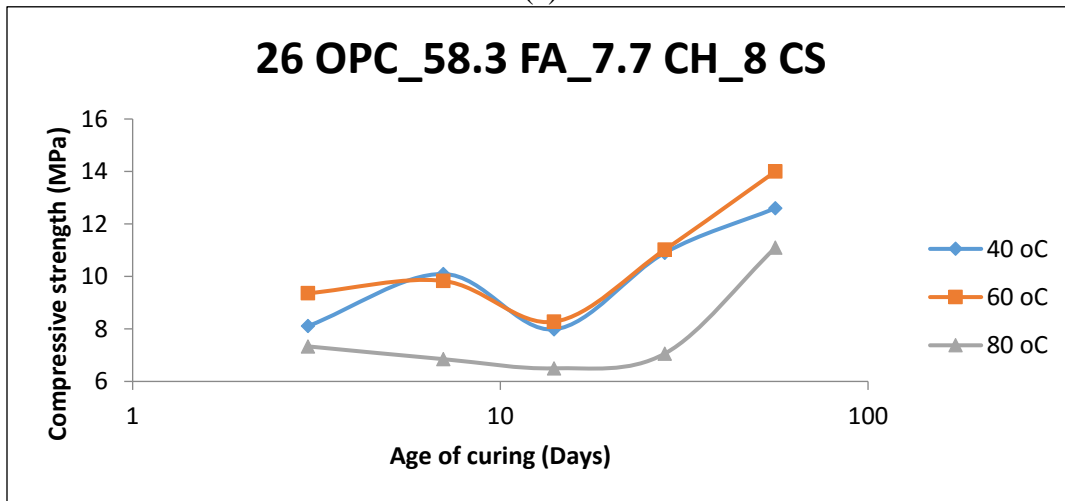


(c)

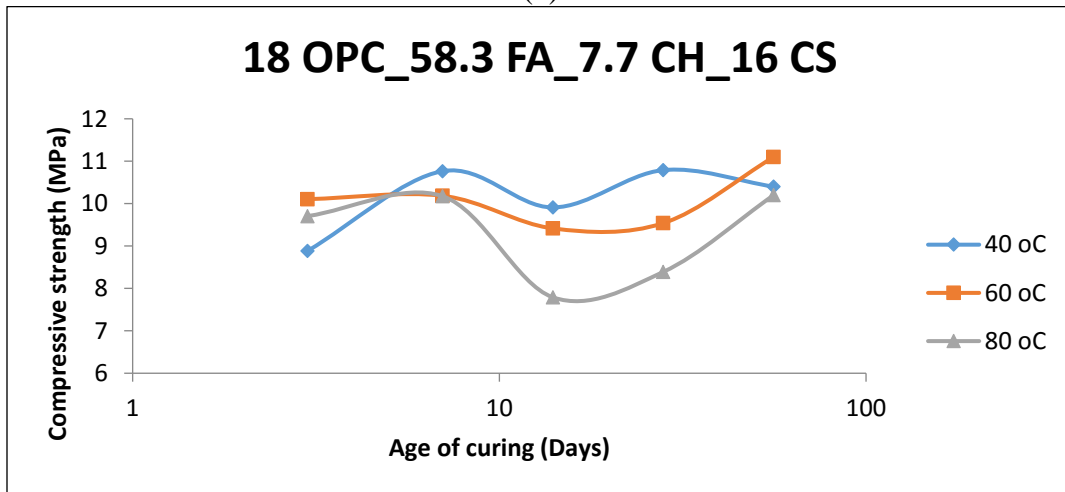
Figure 4.6. Plots for determining k and n in a) 30 OPC_58.3 FA_7.7 CH_4 CS, b) 26 OPC_58.3 FA_7.7 CH_8 CS and c) 18 OPC_58.3 FA_7.7 CH_16CS



(a)



(b)



(c)

Figure 4.7. Compressive strength a) 30 OPC_58.3 FA_7.7 CH_4 CS, b) 26 OPC_58.3 FA_7.7 CH_8 CS and c) 18 OPC_58.3 FA_7.7 CH_16CS in logarithmic scale

4.3 Microstructure

The results of Scanning Electron Microscopy (SEM) and chemical analyses of samples which were performed with the Energy Dispersive Spectroscopy (EDS) technique will be discussed in the following paragraphs.

4.3.1 SEM

Figs. 4.8 and 4.9 shows two SEM micrographs taken from 28 days cured specimens. In contrast with the porous typical interfacial transition zone of Portland cement mixtures, one part geopolymers present a very dense and uniform ITZ.

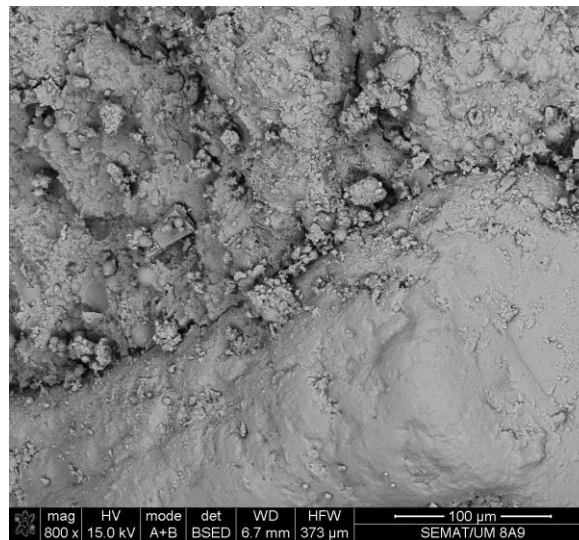


Fig. 4.8 SEM micrograph of interfacial transition zone

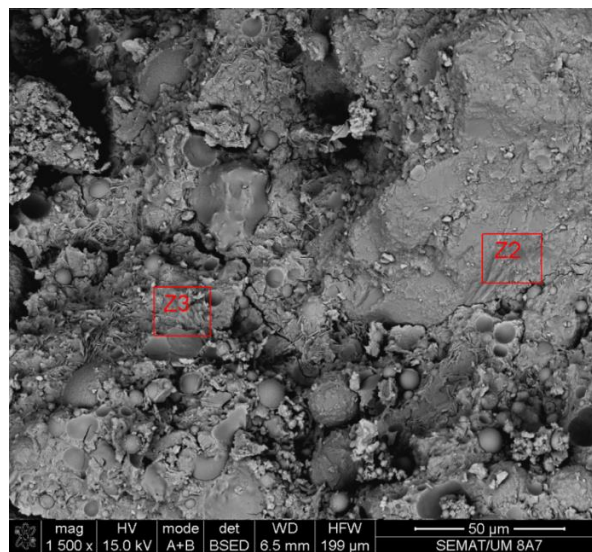


Fig. 4.9 SEM micrograph of hybrid alkaline cement mortar

4.3.2 EDS analysis

The molar ratios of the analyses carried out by EDS are displayed in table 4.9 and 4.10.

Table 4.9 Phase D-Weight ratios

WCa(OH)₂/Wc	WCa/Wc	WFA/Wc	WSP/Wc
0.45	0.12	0.79	0.01
0.5	0.12	0.79	0.01
0.65	0.12	0.79	0.01
0.7	0.12	0.79	0.01

Table 4.10 EDS Atomic ratio analysis

Atomic ratio	Zone	
	Z2	Z3
SiO₂/Al₂O₃	25.6	2.89
Al₂O₃/ Na₂O	2.15	5.44
CaO / SiO₂	0.13	0.5
Na₂O / CaO	0.13	0.12
MgO/Al₂O₃	-	0.15

Typical C/S ratios in CSH of traditional OPC systems go between 1.5 to 2.0 (Diamond, 1976; Richardson, 2000). However, the areas Z2 and Z3, have a much lower C/S ratio which means it has some sodium replacing Ca²⁺ in CSH. Some authors have already demonstrated that sodium incorporation in CSH phase increased as C/S ratio decreases, and therefore they name it as Na-C-S-H (Macphee, 1989). The areas marked as Z2 and Z3 are identified as some form of calcium silicate with traces of some sodium and aluminum in its composition which could be associated to a (N, C)-A-S-H gel. According to Garcia-Lodeiro et al. (2013), these gels usually evolve into compositions with higher calcium and lower aluminum content. Those authors also mention that this is a blank field and that almost nothing has been published concerning the interaction between aluminosilicate materials containing sodium (or potassium or sulphates) in the formation of N-A-S-H or K-A-S-H type cementitious gels.

4.4 FTIR

The FTIR spectra are presented in Fig. 4.10. The mix compositions are presented in Table 4.11. The strong peak band 965 cm⁻¹ is characterized as asymmetric Si-O-Si or Al-O-Si stretching,

which is typical of the polymerization of the silicate group with the formation of CSH (Garcia Lodeiro et al., 2008; Garcia Lodeiro et al., 2009).

A shift to a high wave number occurs when the different spectra are compared. Usually this indicates an increase in the Si content of the gel.

The carbonate bands C-O at around 1415 cm^{-1} and 850 cm^{-1} arise from the reactions of atmospheric CO_2 with calcium hydroxide. This peak intensity changes with the amount of calcium hydroxide.

The broad bands in the region of $1648\text{--}3000\text{ cm}^{-1}$ characterized the spectrum of stretching and deformation vibrations of O-H and H-O-H groups from the weakly bound water molecules.

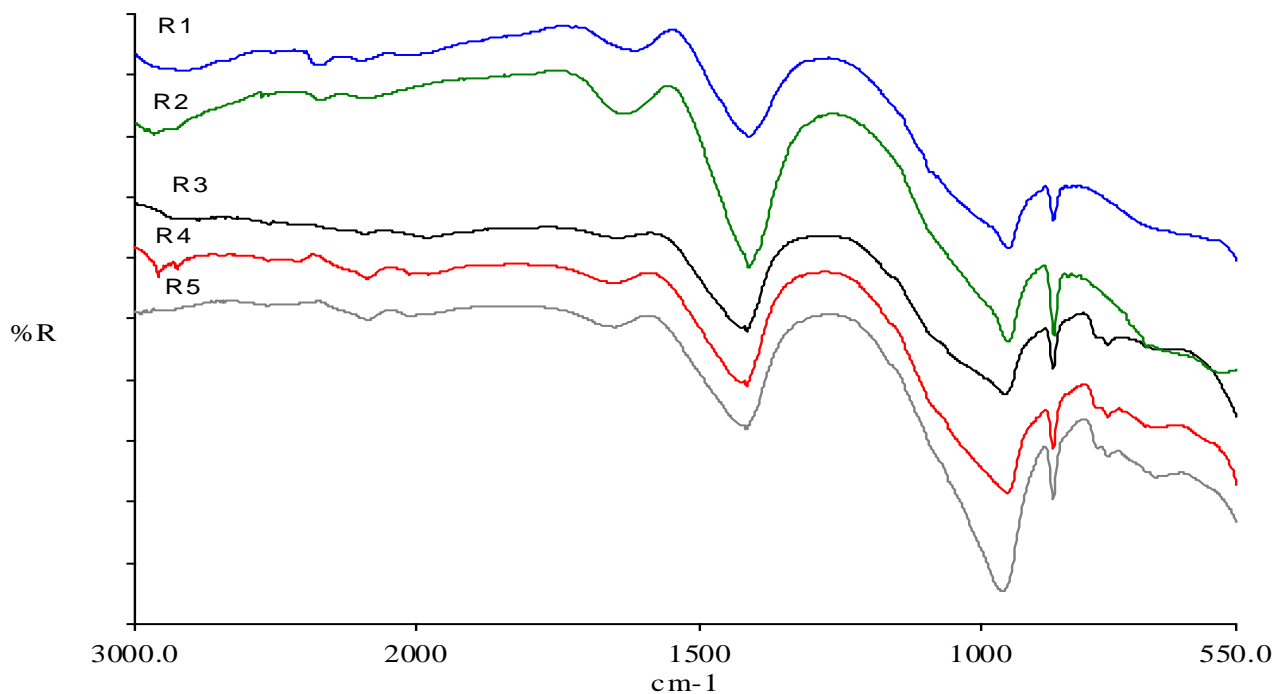


Fig. 4.10 FTIR spectra

4.5 Mix proportioning

For the further investigations by utilizing the obtained results in the previous step 4, new mixes are added in this phase. In addition to the 4 new mixes, one has been selected from the previous part. Based on what were concluded until now, the research will be continued by testing the 5 mixes for obtaining higher compressive results and a high eco-efficient performance. To expand the obtained results, durability tests will also be performed. The compositions of the dry mixes contain the following materials: kaolin, fly ash, ordinary Portland cement (OPC), sodium hydroxide, calcium hydroxide ($\text{Ca}(\text{OH})_2$), water and superplasticizer. These are adapted from the ones presented in the international patent WO 2007/109862 A1 (Zheng et al, 2007).

Table 4.11 Mix composition

Mix	OPC/ Powder*	Fly ash/ Powder	Ca(OH) ₂ / Powder	Calcined stuff**/ Powder	Sand/ Powder	SP/ OPC	Water/ Powder
OPC 100 (R ₁)	100	-	-	-	0.8	0.08	0.35
OPC 70 – FL 30 (R ₂)	70	30	-	-			
OPC 30-FL 58.3-CH 7.7-CS 4 (R ₃)	30	58.3	7.7	4			
OPC 26-FL 58.3-CH 7.7-CS 8 (R ₄)	26	58.3	7.7	8			
OPC 18-FL 58.3-CH 7.7-CS 16 (R ₅)	18	58.3	7.7	16			

*Powder: OPC + Fly ash + $\text{Ca}(\text{OH})_2$ + Calcined stuff

**Calcined stuff has been prepared by mixing kaolin and sodium hydroxide with 2.5/1 ratio.

4.5.1 Compressive strength

Fig. 4.11 shows the compressive strength results. The reduction of OPC content leads to a high reduction on the compressive strength of the mortars. The slow hydration characteristics of fly ash contribute to explain that reduction. The mixture with just 30% OPC (and 58.3 fly ash, 7.7 calcium hydroxide and 4% calcined stuff) shows an almost 40% reduction in compressive strength when compared to the reference mixture. Since this mixture has a higher percentage reduction on OPC content this could mean that the addition of fly ash and calcined stuff could have compensated that reduction. However, the use of increase content in calcined stuff does not seem to compensate the OPC reduction. Thus meaning that the use of 4% calcined stuff seems to be an optimum content.

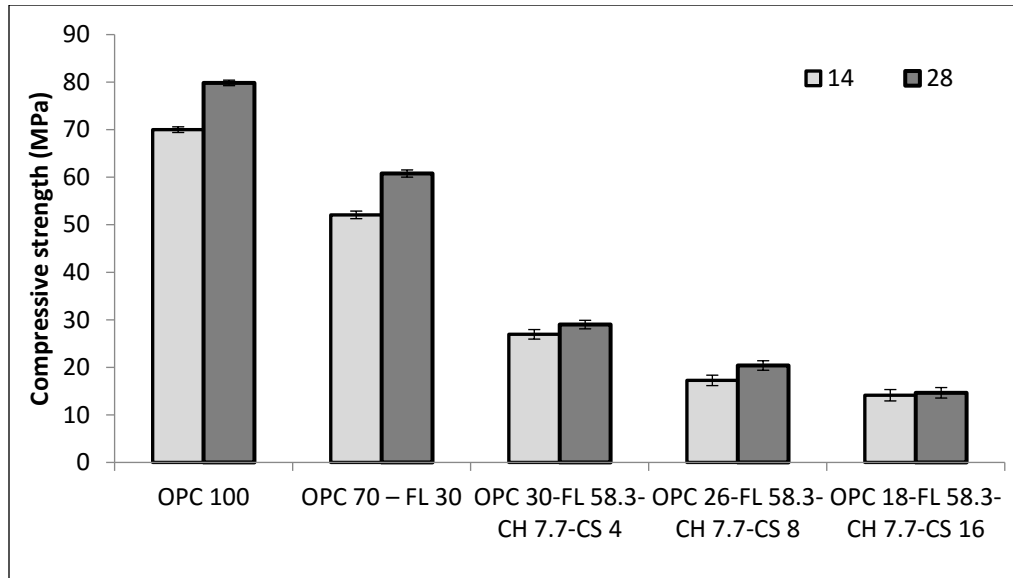


Fig. 4.11 Variation of compressive strength with composition and curing age.

4.6 Durability

Experimental results will be continued on the durability performance of one-part geopolymers concerning penetration of chloride, carbonation resistance and resistance to acid attack.

4.6.1 Efflorescences

Concerning the occurrence of efflorescences, no presence was observed. This confirmed the observations included in the international related patent. The explanations for that can be related to the low amount of (sodium/potassium) as well as to the fact that some sodium/potassium replaced Ca^{2+} in CSH hydration products. Another factor that influences efflorescences is pore volume and permeability. In Portland cement, the water participates in the hydration products so, as the hydration progresses, the pore volume decreases over time. However, two part alkali-activated binders do not have the same pore volume reduction benefit through the conversion of water into a solid via its incorporation into reaction products (Van Deventer et al., 2012), thus needing a very low w/b ratio to ensure low permeability.

4.6.2 Water absorption by immersion

The results of water absorption by immersion are presented in Fig. 4.12. Since all the mixtures have the same w/b ratio they should present a similar open porosity. So the differences between

the several mixtures could be explained by the scatter data because they are small enough for that. Of course the different hydration products present in the different mixtures may contribute for the porosity differences but only in a very slight manner. That is why the mixture already mention in the previous section as having a good compressive strength performance shows the lower open porosity.

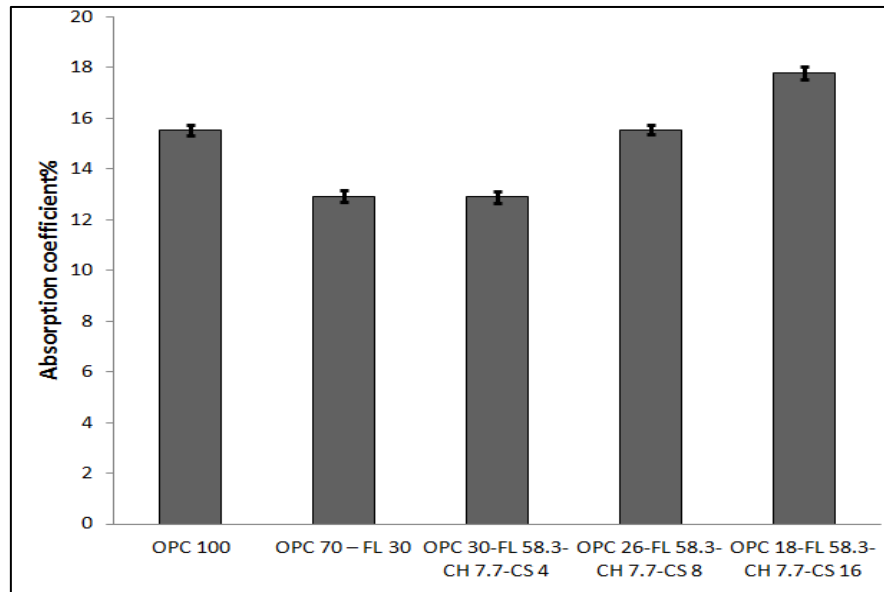


Fig. 4.12 Variation of water absorption by immersion with composition.

4.6.3 Capillarity water absorption

The water absorption capillarity coefficients are showed in Fig. 4.13. The reference mixture shows the best performance. On the opposite side the mixture with 26% OPC 58.3 fly ash, 7.7 calcium hydroxide and 8% calcined stuff clearly shows a very high water absorption by capillarity even at early ages. Such performance is typical of a microstructure with a high amount of capillary pores. Three remaining mixtures show a similar capillarity water absorption coefficient indicating a similar internal capillary pore network.

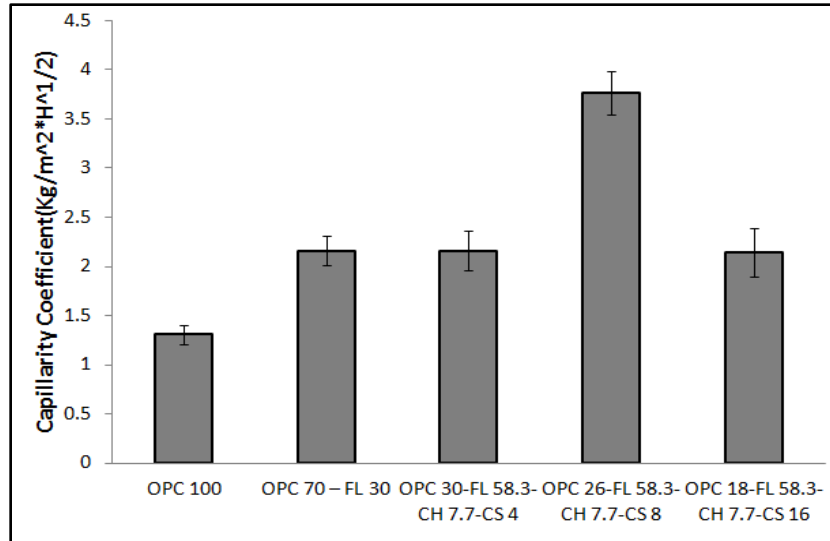


Fig. 4.13 Variation of Water absorption capillarity coefficient with composition

4.6.4 Chloride diffusion

Fig. 4.14 shows the results of the chloride diffusion coefficient. The results are in accordance with the water absorption (open porosity) results. They show that all the mixtures have in the worst case a moderate resistance to chloride diffusion when a comparison is made to the performance of Table 4.12. With the exception of the mixture with 18% OPC 58.3 fly ash, 7.7 calcium hydroxide and 16% calcined stuff. All the other three mixtures in which OPC was partially replaced by fly ash showed a high resistance to chloride diffusion.

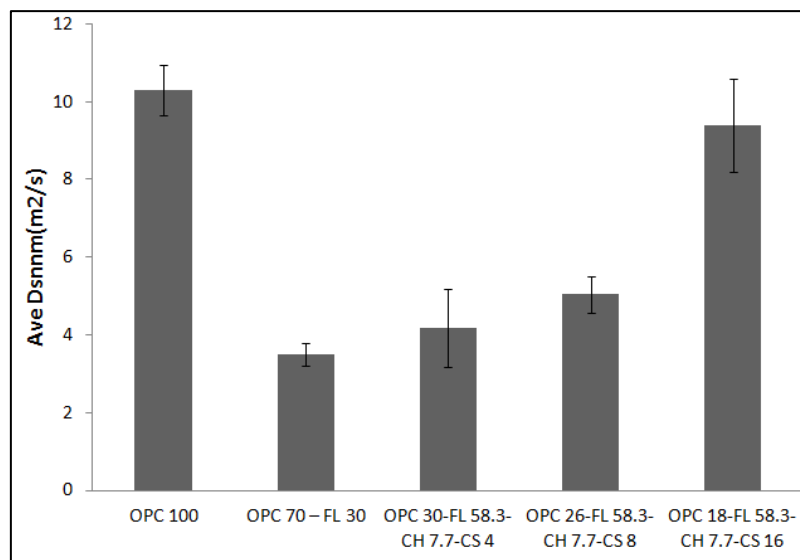


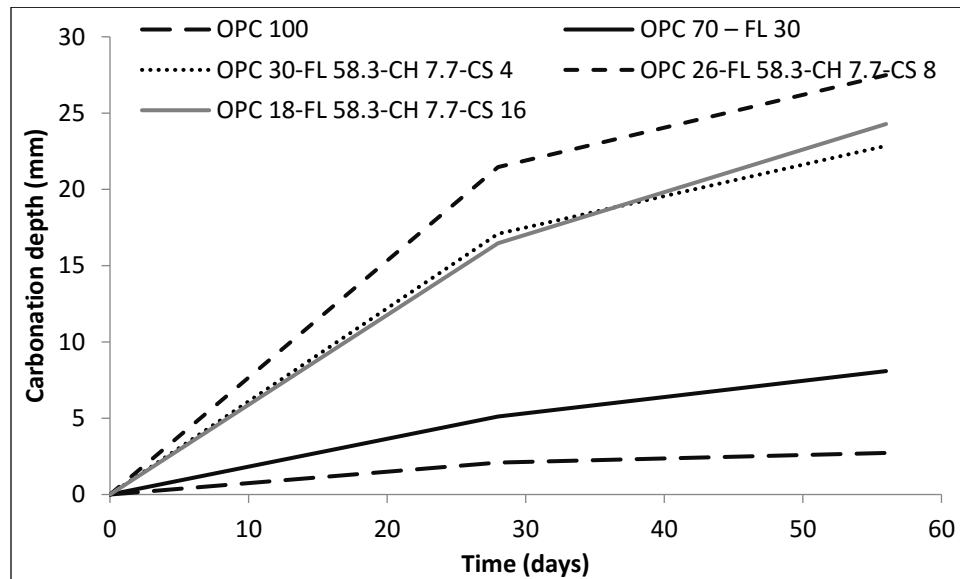
Fig. 4.14 Chloride diffusion coefficient

Table 4.12 Resistance to chloride penetration (Gjorv, 1996)

$\times 10^{-12}$ (m^2/s)	Concrete resistance
>15	Low
10-15	Moderate
5-10	High
2.5-5	Very high
<2.5	Ultra high

4.6.5 Carbonation resistance

Fig. 4.15 shows the results of the carbonation resistance. The 100% OPC based mortar showed the lowest carbonation depth. Replacing 30% OPC by fly ash leads to a higher carbonation depth. Part of the explanation is related to the higher capillarity coefficient of the latter and the other part to the different hydration products.

**Fig. 4.15** Carbonation depth

Previous investigations (Khunthongkeaw et al., 1996) have already reported an increase in concrete carbonation when fly-ash (FA) is used. The mixture with 30% OPC, 58.3 FA, 4% calcined stuff and 7.7% $Ca(OH)_2$ shows a much higher carbonation depth than the second mixture with 30% FA. Since both mixtures have the same capillarity coefficient this means that the carbonation behaviour is related exclusively to the different hydration products. Thus meaning that the new hydration products are proper to carbonation. The mixture with 26% OPC, 58.3 FA, 8%

calcined stuff and 7.7% $\text{Ca}(\text{OH})_2$ shows the highest carbonation depth. This result is not a surprise because this mixture has also the highest water absorption capillarity. The mixture with 18% OPC, 58.3 FA, 16% calcined stuff and 7.7% $\text{Ca}(\text{OH})_2$ shows almost the same carbonation depth as the mixture with 30% OPC and just 4% calcined stuff meaning that difference in composition has little influence on carbonation depth.

4.6.6 Resistance to acid attack

The results of mass loss for specimens immersed in 10% sulphuric acid solutions are shown in Fig. 4.16.

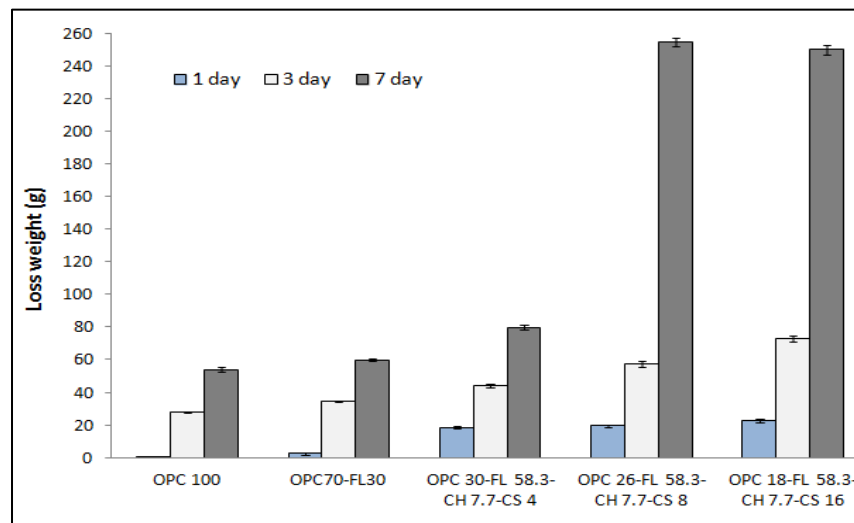


Fig. 4.16 Weight loss of specimens due to acid attack

After 1 day of immersion the best results are shown by the reference mixture and also by the mixture in which 30% OPC was replaced by fly ash. Since the reference mixture has much lower capillary water absorption than the other mixes, this means that in a short term the rate of acid ingress contributes to explain the observed results. However, this is not the case of the one part geopolymeric mixture with 8% calcined stuff because since it has the highest capillarity coefficient it should have a higher weight loss than the other geopolymeric mixtures.

After 3 days of immersion in acid solution, one can confirm that the weight loss is proportional to the OPC content in the mixtures. A higher OPC content is associated to a lower weight loss. High pozzolan content mixtures showed lower resistance to acid attack this results do not confirm previous findings about the fact that the presence of pozzolanic admixtures was found to lower the

detrimental effect of acid attack on concrete (Beddoe and Schmidt, 2009; Goyal et al., 2009) Probably because a denser microstructure typical of pozzolanic based mixtures were not yet formed by the time this mixtures were tested (28 days).

4.7 Conclusions

The investigations concerning mix design, properties and durability of one part geopolymer mixtures allowed for the following conclusions:

Several one part geopolymer mixtures were developed some having a high compressive strength suitable for construction purposes. The results show that there is not a direct linear relationship between the calcium hydroxide content and the compressive strength. Still a general trend was observed linking compressive strength evolution with curing age, which is typical of OPC chemistry. Geopolymeric mixtures with 4% calcined stuff seems to correspond to a good compromise between a low OPC content and an acceptable compressive strength. A reduction of OPC content leads to a reduction on the compressive strength of the mixtures being that the addition of fly ash is not enough to compensate the OPC reduction due to its slow hydration characteristics. Further investigations on mixture composition will be needed in order to select mixtures with a high compressive strength and a high eco-efficient performance. The applicability of the Johnson–Mehl–Avrami–Kolmogorov model to predict the compressive strength of one part-geopolymers was analysed. The degree of reaction of geopolymers was supposed to be related directly to compressive strength and then Avrami constants and exponents were found for all one part geopolymers. It was shown that compressive strength evolution of some one part geopolymers can be found by the proposed equations. The microstructure of one part geopolymers mortars present a very dense and uniform ITZ different of the porous typical interfacial transition zone of Portland cement mixtures. C/S ratio results show that some sodium is replacing Ca^{2+} in CSH which is typical of Na-C-S-H hydration products. FTIR spectra, strong peak band around 965 cm^{-1} was characterized in the one part geopolymers that attributed stretching vibrations Si-O-Si or Al-O-Si mode. No efflorescences, were observed. This may be due to the low amount of alkaline species used as well as to the fact that some sodium replaced Ca^{2+} in CSH hydration products. The durability of OPC mortars and one part geopolymer mortars was assessed by water absorption by immersion, water absorption by capillarity and resistance to acid attack. The results of water

absorption by immersion are very similar for all the mixtures which is due to the fact that they have the same w/b ratio. The capillary water absorption is very high for the one part geopolymeric mixtures with 8% calcined stuff indicating a microstructure with very high amount of capillary pores. The results of resistance to acid attack show that the weight loss is inversely proportional to the OPC content in the mixtures.

CHAPTER FIVE

Performance of foam geopolymers: Two part versus one part

5.1 Introduction

This chapter compares the performance of two part foam geopolymers with the performance of one part geopolymers. The reason for such comparison as to do with the fact that foam geopolymer constitutes a recent research field with high potential in the development of low toxicity thermal insulators and with low thermal conductivity (Prud'homme et al, 2010; Shi et al., 2012, Zhang et al., 2012). Most important the development of materials for energy building related applications is a crucial issue because the increasing demand for worldwide energy, is a major cause for the unsustainable development of our Planet. Between 2007 and 2030 energy demand will grow about 40% reaching 16.8 billion tonnes of equivalent petroleum-TEP (Pacheco-Torgal and Jalali, 2011). The rise in energy consumption has two main reasons, the increase in world population and the fact that there are an increasing number of people with access to electricity. Currently, 1.5 billion people still have no access to electricity (UN, 2010). Besides since urban human population will almost double, increasing from approximately 3.4 billion in 2009 to 6.4 billion in 2050 (WHO, 2014) this will dramatically increase electricity demand. Beyond what energy consumption means in terms of using non-renewable fossil materials, the highest environmental impact of energy consumption has to do with carbon dioxide emissions, generated during the burning of coal and gas for electricity generation in power stations. Given that buildings consume throughout their life cycle, more than 40% of all energy produced (OCDE, 2003), we can easily see the high energy saving potential that this subsector may represent in terms of reducing carbon dioxide emissions. Energy efficiency is the most cost effective way to reduce emissions, improve competitiveness and create employment. The Energy Road Map 2050 (COM 885, 2011) confirmed that higher energy efficiency in new and existing buildings is key for the transformation of the EU's energy system. COM 815 (2011) mentions that the Union's energy efficiency target of saving 20% of energy by 2020 could cut consumers' bills by up to €1000 per household a year and improving Europe's industrial competitiveness and creating up to 2 million new jobs by 2020. The European Energy Performance of Buildings Directive 2002/91/EC (EPBD) has been recast in the form of the 2010/31/ EU by the European Parliament on 19 May 2010. One of the new aspects of the EPBD that reflects an ambitious agenda on the reduction of the energy consumption is the introduction of the concept of nearly zero-energy building (Pacheco-

Torgal et al., 2013). The use of thermal insulation materials constitutes the most effective way of reducing heat losses in buildings thus reducing heat energy needs. These materials are very important for the building material industry representing a 21 billion € market share (Pacheco-Torgal, 2014). With the exception of expanded cork, which is based on a renewable and completely recyclable material, all the other current insulation materials are associated with negative impacts in terms of toxicity. Polystyrene, for example contains anti-oxidant additives and ignition retardants, additionally, its production involves the generation of benzene and chlorofluorocarbons. On the other hand, polyurethane is obtained from isocyanates, which are widely known for their tragic association with the Bhopal disaster. Besides, they release toxic fumes when subjected to fire (Pacheco-Torgal et al., 2012b). Besides recently the European Union approved the Regulation (EU) 305/2011 related to the Construction Products Regulation (CPR) that replaced the current Directive 89/106/CEE, already amended by Directive 1993/68/EEC, known as the Construction Products Directive (CPD). A crucial aspect of the new regulation relates to the information regarding hazardous substances.

5.2 Two part foam geopolymers

The mix parameters were analysed through a laboratory experiment of 54 different two part geopolymeric mortar mixes were, sodium silicate/sodium hydroxide mass ratio (2.5, 3.5, 4.5), activator/binder mass ratio (0.6, 0.8, 1.0), chemical foaming agent type (hydrogen peroxide (H_2O_2) and sodium perborate ($NaBO_3$)) and foaming agent mass ratio content (1%, 2%, 3%).

Table 5.1 Mix compositions (%)

Mix	Fly ash/ Powder*	Ca(OH) ₂ / Powder	Sand/ Powder	Sodium silicate/ Sodium hydroxide	Activator/ Binder	H ₂ O ₂ **	NaBO ₃
FL 90-CH 10	90	10	80	2.5	0.6	1	1
				3.5	0.8	2	2
				4.5	1.0	3	3

*Powder: Fly ash + Ca(OH)₂

**Foam agent to powder

5.2.1 Properties

The results of water absorption by immersion are showed in Fig. 5.1. The lowest water absorption by immersion (11.2%) was in a mixture with an activator/binder ratio of 0.8 a sodium silicate/sodium hydroxide of 4.5 and 3% hydrogen peroxide content. Very similar

and low water absorption values (12.7%) were found for mixtures with 1% hydrogen peroxide and a sodium silicate/sodium hydroxide of 2.5. One with an activator/binder ratio of 0.8 and the other with an activator/binder ratio of 1.0. The highest water absorption by immersion (27%) were found in a mixture with an activator/binder ratio of 1.0 a sodium silicate/sodium hydroxide of 2.5 and 3% hydrogen peroxide content. A similar high water absorption (27%) was found in a mixture with an activator/binder ratio of 1.0 a sodium silicate/sodium hydroxide of 3.5 and 3% sodium perborate content and also in a mixture with an activator/binder ratio of 0.6 a sodium silicate/sodium hydroxide of 4.5 and 3% hydrogen peroxide content. This means that concerning water absorption both foaming agents allow for high porosity mixtures depending on their content and on the ratios activator/binder and sodium silicate/sodium hydroxide.

The results of density are presented in Fig. 5.2. The lowest density results were found in mixtures with an activator/binder ratio of 0.6 and 3% hydrogen peroxide content. One with a sodium silicate/sodium hydroxide of 4.5 (734 kg/m^3) and other with a sodium silicate/sodium hydroxide of 2.5 (749 kg/m^3). As a general trend the increase of foaming agent leads to a lower density. However, the opposite can also take place. That is the case of hydrogen peroxide based mixtures with an activator/binder ratio of 1.0 a sodium silicate/sodium hydroxide of 3.5.

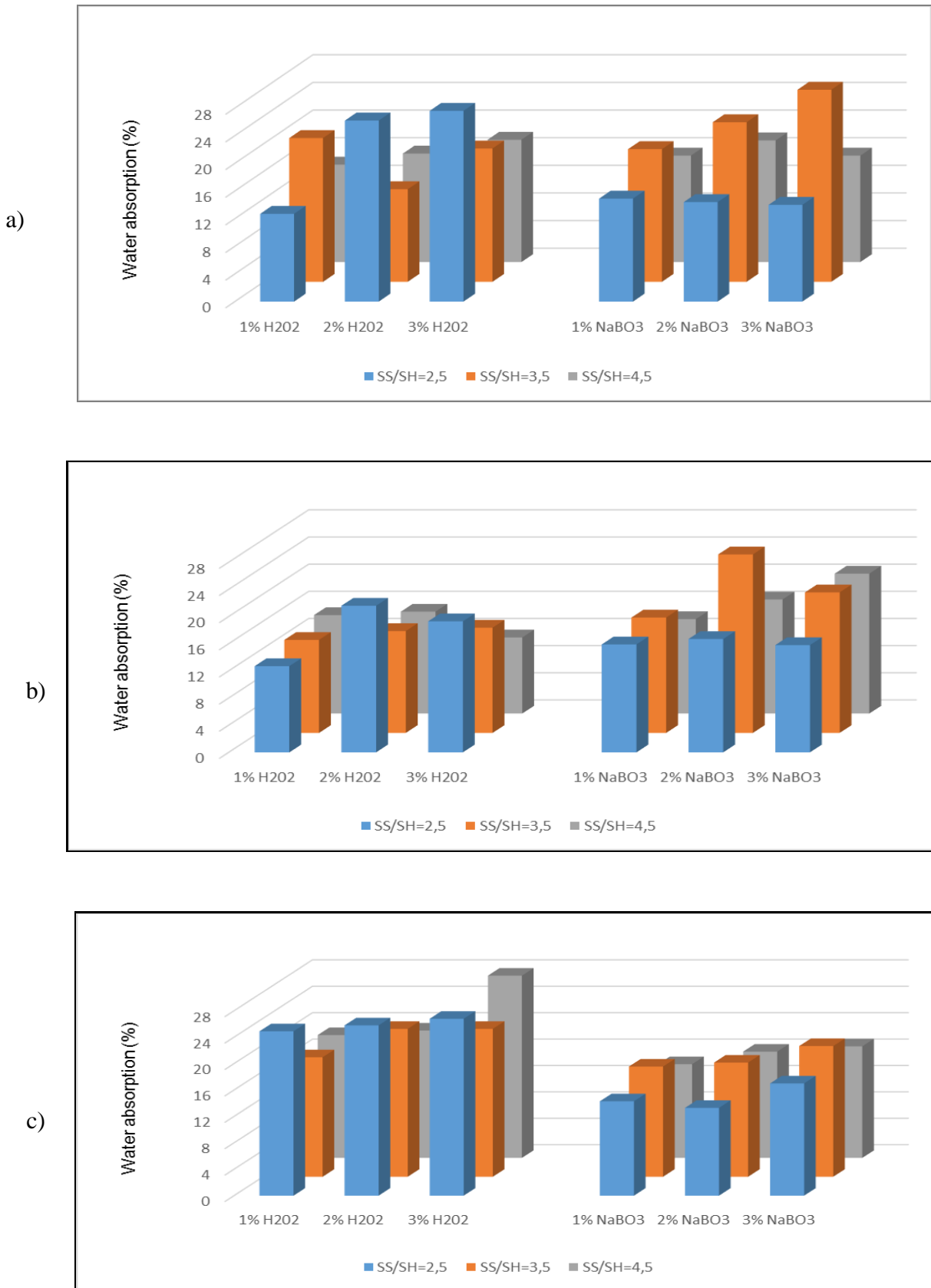


Fig. 5.1 Water absorption by immersion according to activator/binder ratio and sodium silicate/sodium hydroxide mass ratio: a) Activator/binder ratio=1; b) Activator/binder ratio=0.8; Activator/binder ratio=0.6

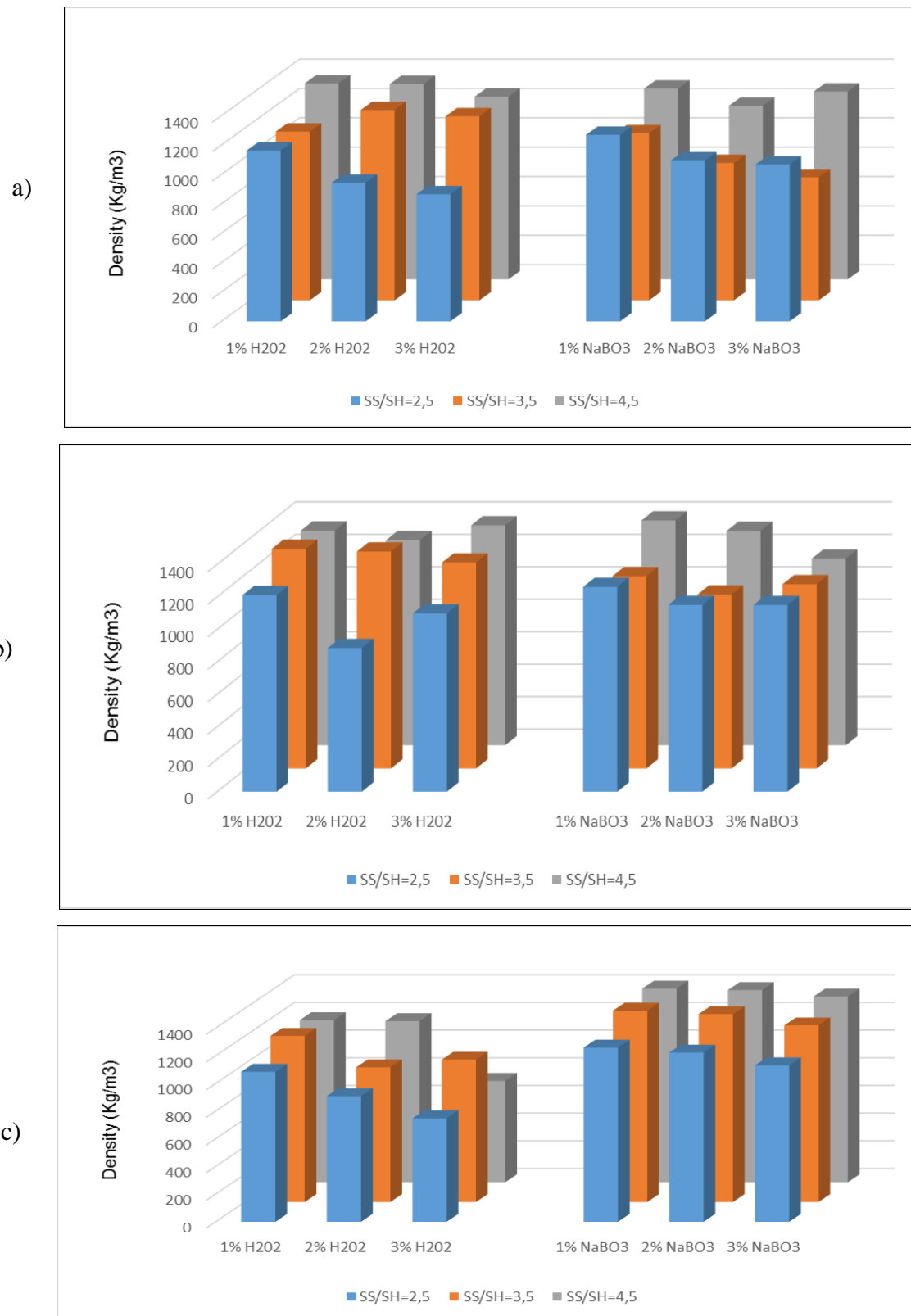


Fig. 5.2 Density according to activator/binder ratio and sodium silicate/sodium hydroxide mass ratio: a) Activator/binder ratio=1; b) Activator/binder ratio=0.8; Activator/binder ratio=0.6

Fig. 5.3 shows the results of the thermal conductivity. Thermal conductivity was executed on specimens, which had low density (lower than 900 kg/m^3) and compressive strength above 3 MPa. The missing values are related to high density mixtures. The lowest thermal conductivity performance was achieved ($0.113 \text{ W/m}\cdot\text{°K}$) in a mixture with an activator/binder ratio of 0.8 a sodium silicate/sodium hydroxide of 2.5 and 3% sodium perborate content. A similar thermal conductivity was obtain in a mixture with the same activator/binder ratio, the same sodium silicate/sodium hydroxide ratio and 1% sodium perborate content ($0.1195 \text{ W/m}\cdot\text{°K}$). A mixture with the same sodium silicate/sodium hydroxide of 2.5 with an activator/binder ratio of 0.6 and 2% hydrogen peroxide content also lead to a low thermal conductivity ($0.1293 \text{ W/m}\cdot\text{°K}$).

Another sodium perborate based mixtures with an activator/binder ratio of 1.0 and a sodium silicate/sodium hydroxide of 4.5 also led to a low thermal conductivity ($0.1187 \text{ W/m}\cdot\text{°K}$). These results outperform the thermal conductivity of commercial autoclaved aerated concrete masonry blocks (Ytong) of around ($0.17 \text{ W/m}\cdot\text{°K}$). No valid statistic correlation was found between thermal conductivity and density (Fig. 5.4). Different sodium silicate/sodium hydroxide ratios and different activator/binder ratios could explain this.

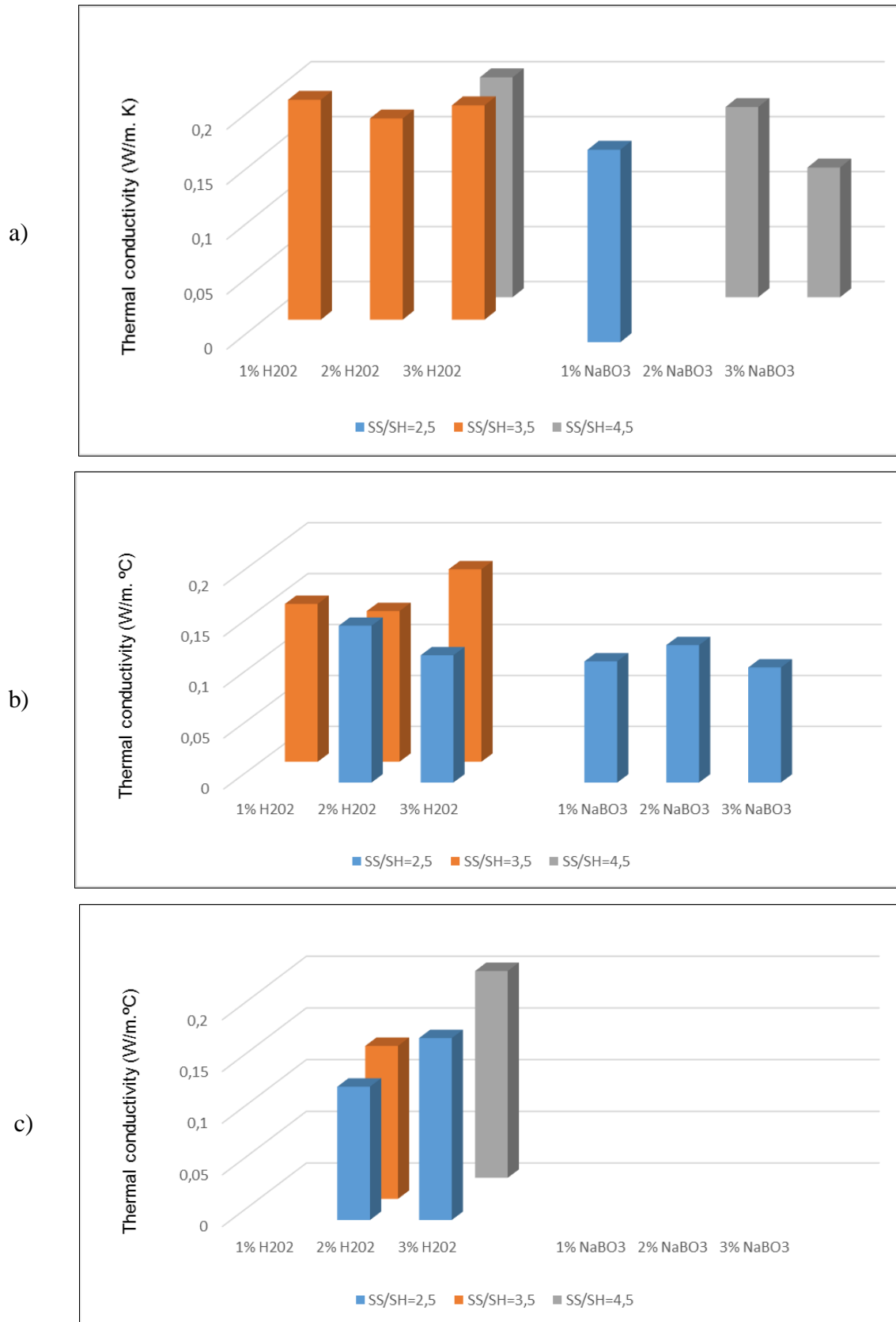


Fig. 5.3 Thermal conductivity according to activator/binder ratio and sodium silicate/sodium hydroxide mass ratio: a) Activator/binder ratio=1; b) Activator/binder ratio=0.8; Activator/binder ratio=0.6

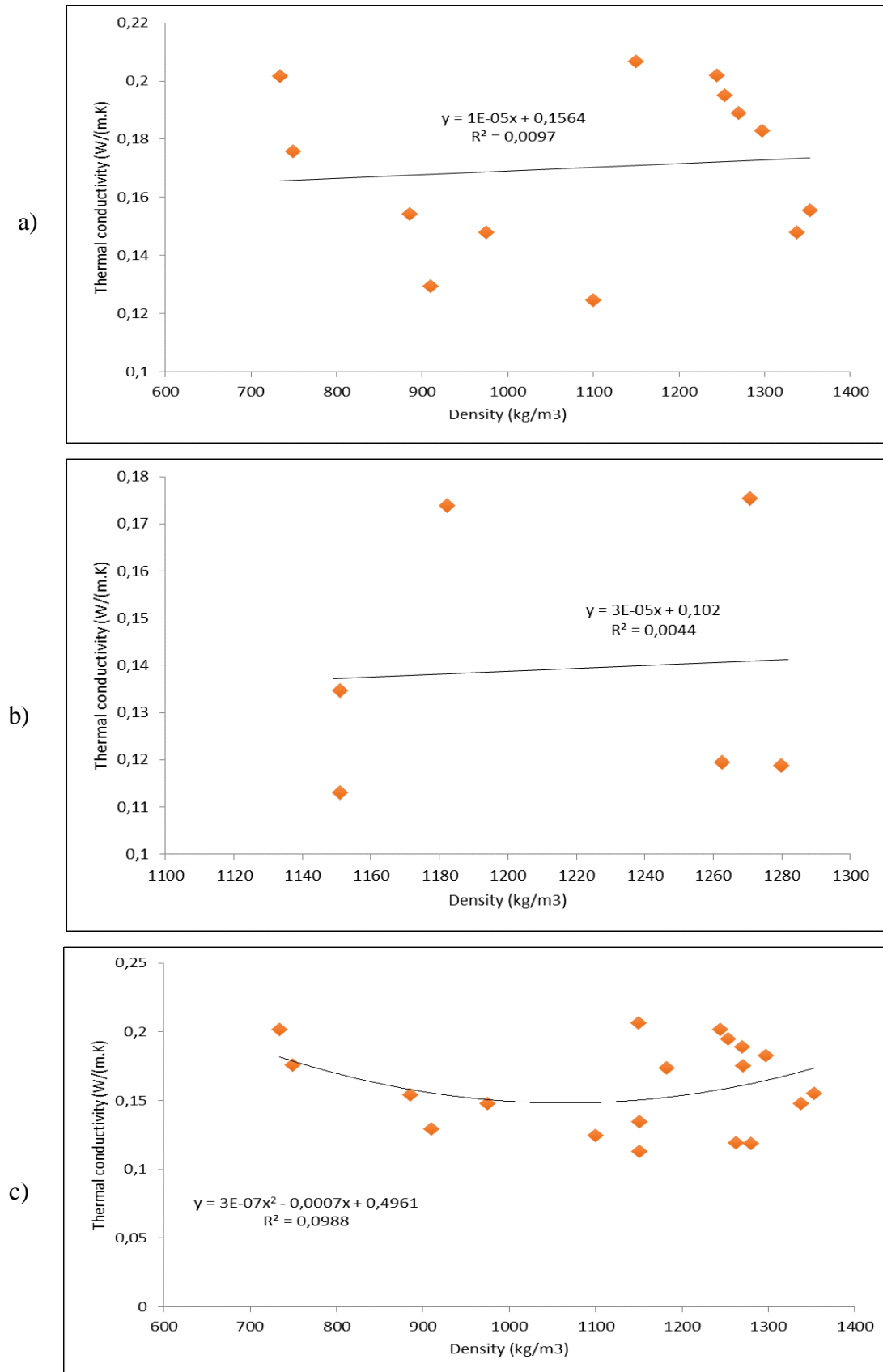


Fig. 5.4 Thermal conductivity versus density: a) Hydrogen peroxide based geopolymers; b) Sodium perborate based geopolymers; c) both

Fig. 5.5 shows the results of the compressive strength. Low compressive strength results (below 3 MPa) were found in hydrogen peroxide mixtures (2 and 3%) with an activator/binder ratio of 0.8 and a sodium silicate/sodium hydroxide of 2.5. It is important to mention that the mixtures with a low thermal conductivity previously mentioned showed a compressive strength in the range of 4.5-6.0 MPa while commercial autoclaved aerated concrete masonry blocks have an average compressive strength above 4,5 MPa.

No valid statistic correlation was found between compressive strength and density due to the variation of the results and the limited number of test samples (Fig. 5.6).

Figs. 5.7-5.9 show the microstructure of three foam geopolymer mixtures. Their composition is shown in table 5.1 while the EDS atomic ratios of two points for each mixture are presented also in table 5.2.

Table 5.2 EDS atomic ratios

	Fly ash	FG A		FG B		FG C	
		Z1	Z2	Z1	Z2	Z1	Z2
SiO₂/Al₂O₃	3.05	19.57	10.33	9.86	9.78	9.92	8.24
Al₂O₃/Na₂O	16.75	0.13	0.14	0.30	0.15	0.45	0.63
CaO/SiO₂	0.05	0.47	0.1	0.27	0.14	0.28	0.28
Na₂O/CaO	0.38	0.78	6.49	1.22	4.35	0.75	0.67
MgO/Al₂O₃	0.13	0.57	0.29	0.27	0.44	0.31	0.38
Fe₂O₃/Al₂O₃	0.19	0.30	0.09	0.14	0.08	0.24	0.16

The microstructure of the three samples shows different level of unreacted fly ash particles. This is consistent with their compressive strength respectively 4.6 MPa, 5.36 MPa and 6.89 MPa. All EDS atomic ratios show a low C/S ratio. Typical C/S ratios in CSH of traditional OPC systems are situated from 1.5 to 2.0 (Diamond, 1976). Meaning there has been some sodium replacing Ca²⁺ in CSH. Some authors have already demonstrated that sodium incorporation in the CSH phase increases as C/S ratio decreases (Macphee, 1989).

All EDS analysis show hydration products with a SiO₂/Al₂O₃ higher than the original SiO₂/Al₂O₃ fly ash ratio which is explained by the Si species added through the used of the sodium silicate. FG B and FG C show similar SiO₂/Al₂O₃ atomic ratios although they used very different sodium silicate contents in their composition. This could mean that the extra Si species have not contributed to the formation of the hardened alkaline aluminosilicate structure and that an optimum sodium silicate content exists.

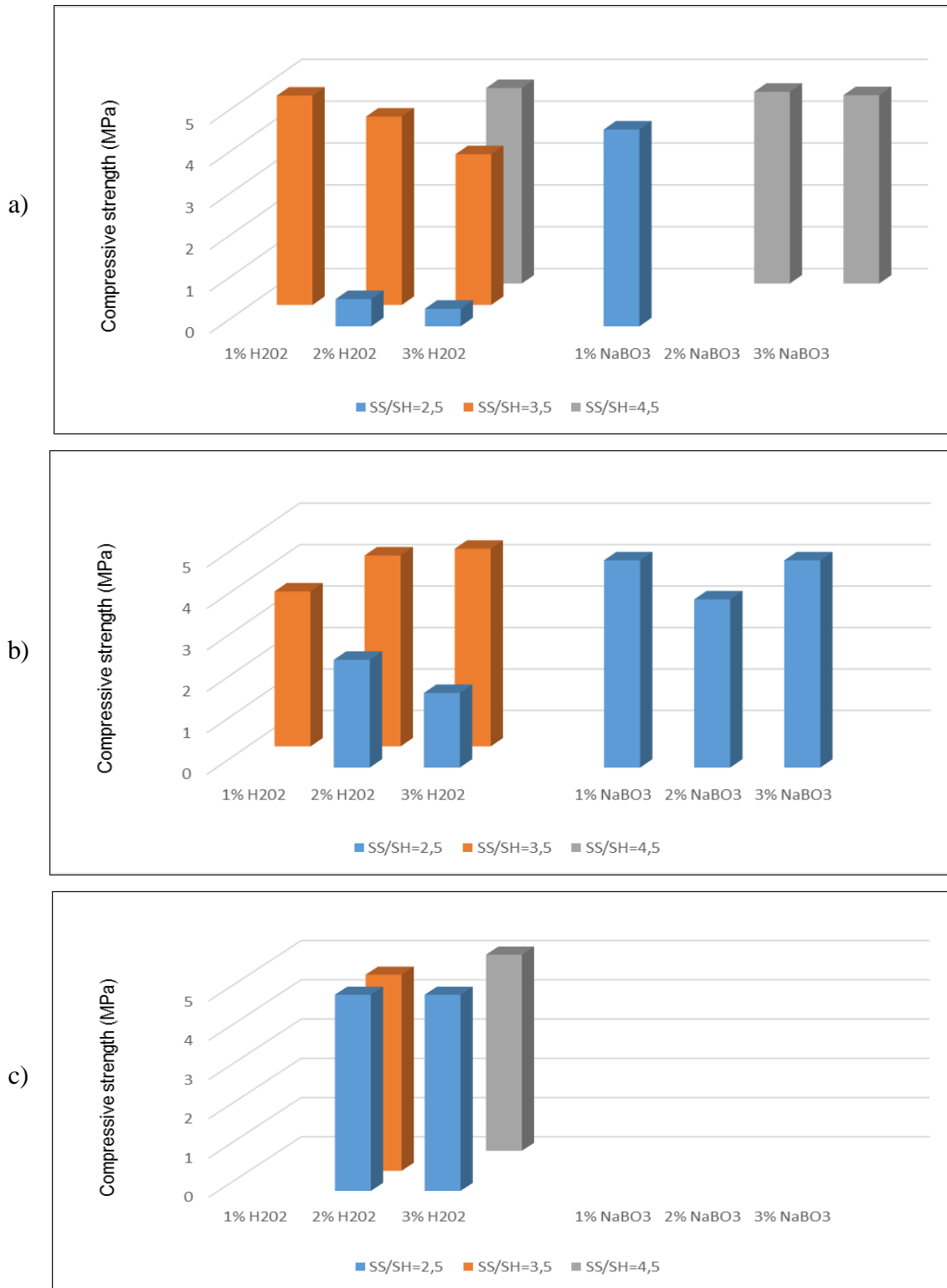


Fig. 5.5 Compressive strength according to activator/binder ratio and sodium silicate/sodium hydroxide mass ratio: a) Activator/binder ratio=1; b) Activator/binder ratio=0.8; Activator/binder ratio=0.6

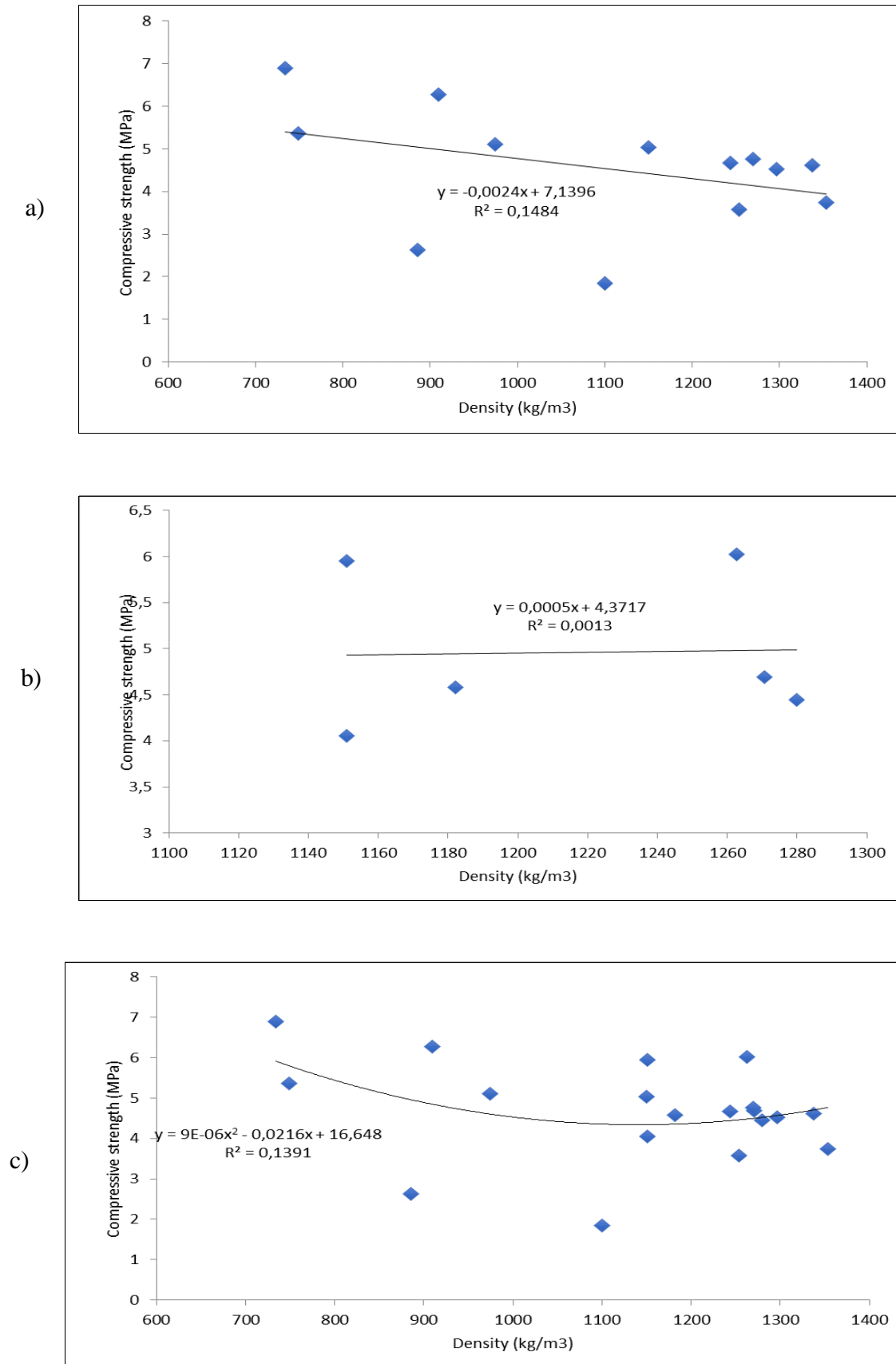


Fig. 5.6 Compressive strength versus density: a) Hydrogen peroxide based geopolymers; b) Sodium perborate based geopolymers; c) both

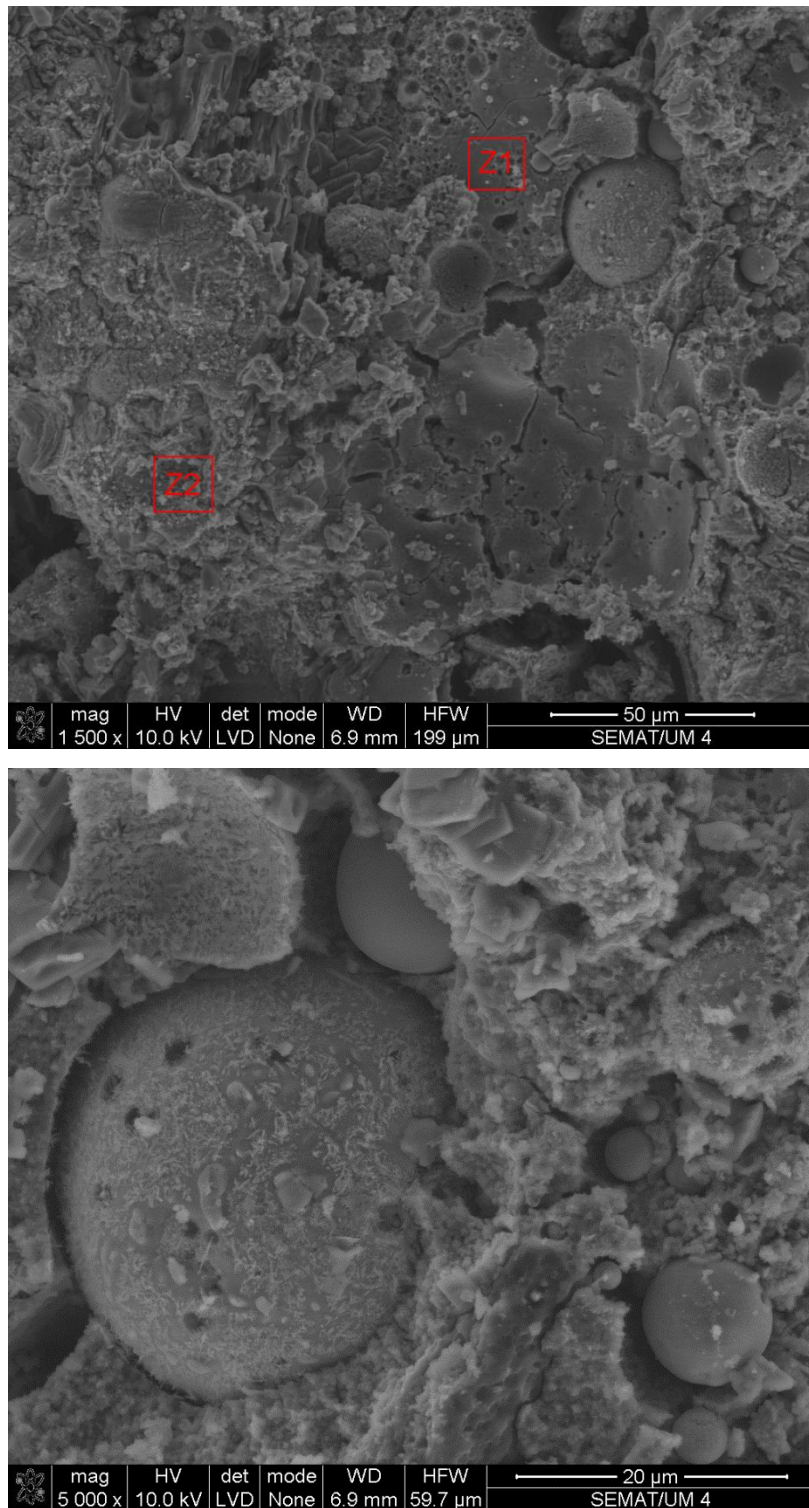


Fig. 5.7 SEM mix FGA

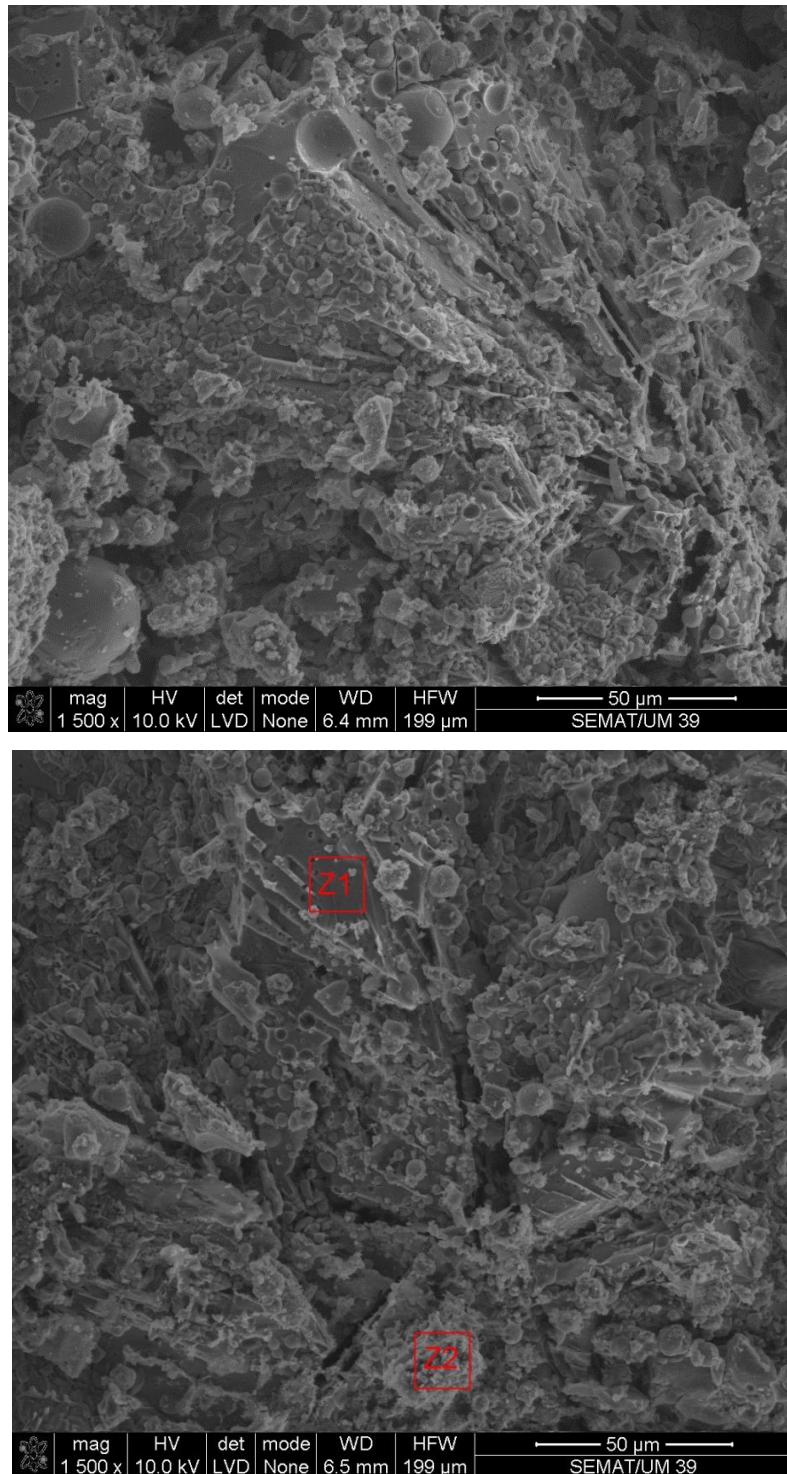


Fig. 5.8 SEM mix FGB

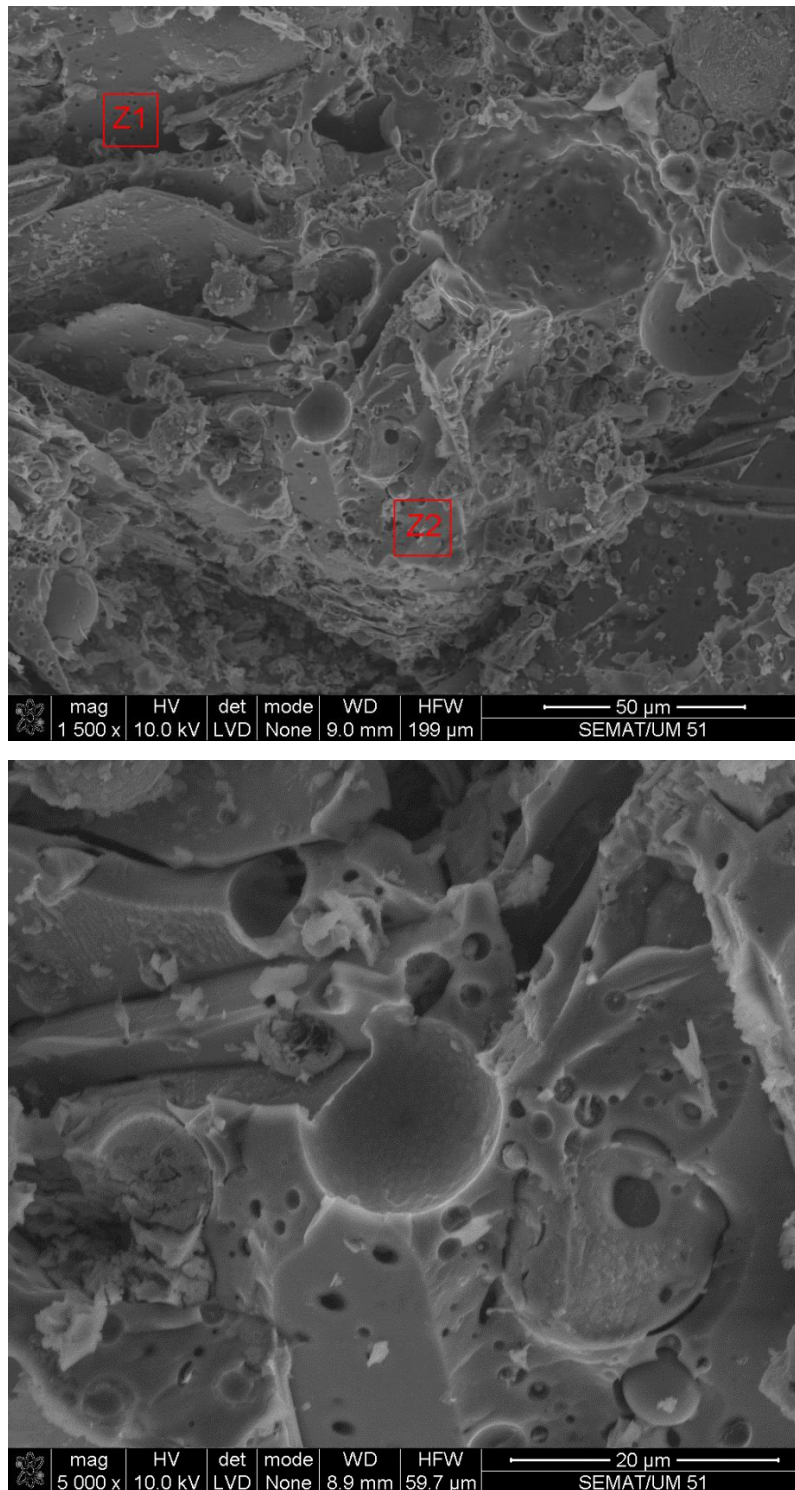


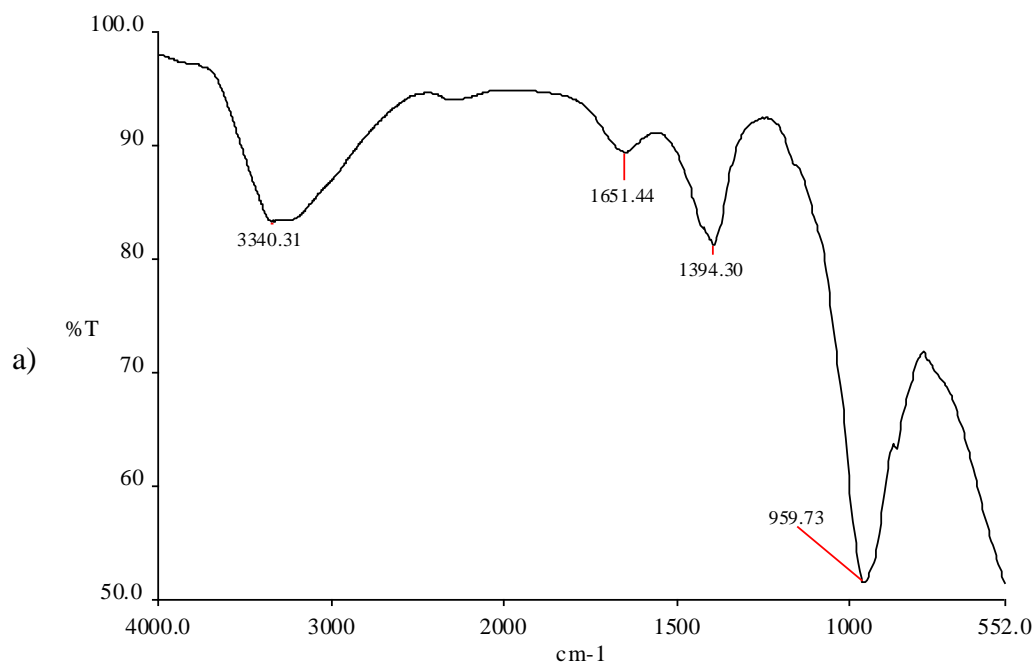
Fig. 5.9 SEM mix FGC

The FTIR spectra of the three hardened foam geopolymer mixtures (table 5.3) are presented in Fig. 5.10. Strong vibration typical of alluminosilicates can be seen. The peak centered around 959 and 965 cm^{-1} is characteristic of a geopolymerization reaction corresponding to the Si–O–Al and Si–O–Si vibration bands. The band at about 864 cm^{-1}

(Fig. 5.10 c) is assigned to Si– OH bending vibration. This mixture had a sodium silicate/sodium hydroxide of 4.5. The absorption band around 1394, 1396 and 1405 cm^{-1} is attributed to stretching vibrations of CO_3^{2-} ions confirming the existence of carbonate species (Fernandez-Jimenez and Palomo, 2005). Atmospheric CO_2 enter in geopolymer to reacting with unhydrated sodium to form sodium carbonate.

Table 5.3 Content of geopolymer samples used for FTIR

Sample	Activator/ Binder	Sodium silicate/sodium hydroxide mass ratio (SS/SH)	Foam Agent type	Foam agent content
FG A	1	2.5	NaBO_3	1%
FG B	0.6		H_2O_2	3%
FG C		4.5		



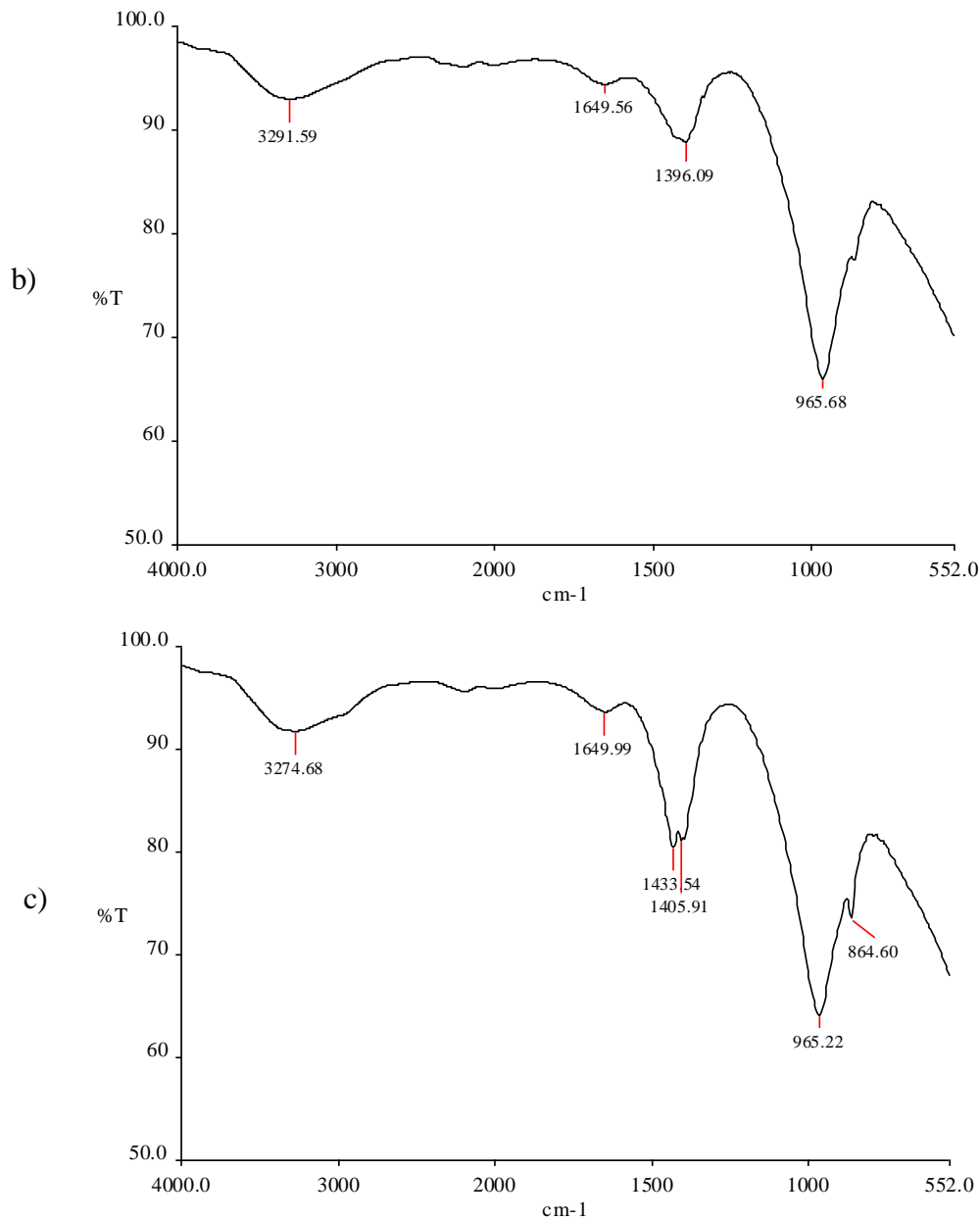


Fig. 5.10 FTIR bands of foam geopolymers: a) FGA; b) FGB; c) FGC

5.2.2 Cost analysis

Since the sodium perborate has a cost 50% higher than the hydrogen peroxide it is important to assess how can this influence the overall cost performance of the different mixtures. Fig. 5.11 shows the cost of the foam geopolymer mixtures according to the activator/binder ratio and sodium silicate/sodium hydroxide mass ratio. The lower the activator/binder ratio, the lower the cost. This is because the cost percentage of foaming agents is just around 10% the total cost (Table 5.4).

Table 5.4 Cost of the materials (euro/kg)

Calcium hydroxide	Fly ash	Sodium silicate	Sodium hydroxide	Water	H ₂ O ₂	NaBO ₃
0.3	0.03	0.53	0.85	0.001	0.98	1.5

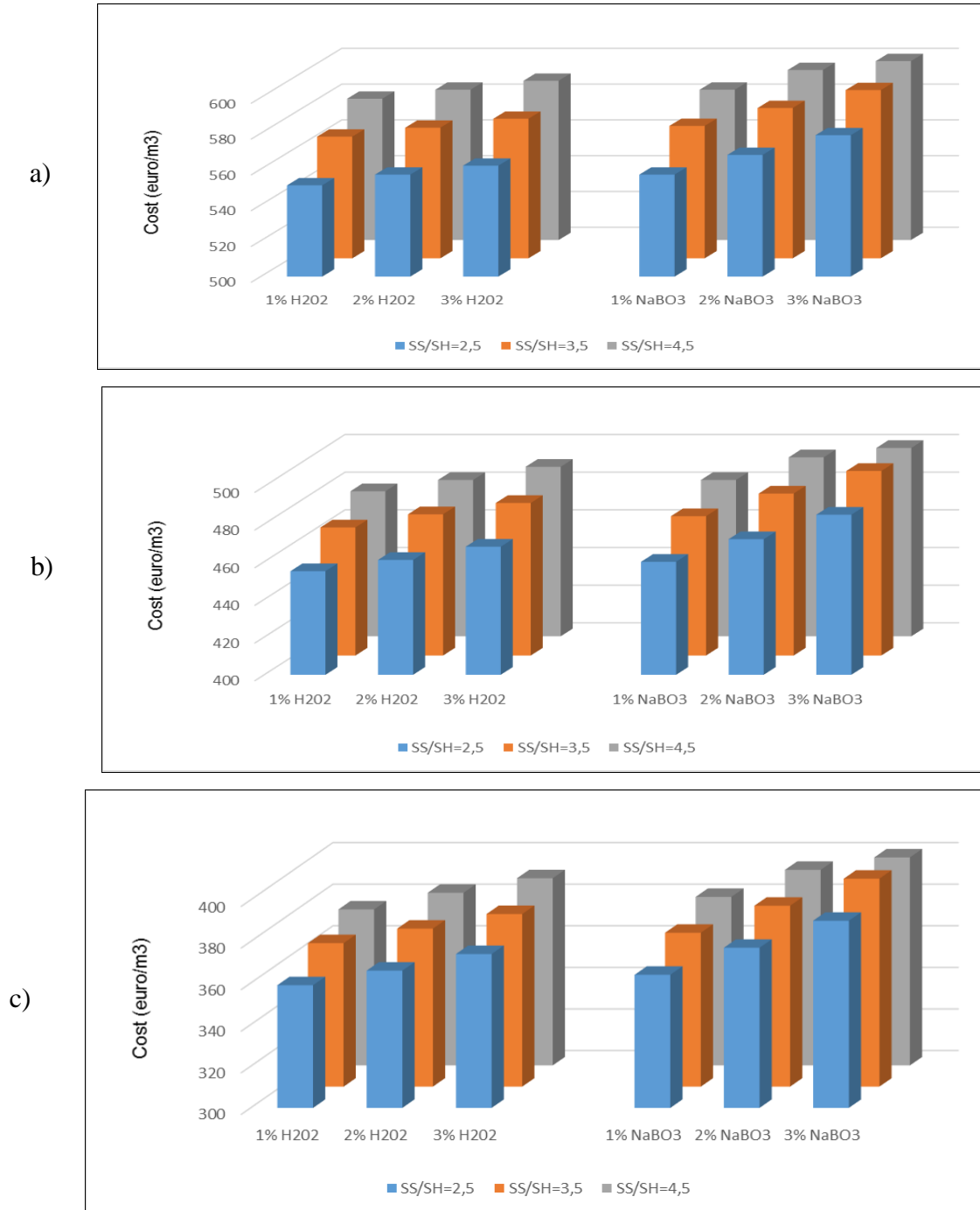


Fig. 5.11 Cost according to activator/binder ratio and sodium silicate/sodium hydroxide mass ratio: a) Activator/binder ratio=1; b) Activator/binder ratio=0.8; Activator/binder ratio=0.6

Alkaline activators being responsible for 80% of the cost. Current investigations aiming to replace sodium silicate by low cost waste glass (Puertas et al., 2014) will increase the cost efficiency of foam geopolymer mixtures. Fig. 5.12 shows the cost to thermal resistance ratio. Fig. 5.13 shows the cost to thermal resistance ratio for several activator/binder ratios. The mixture with the higher performance uses sodium perborate with a activator/binder ratio of 1.0 and sodium silicate/sodium hydroxide mass ratio of 4.5.

Hydrogen peroxide based mixtures (3% and 2% content) with and activator/binder ratio of 0.8 and a sodium silicate/sodium hydroxide mass ratio of 2.5 and 3.5 also present a low cost to thermal resistance ratio.

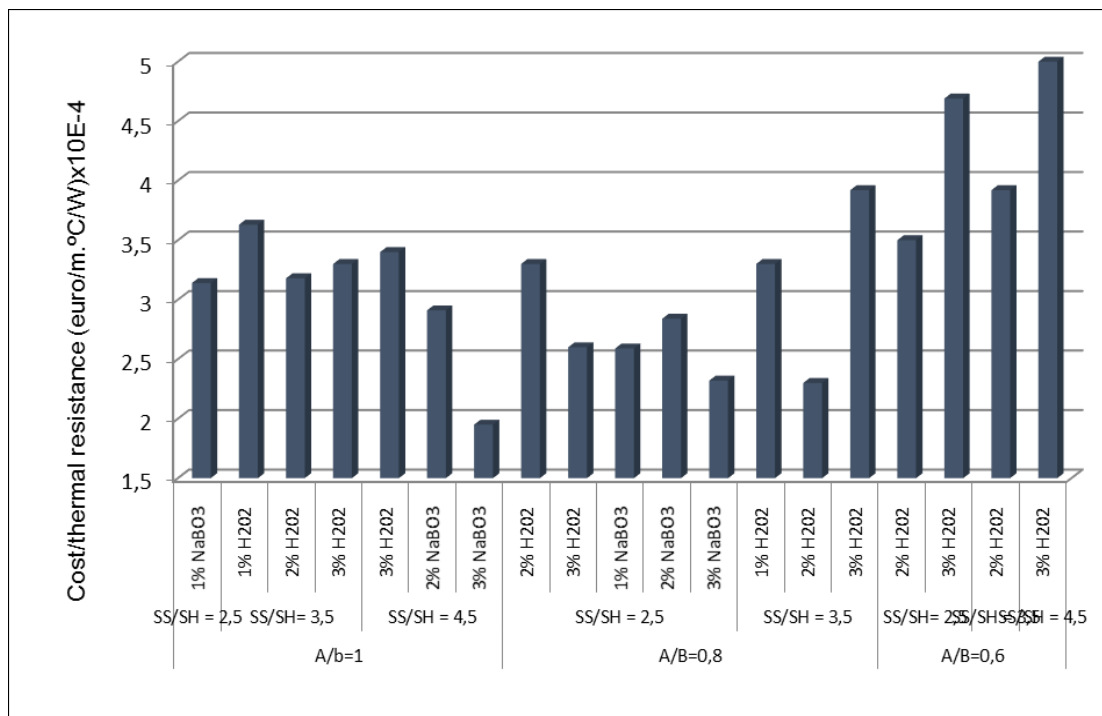


Fig. 5.12 Cost to thermal resistance ratio

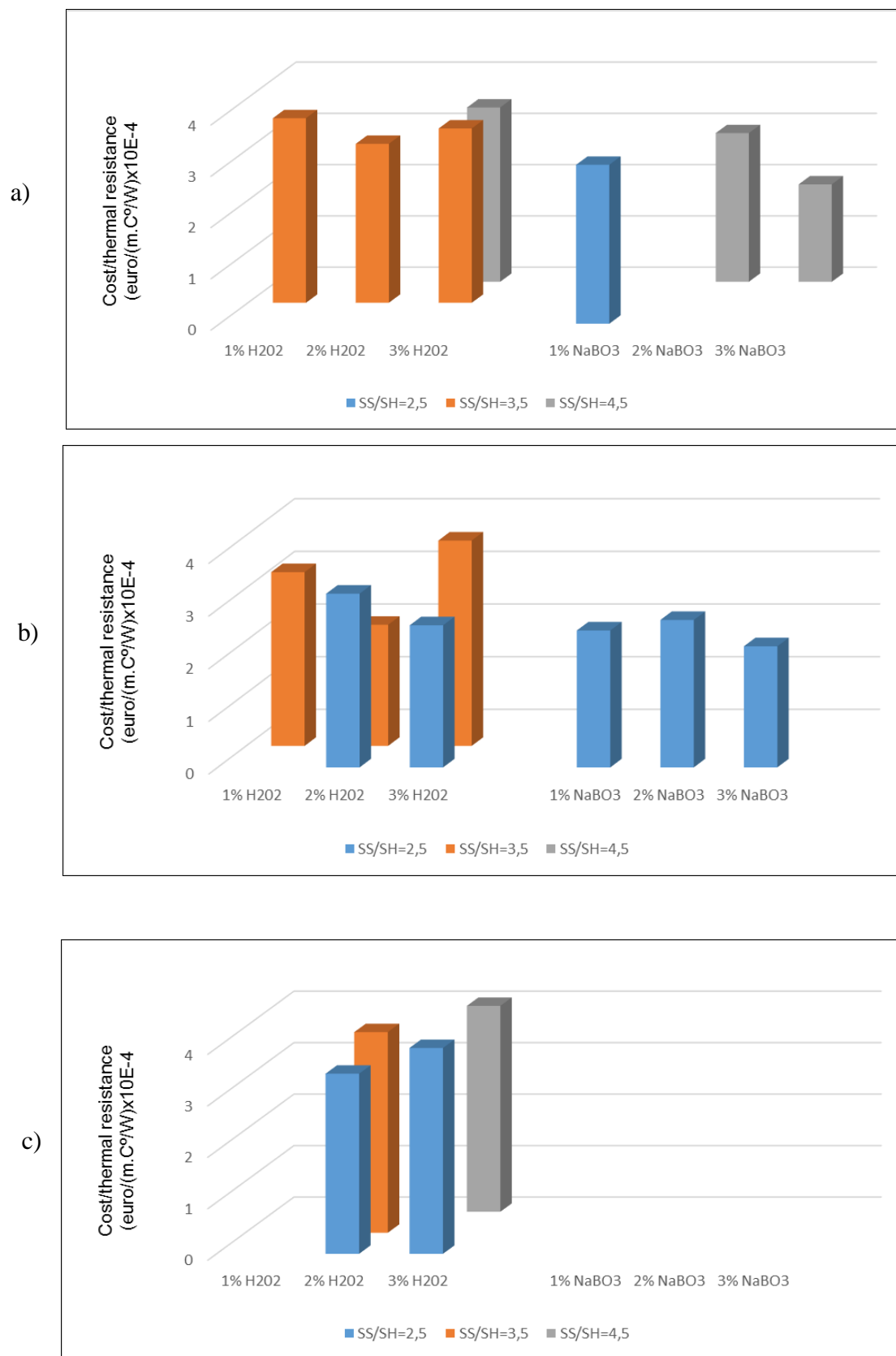


Fig. 5.13 Cost to thermal resistance ratio:

a) Activator/binder ratio=1; b) Activator/binder ratio=0.8; Activator/binder ratio=0.6

5.3 One part foam geopolymers

The one part geopolymer mixtures used to produce the foam geopolymer are presented in table 5.5. The influence of three foaming agents namely aluminium powder (0.5% - 1.5%), NaBO₃ (3%-5%) and H₂O₂ (3%-5%) was analysed.

Table 5.5 Composition of one-part geopolymer mixtures

Mix	OPC/ Powder*	Fly ash/ Powder	Calcined /Powder	Ca(OH) ₂ / Powder	Sand/ Powder	SP/ OPC	W/ Powder
100 OPC	100%	-	-	-	80%	0.8%	35%
30 OPC_70 FA	30%	70%	-	-			
30 OPC_58.3 FA_4 CS_7.7 CH	30%	58.3%	4%	7.7%			
26 OPC_58.3 FA_8 CS_7.7 CH	26%	58.3%	8%	7.7%			
18 OPC_58.3 FA_16 CS_7.7 CH	18%	58.3%	16%	7.7%			

*Powder: OPC + Fly ash + Calcined kaolin and sodium hydroxide + Ca(OH)₂

*Calcined stuff has been prepared by mixing kaolin and sodium hydroxide with 2.5/1 ratio.

5.3.1 Properties

The results of X-ray diffraction are presented in Fig. 5.14. A small mullite crystalline phase is detected in all the calcined kaolin based mixtures. A clear calcite peak is common to the calcined kaolin mixtures. The clear crystalline structure in these mixtures contrasts with the amorphous structures of traditional two part geopolymers. The different foaming agents (aluminum powder and hydrogen peroxide) seems not to have altered the crystalline phases of the hardened material. The exception being the clear calcite silicate oxide in the mixture containing 5% oxygen peroxide. Results of SEM are presented in Fig. 5.15 Also the mixtures have the following compressive strength after 28 days curing (2.3, 2.2, 7 and 8.7). The mixtures associated to lower compressive strength show lesser dense microstructure. This is clearer in the mixture 30 OPC_58.3 FA_4 CS_7.7 CH (5% H₂O₂) with 5% hydrogen peroxide foaming agent. Concerning the EDS molar ratios (Table 5.6). Several areas (Z2 e Z3 in mixture with 3.5% H₂O₂ and Z2 in mixture with 0.5% aluminum powder) in the one-part geopolymer mixture show lower C/S ratio typical of sodium incorporation in the CSH phase into Na-C-S-H gel. That usually evolve into compositions with higher calcium and lower aluminum content (with the C-A-S-H gel proposed to be more stable than N-A-S-H, at high pH) (Garcia-Lodeiro et al., 2013).

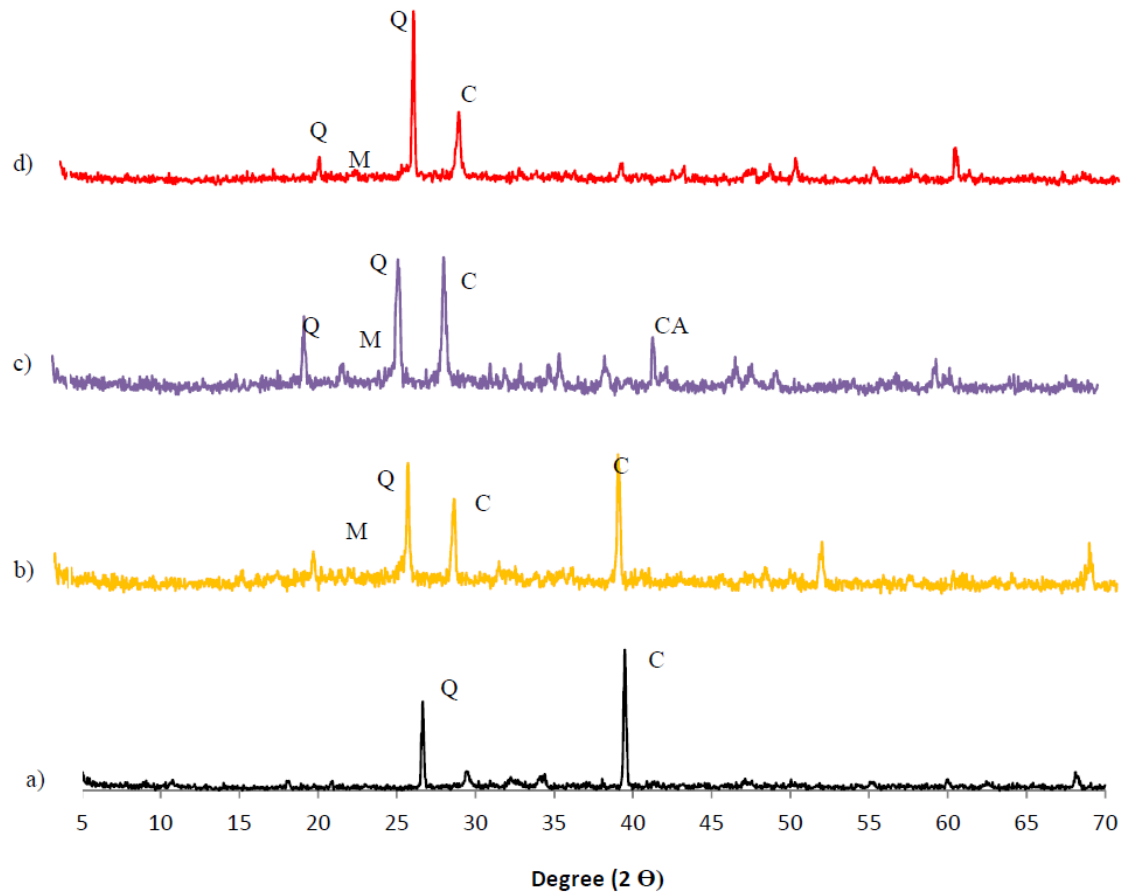


Fig. 5.14 XRD patterns of: a) 100 OPC (1.5% AL); b) 30 OPC_58.3 FA_4 CS_7.7 CH (0.5% AL); c) 30 OPC_58.3 FA_4 CS_7.7 CH (5% H₂O₂); d) 30 OPC_58.3 FA_4 CS_7.7 CH (3.5% H₂O₂); M-Mullite; Q-Quartz; C-Calcite; CA-Calcite silicate oxide

Table 5.6 EDS atomic ratios

	100 OPC		30 OPC_58.3 FA_4 CS_7.7 CH					
	1.5% AL		3.5% H ₂ O ₂			5% H ₂ O ₂	0.5% AL	
	Z ₁	Z ₂	Z ₁	Z ₂	Z ₃	Z ₁	Z ₁	Z ₂
SiO ₂ /Al ₂ O ₃	1.41	3.96	8.81	6.08	4.41	5.86	2.08	5.84
Al ₂ O ₃ / Na ₂ O	---	---	0.47	2.73	4.53	---	6.20	6.66
CaO / SiO ₂	6.57	3.32	5.08	0.46	0.08	6.55	2.40	0.42
Na ₂ O / CaO	---	---	0.04	0.13	0.61	---	0.03	0.06
MgO/Al ₂ O ₃	0.57	3.84	2.32	0.54	---	---	---	---

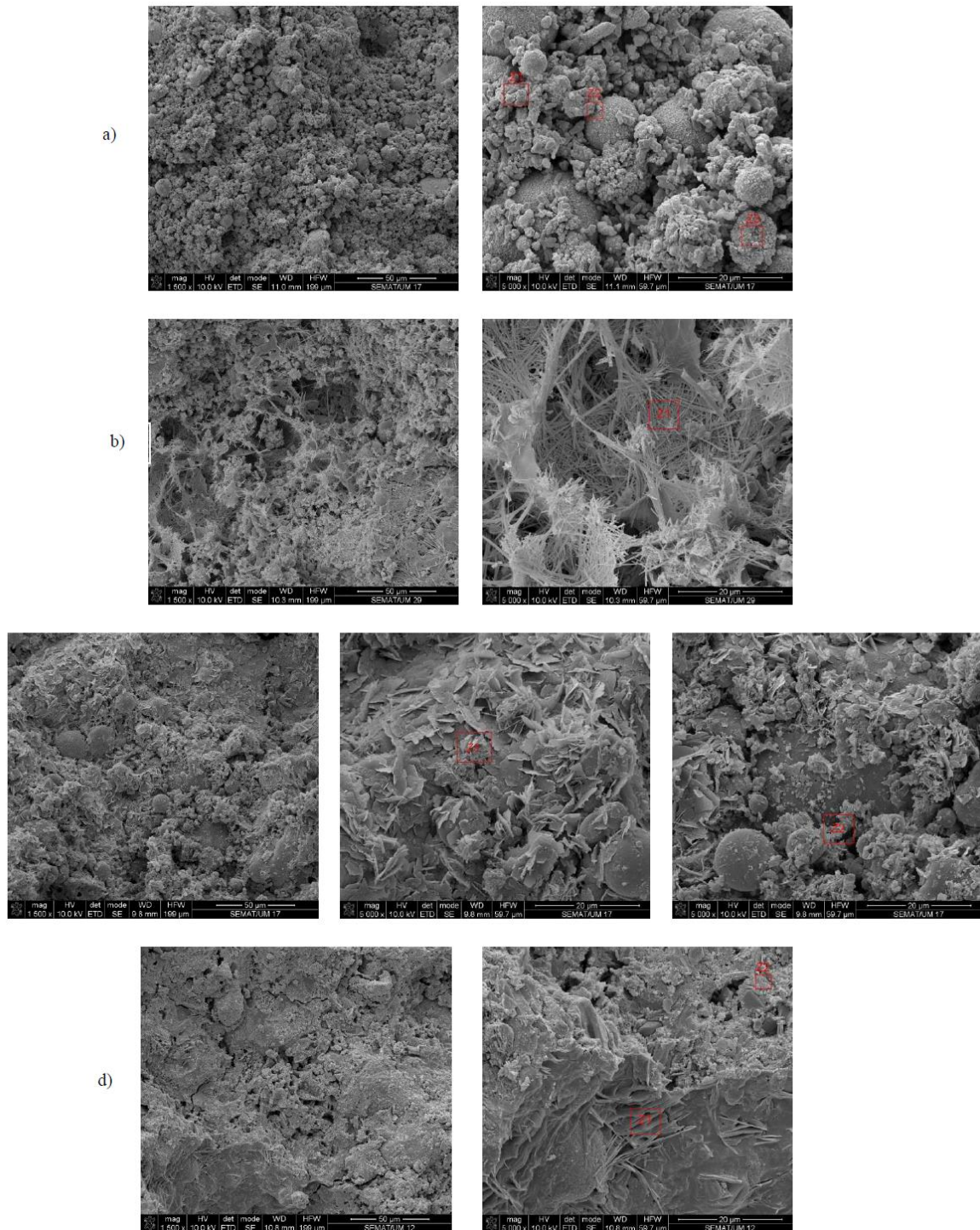


Fig. 5.15 SEM images of: a) 30 OPC_58.3 FA_4 CS_7.7 CH (3.5% H₂O₂);
 b) 30 OPC_58.3 FA_4 CS_7.7 CH (5% H₂O₂); c) 30 OPC_58.3 FA_4 CS_7.7 CH (0.5% AL);
 d) 100 OPC (1.5% AL);

Results of compressive strength of one-part geopolymer mortars are shown in Fig. 5.16. For mortars based only in Portland cement, increase of the aluminium content leads to a decrease in compressive strength.

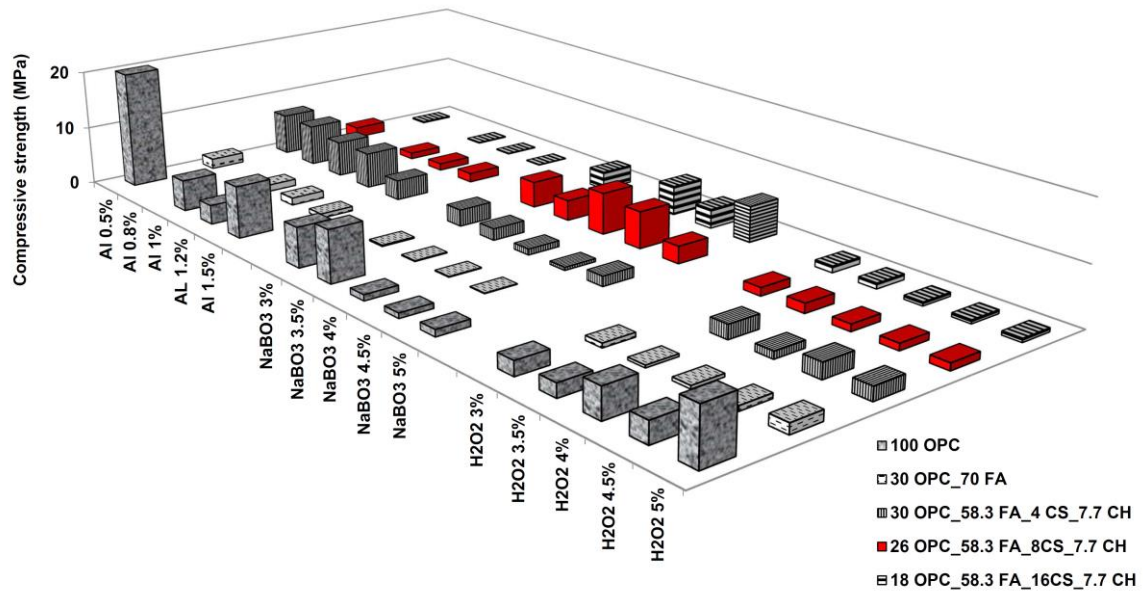


Fig. 5.16 Compressive strength

Except when the aluminium content increases from 1.2% to 1.5% which leads to increase of compressive strength. The reaction of aluminium powder in the alkaline environment liberates Al_2O^- and hydrogen gas (H_2) according to the equation 1 (Arellano et al., 2010):



When the NaBO_3 is used as foaming agent in Portland cement mortars a trend on compressive strength decreased with foaming agent increased. Although one exception is detected when NaBO_3 increased from 3% to 3.5% that leads to an increase in compressive strength. Concerning the use of H_2O_2 the increase of foaming agent shows a minor increase in the compressive strength but when the foaming agent is increased 4% to 4.5% compressive strength decreased. Comparing the performance of the different foaming agents on Portland cement mortars it is observed that the higher compressive strength (20.24 MPa) was recorded for a 0.5% AL content. Concerning the mixture 30 OPC_70 FA, the increase of the aluminium content results in a decrease in compressive strength.

Except when it increased from 1% to 1.2% lead to slight compressive strength increase. When the NaBO_3 is used a trend on compressive strength decrease with foaming agent increase can be found. In respect to the use of H_2O_2 the increase of foaming agent from

3%-3.5% leads to decrease the compressive strength. In an alkaline environment oxygen peroxide decomposes into water and oxygen.

In general, it can be stated that the results gathered for compressive strength of the mixture 30 OPC_70 FA with different foam agents are taken place in a lower range in compare to other compressive strengths of one-part geopolymer mortars. Regarding the mixture 30 OPC_58.3 FA_4 CS_7.7 CH an increase of the aluminium content results in a reduction for compressive strength. Increasing NaBO_3 from 1% to 5% reduced the compressive strength with some exceptions. The exceptions were found when the NaBO_3 content increased from 1% to 2% and 4.5% to 5%. Since, no specific trend was observed in compressive strength of the mixture 30 OPC_58.3 FA_4 CS_7.7 CH that used H_2O_2 .

Comparing the performance of the different foaming agents the higher compressive strength (7 MPa) took place for a 0.5% AL content. Additionally, two similar compressive strength recorded for this mixture with 1% AL (6 MPa) and 1.2% AL (6.04 MPa). Results of compressive strength in mixture 26 OPC_58.3 FA_8 CS_7.7 CH show that there is an increase in compressive strength when the Al content increased. The increase in density can related to pore collapses as suggested by these authors (Masi et al., 2014). Those authors also confirm that aluminium powder is very reactive requiring a much less amount than hydrogen peroxide to obtain similar densities. However since the former costs 33 more than the later (section 5.3.2) it is important to compare the economic performance of the different mixtures. Although an exception discovered when the aluminium content increased from 0.5% to 1%. Since, no specific trend was observed in compressive strength of the mixture 30 OPC_58.3 FA_4 CS_7.7 CH that used NaBO_3 . Concerning the use of H_2O_2 result in constant trend in compressive strength with an exception. An increase of H_2O_2 content between 3% to 3.5% lead to a slight increase in the compressive strength. The higher compressive strength (6.99 MPa) registered for a 4% NaBO_3 content.

Concerning the mixture 18 OPC_58.3 FA_16 CS_7.7 CH, an increase in the aluminium content leads to a decrease in compressive strength. When the NaBO_3 is used as foaming agent a trend on compressive strength increase with foaming agent increase can be noticed. Except when the NaBO_3 increased from 4% to 4.5% lead to a compressive strength reduction. Respect to the use of H_2O_2 the increase of foaming agent results in reduction of compressive strength. By comparing the performance of the different

foaming agents it can be concluded that the higher compressive strength (6.11 MPa) was measured for a 5% NaBO_3 content. The overall results show that several mixtures show a compressive strength similar to the one of commercial cellular concrete blocks (6.5 MPa).

However most mixtures comply with the compressive strength requirement (≥ 1.4 MPa) of the grades 4 and 5 of the Korean Industrial Standard code for foam concrete for floor heating systems (Yang et al., 2014).

Results of water absorption of one-part geopolymer mortars are shown in Fig. 5.17. For mortars based on Portland cement, the increase of the aluminium content does not leads to a relevant change in water absorption. When it increases from 1.2% to 1.5% leads to the slight water absorption decrease. When the NaBO_3 is used as foaming agent in Portland cement mortars a trend on water absorption increase with foaming agent increase can be noticed. However, some exceptions are detected. The increase from 3% to 3.5% and the increase from 4% to 4.5% that lead to a water absorption reduction. Concerning the use of H_2O_2 the increase of foaming agent from 3% to 3.5% shows a minor increase in the water absorption but when the foaming agent is increased above 3.5% no water absorption is detected. Comparing the performance of the different foaming agents on Portland cement mortars it is seen that the highest water absorption (62%) took place for a 5% NaBO_3 content.

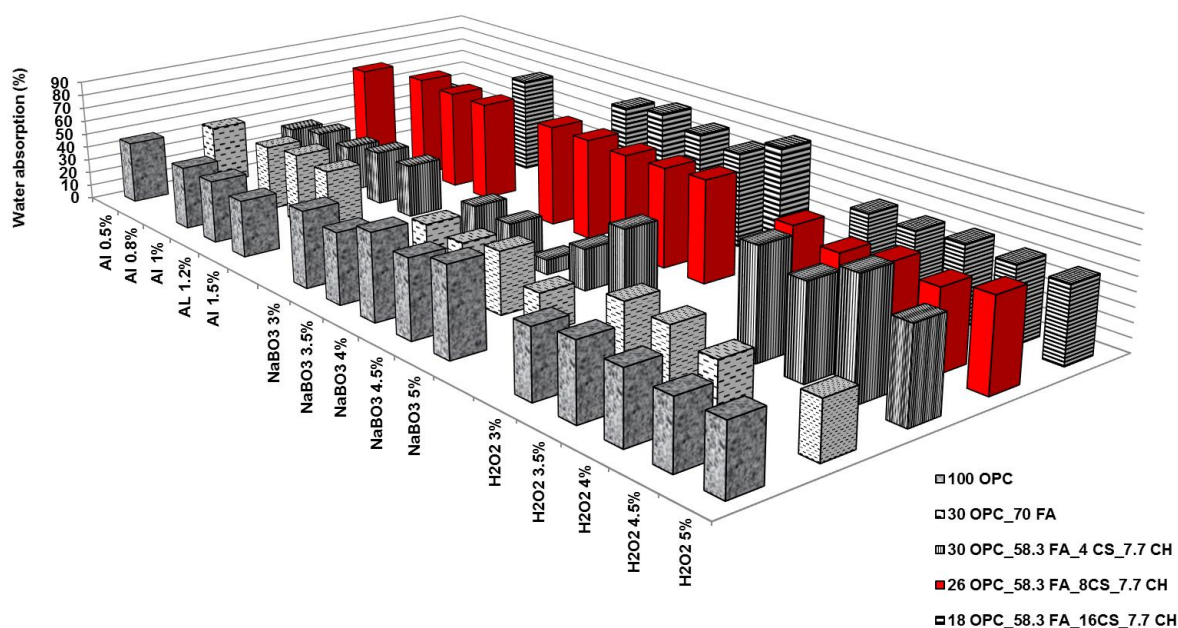


Fig. 5.17 Water absorption

However, this mixture shows a foaming efficiency (water absorption/foaming agent content= 12) that is lower than other mixtures based on aluminium foaming agent that show higher water absorption levels with just 0.5% content (efficiency= 90). Concerning the mixtures 30 OPC_70 FA, the increase of the aluminium content leads to a slight increase in water absorption. When the aluminium increases from 1.2% to 1.5% a slight water absorption decrease was detected. When the NaBO_3 is used as foaming agent in this mixture a trend on water absorption decrease with foaming agent increase registered.

However, there was an exception. When the NaBO_3 increased from 4% to 4.5% leads to a water absorption reduction. Regarding the use of H_2O_2 the increase of foaming agent depicts a minor decrease in the water absorption but when the foaming agent is increased above 4% slight increase in water absorption is detected. Comparing the performance of the different foaming agents on the mixture 30 OPC_70 FA it is revealed that the higher water absorption (50.53%) recorded for 1.5% Al content. In respect to the mixtures 30 OPC_58.3 FA_4 CS_7.7 CH, an increase of the aluminium content leads to an increase of water absorption. The increase from 0.8% to 1% and 1.2% to 1.5% decrease the water absorption. When the NaBO_3 is used as foaming agent, a decrease was detected by increasing foam agent content. Although some exceptions were detected from 1% to 2% and 4% to 5% which lead to water absorption increase.

Concerning the use of H_2O_2 the increase of foaming agent leads to reduce in water absorption with one exception. The exception was monitored in an increase of foam agent from 4% to 4.5% which leads to increase in water absorption. Comparing the performance of the different foaming agents it is found that the higher water absorption (81.07%) took place for a 4.5% H_2O_2 content. This corresponds to an efficiency of $(81.07/4.5= 18)$ while Al mixtures show high efficiencies $(40/1.2=33.3)$. Concerning the mixtures 26 OPC_58.3 FA_8 CS_7.7 CH, an increase of the aluminium content leads to a slight decrease in water absorption with one exception. The exception was measured when the use of AL increased from 0.5% to 1% and a minor increase in the water absorption was detected.

When the NaBO_3 is used as foaming agent a trend on water absorption is almost constant with no increase, regardless increasing foam agent content. In respect to the use of H_2O_2 the increase of foaming agent shows no change in the water absorption. The

performance of different foaming agents on this mixture showed that the higher water absorption (72.72%) was registered for a 3% NaBO_3 content. Additionally, some similar high water absorptions observed for this mixture with 1.2% Al (72.31%), 1.5% AL (72.22%), 3.5% NaBO_3 (72.27%), and 5% NaBO_3 (72.70%). Concerning the mixture 30 OPC_58.3 FA_16 CS_7.7 CH, an increase of the aluminium content leads to an increase in water absorption. When the NaBO_3 is used a trend on water absorption reduction with foaming agent content increase can be noticed. However, some exceptions are acquired.

The increase of NaBO_3 from 3% to 3.5% and the increase of NaBO_3 from 4.5% to 5% lead to a water absorption increase. Regarding the use of H_2O_2 , by increasing foam agent content no increase in water absorption is discovered. Comparing the performance of the different foaming agents on the mixture 30 OPC_58.3 FA_16 CS_7.7 CA it is seen that the higher water absorption (81.48%) took place for a 5% NaBO_3 content.

The results of bulk density of one-part geopolymer mortars are shown in Fig. 5.18. For mortars based on Portland cement an increment in the aluminium content leads to a decrease in bulk density. When the NaBO_3 is employed in Portland cement mortars a trend on bulk density decrease with foaming agent content increase can be noticed.

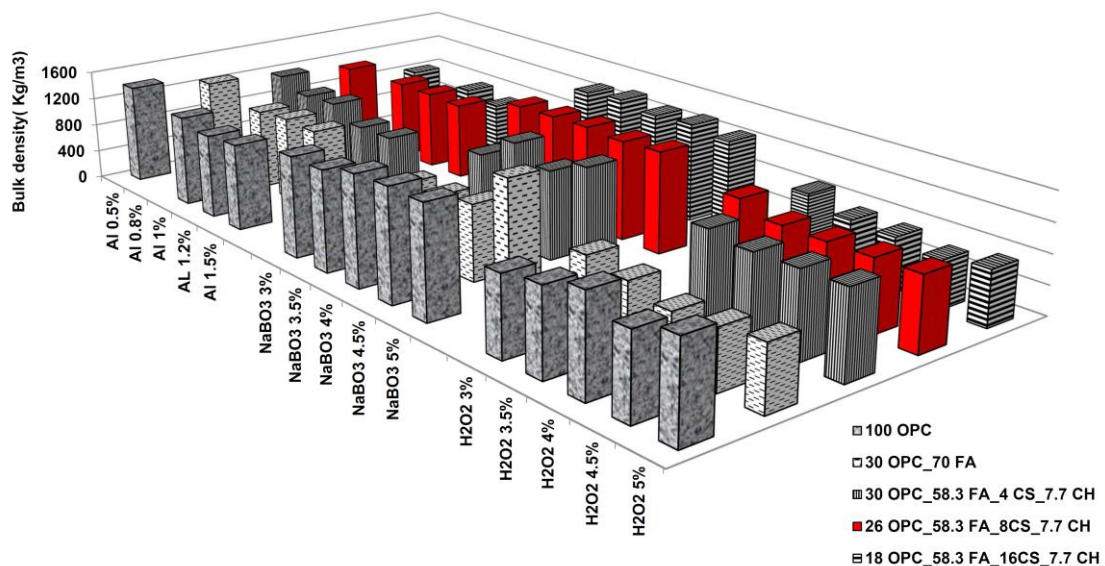


Fig. 5.18 Bulk density

Concerning the use of H_2O_2 the increase of foaming agent show a minor increase in the bulk density but when the foaming agent is increased between 4% to 4.5% slight decrease in bulk density was detected. Regarding the performance of the different foaming agents

on Portland cement mortars it is revealed that the lowest bulk density (1067 kg/m^3) recorded for a 3% H_2O_2 content. Concerning the mixture 30 OPC_70 FA the increase of the aluminium content leads to decrease in bulk density. Except when it increases from 1% to 1.2% lead to the slight bulk density increase. When the NaBO_3 is used a trend can be noticed on bulk density increase. Regarding the use of H_2O_2 the increase of foaming agent from 3% to 4% show a decrease in the bulk density but when the foaming agent is increased above 4% an increase in the bulk density were registered. The lowest bulk density (785 kg/m^3) took place for a 4.5% H_2O_2 content. In respect to results of bulk density for mixture 30 OPC_58.3 FA_4 CS_7.7 CH increasing the aluminium content leads to reduce bulk density. Except when it increases from 0.8% to 1% which lead to the slight bulk density increase. Increasing the NaBO_3 content results in increasing bulk density, except when it increases from 4% to 4.5% which leads to the slight bulk density decrease. Concerning the use of H_2O_2 the increase of foaming agent show a constant trend in bulk density results. Comparing the obtained results by using different foaming agents it is observed that the lowest bulk density (821 kg/m^3) took place for a 1.2% Al content.

Concerning the mixture 26 OPC_58.3 FA_8 CS_7.7 CH an increasing the aluminium content from 0.5% to 1% leads to slight increase in bulk density. By increasing Al content more than 0.8% results in constant trend in bulk density and no increase was detected.

Respect to the increase in NaBO_3 content as foam agent, no change was observed. When NaBO_3 content increased from 4% to 4.5% a slight increase in bulk density was noticed.

The use of H_2O_2 shows a slight decrease from 3% to 3.5%. Increasing H_2O_2 content more than 3.5% did not show any change in bulk density. Comparing the results obtained from using different foaming agents, it is revealed that the lowest bulk density (980 kg/m^3) measured for a 4% H_2O_2 content. Concerning the mixture 18 OPC_58.3 FA_16 CS_7.7 CH. the increase of the aluminium content leads to reduce of bulk density. Increasing of NaBO_3 content, results in reduction of bulk density. However some exceptions were detected. Increasing NaBO_3 from 3% to 3.5% and 4% to 4.5% lead to slight increase in bulk density. The increase of H_2O_2 foam agent content leads to decrease of bulk density. Except from 4.5% to 5% which show an increase in the bulk density. The lowest bulk density (654 kg/m^3) recorded for a 4.5% H_2O_2 content.

Fig. 5.19 presents the results of thermal conductivity performance of some one part foam geopolymer mixtures. Thermal conductivity test was not carried out on all one-part geopolymer mixtures. Instead, two criteria were considered to select the mixtures for thermal conductivity testing, a) Mixtures with compressive strength greater than 2 MPa; b) Mixtures with bulk density lower than 1100 kg/m^3 . The lowest thermal conductivity performance (0.132 W/m.K) was recorded for one-part geopolymer mortars, in mix 30 OPC+58.3 FA+4 CS_7.7 CH and 1.2% Al. Furthermore, a close value of thermal conductivity was measured for the same mixture with 1.5% aluminium powder. As the thermal conductivity of commercial autoclaved aerated concrete masonry blocks (Ytong) is around (0.17 W/m.K), similar thermal conductivity performances can be considered acceptable for thermal insulator like cementitious materials. The mixture 26 OPC+58.3 FA+8 CS_7.7 CH with 3.5% hydrogen peroxide shows an acceptable thermal conductivity of 0.16 W/m.K because it fits the threshold of the grades 4 and 5 of the Korean Industrial Standard code for foam concrete for floor heating systems (Yang et al., 2014).

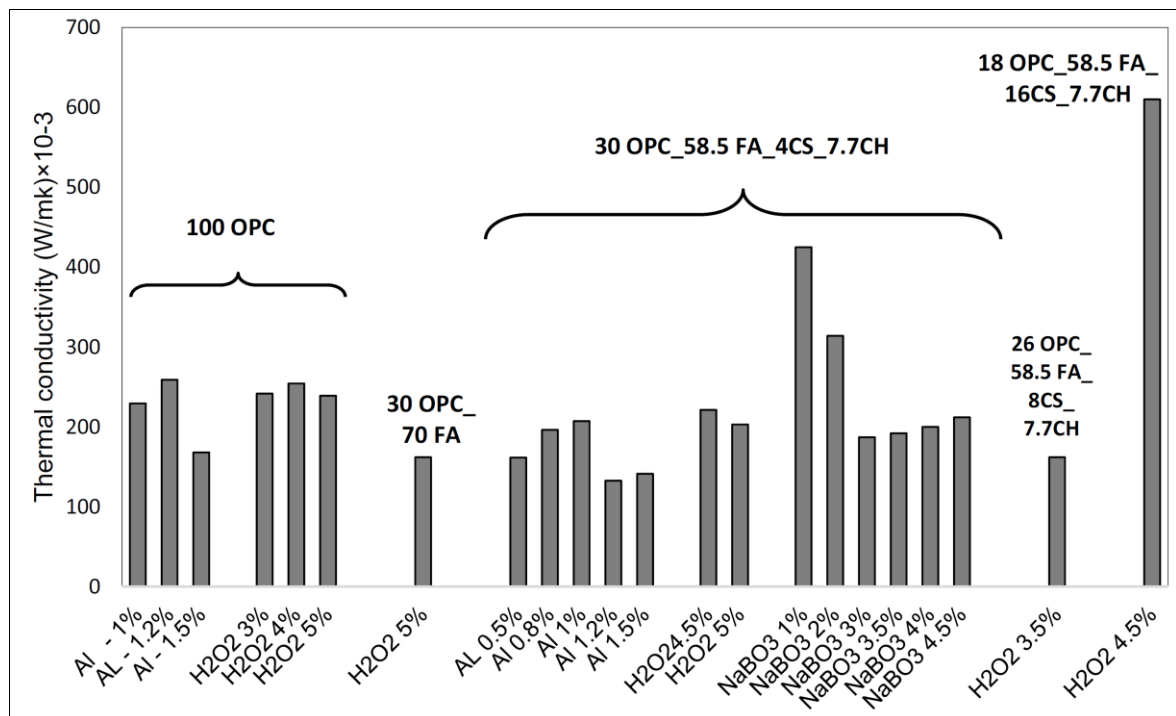


Fig. 5.19 Thermal conductivity

5.3.2 Cost analysis

The cost of materials are listed in Table 5.7 which shows that the Al powder foaming agent has a much higher cost than the other two foaming agents. The cost of mixtures is presented in Fig. 5. 20.

Table 5.7 Costs of the materials (euro/kg)

Sand	OPC	Ca (OH) ₂	Fly ash	Kaolin	Sodium hydroxide	Water	SP	H ₂ O ₂	NaBO ₃	AL
0.02	0.1	0.3	0.03	0.29	0.85	0.1	0.82	0.98	1.5	32.4

The results show that using Al powder leads to a significant increase of the cost of geopolymers mixtures. The most cost-efficient mixtures (67 euro/m³) were obtained for 26 OPC+58.3 FA+8 CS+7.7 CH with 3.5% hydrogen peroxide foaming agent. The use of mixtures based on aluminium powder is not feasible because they are not cost-efficient at all. The mixture based on aluminium powder foaming agent with the lowest cost (30 OPC+58.3 FA+4 CS+7.7 CH) costs more than 200 euro/m³. This represents more than twice the cost of Ytong masonry blocks (70-80 euro/m³). It is worth remember that foam mortars based on classical two part geopolymers have a cost above 300 euro/m³ (Abdollahnejad et al., 2015). Fig. 5.20 also includes cost simulations for two scenarios: a) Carbon social cost of 34.7 euro/ton as per US study (Standford, 2015); b) Carbon social cost of 206.3 euro/ton (Moore and Diaz, 2015). When the cost of the mixtures includes the cost of carbon dioxide emissions mixtures based on hydrogen peroxide show a high increase in its cost. A minor increase is noticed in aluminium powder based mixtures. The results confirm that in both scenarios the mixture 26 OPC+58.3 FA+8 CS+7.7 CH with 3.5% hydrogen peroxide foaming agent is still the most cost-efficient. The results of the cost to thermal resistance ratio are presented in Fig. 5.21 The best ratio was detected for the mixture 26 OPC+58.3 FA+8 CS+7.7 CH around 10 euro/(m.K/W).

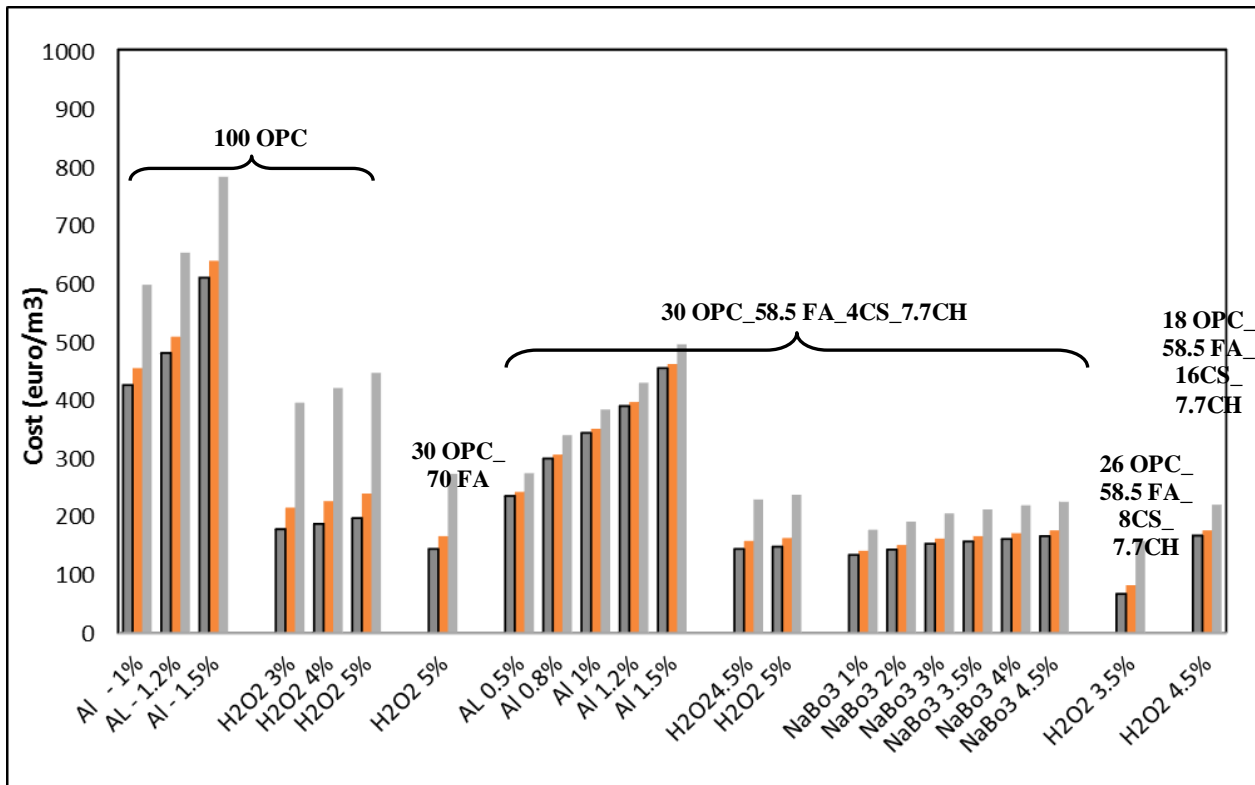


Fig. 5.20 Cost of one-part geopolymer mixtures: Gray bars) Materials cost; Red bars) Materials cost for a carbon cost in scenario 1; Green bars) Materials cost for a carbon cost in scenario 2

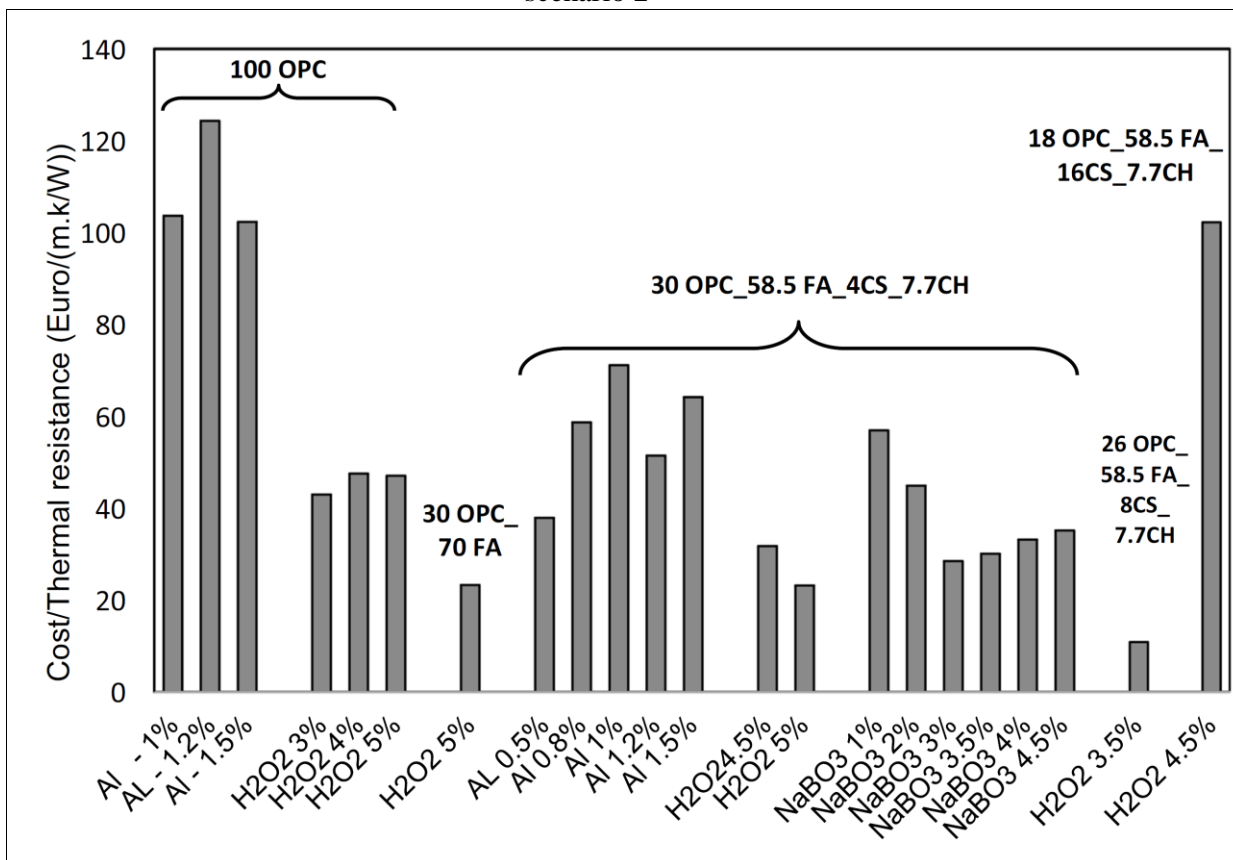


Fig. 5.21 Cost to thermal resistance ratio

5.3.3 Global warming potential

The global warming potential GWP (KgCO_2e) was assessed using EcoInvent database. Fig. 5.22 presents the global warming potential to thermal resistance ratio. The results show that mixtures with similar thermal conductivity performance have a much different global warming potential to thermal resistance ratio. This parameter is influenced by the percentage of Portland cement. Higher percentages are associated with higher ratios of global warming potential to thermal resistance ratios. Even the mixtures containing sodium hydroxide have a lower ratio because although the GWP of NaOH is 2.65 higher than the GWP of Portland cement the amount of OPC used in those mixtures is much higher. The mixture 26 OPC+58.3 FA+8 CS+7.7 CH with 3.5% hydrogen peroxide foaming has a global warming potential of $443 \text{ KgCO}_{2\text{eq}}/\text{m}^3$.

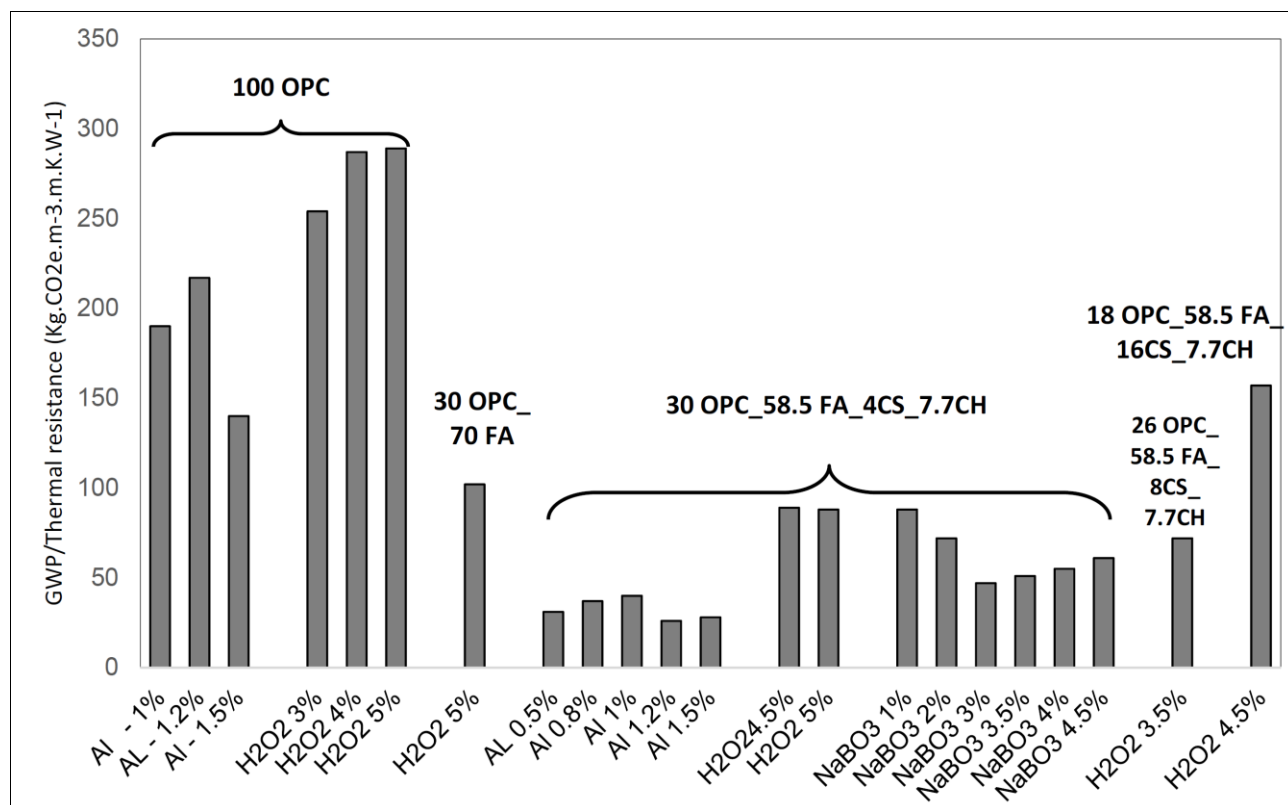


Fig. 5.22 Global warming potential to thermal resistance ratio

5.4 Conclusions

The results of two part foam geopolymers show that the sodium perborate over performs hydrogen peroxide leading to a lower overall thermal conductivity of foam geopolymers.

The use of an activator/binder ratio of 0.8 and a sodium silicate/sodium hydroxide of 2.5 led to the lowest thermal conductivity. Mixtures with a low thermal conductivity of around 0.1 W/(m.°K) and a compressive strength of around 6 MPa were achieved. The cost analysis show the foaming agents are responsible for a small percentage of foam geopolymers total cost (less than 10%) being that the alkaline activators are responsible for more than 80%.

Concerning foam one part geopolymer mixtures the results show that the use of aluminium powder is very effective in obtaining foam materials with low thermal conductivity. An increase of bulk density with aluminium powder content was noticed that could be related to pore collapses. Aluminium powder allows the production of mortar mixtures with a compressive strength above 6MPa however, its high cost means they are commercially useless when facing the competition of commercial cellular concrete. The mortar mixture based on aluminium powder mortar with the lowest cost (30 OPC+58.3 FA+4 CS+7.7 CH) costs more than 200 euro/m³. This represents more than twice the cost of Ytong masonry blocks (70-80 euro/m³). It is worth remember that foam mortars based on classical two part geopolymers have a cost above 300 euro/m³ which shows that two part geopolymers are not a cost-effective solution for thermal insulation materials. The mixture 26 OPC+58.3 FA+8 CS+7.7 CH with 3.5% hydrogen peroxide shows an acceptable compressive strength and thermal conductivity complying with the requirements of the grades 4 and 5 of the Korean Industrial Standard code for foam concrete for floor heating systems (≥ 1.4 MPa and ≤ 0.16 W/m.K). This mixture is cost efficient (67 euro/m³) and has a low global warming potential of 443 KgCO_{2eq}/m³. When the cost of the mixtures includes the cost of carbon dioxide emissions mixtures based on hydrogen peroxide show a high increase in its cost. A minor increase is noticed in aluminium powder based mixtures. The results confirm that in both carbon dioxide social cost scenarios the mixture 26 OPC+58.3 FA+8 CS+7.7 CH with 3.5% hydrogen peroxide foaming agent is still the most cost-efficient.

6.1 Conclusions and suggestions for further investigations

The production of Portland cement as the essential constituent of concrete requires considerable energy, releasing a significant amount of carbon dioxide and other greenhouse gases (GHGs) into atmosphere. Environmental concerns regarding the high CO₂ emissions related to the production of ordinary Portland cement (OPC) led to research efforts on the development of eco-efficient alternative binders.

Geopolymers constitute promising inorganic binders alternative to OPC which are based on aluminosilicates by-products and alkali activators. The geopolymerization technology is a complex chemical process evolving dissolution of raw materials, transportation, orientation and polycondensation of the reaction products. However, there are still many drawbacks associated with traditional two part geopolymer mixes. The caustic alkaline solutions needed to form the geopolymers make the handling and application of geopolymers difficult. Also, workability is generally poor and not easily adjustable due to a sticky and thick mortar that is generated during processing. The system is also sensitive to the ratio of alkaline and soluble silicate, which is difficult to control in practice. Also two part geopolymers carbon footprint is dependent on the fact that sodium silicate usage is avoided. The durability of two part geopolymers is also subject of some controversy. Some authors state that the durability of these materials constitutes the most important advantage over Portland cement others argue that it is an unproven issue. For instance current two part geopolymeric mixes can suffer from efflorescence originated by the fact that alkaline or soluble silicates that are added during processing cannot be totally consumed during geopolymerisation. This leads to high permeability and water absorption due to the movement of alkali together with water to the geopolymer surfaces. Therefore, new and improved geopolymer mixes are needed.

The discovery of one-part geopolymers is considered as a key event on the evolution of low carbon geopolymer technology in the “just add water” concept. However they were associated with very low compressive strength. Some authors even report a compressive strength decrease with time for one-part geopolymers based on calcined red mud and sodium hydroxide blends. The present thesis aimed to develop some one part geopolymer mixtures that could be of some use for the construction industry. The experimental and numerical results allows for the following conclusions

Several one part geopolymer mixtures were developed some having a high compressive strength suitable for construction purposes. The results show that there is not a direct linear relationship between the calcium hydroxide content and the compressive strength. Still a general trend was observed linking compressive strength evolution with curing age, which is typical of OPC chemistry. The applicability of the Johnson–Mehl–Avrami–Kolmogorov model to predict the compressive strength of one part-geopolymers was analysed. The degree of reaction of geopolymers was supposed to be related directly to compressive strength and then Avrami constants and exponents were found for all one part geopolymers. It was shown that compressive strength evolution of some one part geopolymers can be found by the proposed equations. The microstructure of one part geopolymers mortars present a very dense and uniform ITZ different of the porous typical interfacial transition zone of Portland cement mixtures. C/S ratio results show that some sodium is replacing Ca^{2+} in CSH which is typical of Na-C-S-H hydration products. No efflorescences, no presence was observed. This may be due to the low amount of alkaline species used as well as to the fact that some sodium replaced Ca^{2+} in CSH hydration products.

The investigations on foam geopolymers show that in two part mixtures the sodium perborate over performs hydrogen peroxide leading to a lower overall thermal conductivity. The use of an activator/binder ratio of 0.8 and a sodium silicate/sodium hydroxide of 2.5 led to the lowest thermal conductivity. Mixtures with a low thermal conductivity of around $0.1 \text{ W}/(\text{m}\cdot\text{K})$ and a compressive strength of around 6 MPa were achieved. The cost analysis show the foaming agents are responsible for a small percentage of foam geopolymers total cost (less than 10%) being that the alkaline activators are responsible for more than 80%. Concerning one part geopolymers the results show that the use of aluminium powder is very effective in obtaining foam materials with low thermal conductivity. An increase of bulk density with aluminium powder content was noticed that can be related to pore collapses. Aluminium powder allows the production of mortar mixtures with a compressive strength above 6MPa however its high cost means they are commercially useless when facing the competition of commercial cellular concrete. The mixture 26 OPC+58.3 FA+8 CS+7.7 CH with 3.5% hydrogen peroxide shows an acceptable compressive strength and thermal conductivity complying with the requirements for foam concrete for floor heating systems ($\geq 1.4 \text{ MPa}$ and $\leq 0.16 \text{ W}/(\text{m}\cdot\text{K})$). This mixture is cost efficient (67 euro/ m^3) and has a low global warming potential of 443 kg $\text{CO}_2\text{eq}/\text{m}^3$. The results confirm that in both carbon dioxide social cost scenarios the mixture 26 OPC+58.3 FA+8 CS+7.7 CH with 3.5% hydrogen peroxide foaming agent is still the most cost-efficient.

Concerning applications foam one part geopolymers could also be used in the production of lightweight masonry units an issue that should merit future investigations. Other issues that should be investigated include the assessment of alkali-silica reaction not only because of its alkali components but also because of the presence of calcium. The study of the pH conditions of these materials is needed because this is crucial to prevent the corrosion of steel reinforcement. The study of one part geopolymer mixtures based on other by products and industrial wastes with pozzolanic properties will also be needed to enhance the body of knowledge of these materials.

REFERENCES

Abdollahnejad Z., Pacheco-Torgal F., Aguiar A., “Mix design, properties and cost analysis of fly ash-based geopolymer”, *Construction and Building Materials*, 2015; 8: 18-30.

Abdollahnejad Z., Hlavacek P., Miraldo S., Pacheco-Torgal F., Aguiar J., “Compressive strength, microstructure and hydration products of hybrid alkaline cements”, *Materials Research*. 2014; 17:221-227.

Allahverdi A., Najafi Kani E., “Construction wastes as raw materials for geopolymer binders”, *International Journal of Civil Engineering*. 2009; 7:154–60.

Allahverdi A., Škvára F., “Nitric acid attack on hardened paste of geopolymeric cements- Part 1”, *Ceramics-Silikaty*, 2001; 45:81–8.

Allahverdi A., Škvára F., “Sulfuric acid attack on hardened paste of geopolymer cements- Part 2”, *Corrosion mechanism at mild and relatively low concentrations – Part 2. Ceramics-Silikaty*, 2005; 45:1–4.

Allahverdi A., Škvára F., “Sulfuric acid attack on hardened paste of geopolymer cements- Part 1”, *Mechanism of corrosion at relatively high concentrations. Ceramics-Silikaty*. 2005; 49:225–9.

Al-Otaibi S., “Durability of concrete incorporating GGBS activated by water-glass”, *Construction and Building Materials*, 2007; 22(10): 2059–2067.

Aperador W., de Gutiérrez R., Bastidas D., “Steel corrosion behavior in carbonated alkali-activated slag concrete”, *Corrosion Science*. 2009; 51:2027–33.

Arshad M., Maaroufi A., “Relationship between Johnson–Mehl–Avrami and Šesták–Berggren models in the kinetics of crystallization in amorphous materials”, *Journal of Non-Crystalline Solids*. 2015; 413:53–58.

Arellano Aguilar R.; Burciaga Díaz O., Escalante García J.I., “Lightweight concretes of activated metakaolin-fly ash binders, with blast furnace slag aggregates”, *Construction and Building Materials*, 2010; 24: 1166–1175.

ASTM C373-14a, Standard Test Method for Water Absorption, Bulk Density, Apparent Porosity, and Apparent Specific Gravity of Fired White ware Products, Ceramic Tiles, and Glass Tiles, ASTM International, West Conshohocken, PA, 2014.

Bakharev T., “Geopolymeric materials prepared using class F fly ash and elevated temperature curing”, *Cement and Concrete Research*, 2005; 3: 1224 – 1232.

Bakharev T., Sanjayan J.G., Cheng Y.B., “Resistance of alkali-activated slag to alkali–aggregate reaction”, *Cement and Concrete Research*, 2001; 31:331–4.

Bakharev T., Sanjayan J.G., Cheng Y.B., “Resistance of alkali-activated slag concrete to alkali–aggregate reaction”, *Cement and Concrete Research*, 2000; 31(2): 331–334.

Bakharev T., Sanjayan J.G., Cheng Y.B., “Resistance of alkali-activated slag concrete to acid attack”, *Cement and Concrete Research*, 2003; 33:1607–11.

Bakharev T., Sanjayan J.G., Cheng Y.B., “Sulfate attack on alkali-activated slag concrete”, *Cement and Concrete Research*, 2002; 31:211–6.

Boron J.B., Inorganic Chemistry Encyclopedia of Inorganic Chemistry, 1994, Ed. R. Bruce King, John Wiley & Sons ISBN 0-471-93620-0

Bernal S., de Gutiérrez R., Pedraza A., Provis J., Rodriguez E., Delvasto S., “Effect of binder content on the performance of alkali-activated slag concretes”, Cement and Concrete Research, 2011; 41:1–8.

Bernal S., de Gutiérrez R., Pedraza A., Provis J., Rose V., “Effect of silicate modulus and metakaolin incorporation on the carbonation of alkali silicate-activated slags”, Cement and Concrete Research, 2010; 40:898–907.

Bortnovsky O., Dvorakova K., Roubicek P., Bousek J., Prudkova Z., Baxa P., Barbosa, Valeria F., MacKenzie, K. J. D., Thaumaturgo C., “Synthesis and characterization of materials based on inorganic polymers of alumina and silica: Sodium polysialate polymers”, International Journal of Inorganic Polymers, 2000; 3: 309-317.

Bortnovsky O., Dvorakova K., Roubicek P., Pousek J., Prudkova Z., Baxa P., “Development, properties and production of geopolymers based on secondary raw materials”, In: Alkali activated materials – research, production and utilization 3rd conference, Prague, Czech Republic. 2007; 83–96.

Buchwald A., Dombrowski K., Weil, M. “The influence of calcium content on the performance of geopolymeric binder especially the resistance against acids”, Proceedings of the World Geopolymer, Geopolymer Green Chemistry and Sustainable Development Solutions, 2005; 35-39.

Buchwald A., Kaps Ch., Hohmann M., “Alkali-activated binders and pozzolan cement binders- compete binder reaction or two sides of the same story?”, In proceeding of 11 International conference on the Chemistry of cement, Durban, South Africa, 2003; 1238-1246.

Brooks R., Bahadory M., Tovia F., Rostami H., “Properties of alkali-activated fly ash: high performance to lightweight”, International Journal of Sustainable Engineering, 2010; 3:211–8.

BS EN 1015-18. Methods of test for mortar for masonry. Determination of water absorption coefficient due to capillary action of hardened mortar, 2002.

Chen Y., Pu X., Yang C., Ding Q., “Alkali aggregate reaction in alkali slag cement mortars”, Wuhan University of Technology-Mater, Sci. Ed. 2002; 17(3): 60–62.

Cyr, M., Pouhet R., “Resistance to alkali-aggregate reaction (AAR) of alkali-activated binders. In Handbook of Alkali-Activated Cements, Mortars and Concretes”, 397-422 (Eds) Pacheco-Torgal, F.; Labrincha, J.; Palomo, A.; Leonelli, C.; Chindapasirt, P., WoddHead Publishing, 2014, Cambridge, UK.

COM (2011) 885/2. Energy Roadmap 2050.

COM 815 (2011) Progress report on the Europe 2020 strategy

Damtoft J., Lukasik J., Herfort D., Sorrentino D., Gartner E., “Sustainable development and climate change initiatives”, Cement and Concrete Research, 2008; 38:115–27.

Davidovits J., “Properties of geopolymers cements. In: Proc of the 1st international conference on alkaline cements and concretes”, Ukraine: Scientific Research Institute on Binders and Materials Kiev, 1994a; 131–49.

Davidovits J., High-alkali cements for 21st century concretes. In Concrete Technology, Past, Present and Future. Metha, P.K, American Concrete Institute, Farmington Hills, MI. Ed. 1994b; 383–397.

Davidovits J., Geopolymers: inorganic polymeric new materials. J Therm Anal. 1991; 37:1633–56.

Davidovits J, Comrie DC, Paterson JH, Ritcey DJ., “Geopolymeric concretes for environmental protection”, ACI ConcrInt, 1990; 12:30–40.

Davidovits J., “Synthesis of new high temperature geo-polymers for reinforced plastics/composites”, SPE PACTEC 79 Society of Plastic Engineers, Brookfield Center, 1979; 151-154.

Davies D., Oberholster RE., “Alkali–silica reaction products and their development”, Cement and Concrete Research, 1988; 18:621–35.

Development, properties and production of geopolymers based on secondary raw materials. In: Alkali activated materials – research, production and utilization 3rd conference, Prague, Czech Republic. 2007; 83–96.

Duxson P., Van Deventer J., In: Provis J., Van Deventer J., editor. Geopolymers, structure, processing, properties and applications. Cambridge, UK: Woodhead Publishing Limited Abington Hall; 2009 [ISBN -13: 978 1 84569 449 4].

Duxson P., Provis J., Lukey G., Van Deventer J., “The role of inorganic polymer technology in the development of green concrete”, Cement and Concrete Research. 2007; 37:1590–7.

Dolezal J., Skvara F., Svoboda P., Sulc R., Kopecky L., Pavlasova S., Myskova L., Lucuk M., Dvoracek K., “Concrete based on fly ash geopolymers. In: Alkali activated materials – research”, production and utilization 3rd conference, Prague, Czech Republic, 2007; 185–97.

Diamond S., C/S mole ratio of CSH gel in a mature C₃S paste as determined by EDXA. Cement and concrete Research 6, 1976; 413-416.

Damjanovic A., Genshaw M., Bockris J., “Hydrogen peroxide formation in oxygen reduction at gold electrodes: II”, Alkaline Solution, J.Electroanalytical Chem. Interfacial Electrochem 15. 1967; 173–180.

Diamond S., “C/S mole ratio of CSH gel in a mature C₃S paste as determined by EDXA”, Cement and Concrete Research, 1976; 6: 413-416.

ERMCO Statistics of the year 2010. Boulevard du Souverain 68, B-1170, Brussels, Belgium; 2011.

Feng J., Zhang R., Gong L., Li Y., Cao W., Cheng X., “Development of porous fly ash based geopolymer with low thermal conductivity”, Materials and Design, 2015; 65: 529–533.

Fernandez-Jimenez A., Palomo A., “Composition and microstructure of alkali activated fly ash binder: Effect of the activator”, Cement and Concrete Research, 2005a; 35: 1984-1992.

Fernandez-Jimenez A., Palomo A., “Mid-infrared spectroscopic studies of alkali activated fly ash structure”, Microporous Mesoporous, 2005b; 86: 207–14.

Fernandez-Jimenez A, Puertas F., “The alkali–silica reaction in alkali-activated slag mortars with reactive aggregate”, Cement and Concrete Research, 2002; 32: 1019–24.

- Fernandez-Jimenez A., Palomo A., Puertas F., “Alkali activated slag mortars. Mechanical strength behaviour”, *Cement and Concrete Research*, 1999; 29: 1313–21.
- Fu Y., Cai L., Wu Y., “Freeze–thaw cycle test and damage mechanics models of alkali-activated slag concrete”, *Construction and Building Materials*, 2011; 25:3144–8.
- Flatt R., Roussel R., Cheeseman C.R., “Concrete: An eco-material that needs to be improved”, *Journal of the European Ceramic Society*, 2012;32: 2787-2798.
- Galiano Y., Pereira C., Vale J., “Stabilization/solidification of a municipal solid waste incineration residue using fly ash-based geopolymers”, *Hazard Mater*, 2011; 185: 373–81.
- García-Lodeiro I., Palomo A., Fernández-Jiménez A., “Alkali – aggregate reaction in activated fly ash systems”, *Cement and Concrete Research*, 2007; 3: 175–83.
- Garcia Lodeiro I., Fernandez-Jimenez A., Blanco M.T., Palomo A., “FTIR study of sol-gel Synthesis of cementitious gels: CSH and NASH.”, *Journal of Sol–Gel Science Technology*, 2008;45: 63–72.
- Garcia Lodeiro I., Macphee D., Palomo A., Fernandez-Jimenez A., “Effect of alkalis on fresh CSH gels. FTIR analysis”, *Cement and Concrete Research*, 2009;39: 147–53.
- Lodeiro G., Fernandez-Jimenez A., Palomo A., “Alkali-activated based concrete”, ISBN 978-0-85709-424-7, In *Eco-efficient concrete. Geopolymers*, Ed. F.Pacheco-Torgal, S.Jalali, J. Labrincha & V.M. John, Woodhead Publishing Limited Abington Hall, Cambridge, UK. 2013; 439-487.
- Gartner E., “Industrially interesting approaches to low-CO₂ cements”, *Cement and Concrete Research* 2004. ;34:1489–98.
- Gifford P.M., Gillott J.E., “Alkali-silica reaction (ASR) and alkali-carbonate reaction (ACR) in activated blast furnace slag cement (ABFSC) concrete”, *Cement and Concrete Research*, 1996;26(1): 21–26.
- Glukhovskiy V.D., “Slag-alkali concretes produced from fine-grained aggregate”, Kiev: VishchaShkolay; 1981.
- Gourley J.T., Johnson G.B., “Evelopments in geopolymer precast concrete”, In: Quentin S, editor. *Proc of geopolymer 2005 world congress*. France: Geopolymer Green Chemistry and Sustainable Development Solutions, 2005; 139–43.
- Goyal S., Kumar M., Sidhu D.S., Bhattacharjee B., “Resistance of mineral admixture concrete to acid attack”, *Journal of Advanced Concrete Technology*, 2009;7: 273–83.
- Gjørsv O.E., “Performance and serviceability of concrete structures in the marine environment”, *Proceedings, Odd E. Gjørsv Symposium on Concrete for Marine Structures*, Ed. por P.K. Mehta, CANMET/ACI, 1996; 259-279.
- Habert G., de Lacaillerie J., Roussel N., “An environmental evaluation of geopolymer based concrete production: reviewing current research trends”, *Journal of Cleaner Production*, 2011; 11:1229–38.

- Hermann E., Kunze C., Gatzweiler R., Kiebig G., Davidovits J., “Solidification of various radioactive residues by geopolymer with special emphasis on long term stability”, In: Proc of 1999 geopolymer conference; 1999; 211–28.
- Hill C. N. A., “Vertical Empire: The History of the UK Rocket and Space Programme”, 1950–1971. Imperial College Press. 2001;[ISBN 978-1-86094-268-6].
- IUPAC. Compendium of Chemical Terminology, 2nd ed. (the "Gold Book"). Compiled by A. D. McNaught and A. Wilkinson. Blackwell Scientific Publications, Oxford, 1997.
- IPCC, Intergovernmental Panel on Climate Change. 4th Assessment report. In: Parry ML, editor. Assessment of observed changes and responses in natural and managed systems. Climate change: impacts, adaptation and vulnerability. Contribution of working group II to the 4th assessment report of the Intergovernmental Panel on Climate Change. Cambridge Univ. Press; 2007; 79–131.
- Jiang W., Silsbee M.R., Breval E., Roy M.D., “Alkali-activated cementitious materials in chemically aggressive environments”, In: Young JF, editor. Mechanisms of chemically degradation of cement-based systems. E&FN SPON London. 1997; 289–96.
- Juenger M., Winnefeld F., Provis J., Ideker J., “Advances in alternative cementitious binders”, Cement and Concrete Research, 2011;41:1232–43.
- Keawpapasson P., Tippayasam C., Ruangjan S., Thavorniti P., Panyathanmaporn T., Fontaine A., Leonelli C., Chayasuwa D., “Metakaolin-Based Porous Geopolymer with Aluminium Powder”, Key Engineering Materials. 2014; 608: 132-138.
- Kolousek J., Brus J., Urbanova M., Andertova J., Hulinsky V., Vorel J., “Preparation, structure and hydrothermal stability of alternative (sodium silicate-free) geopolymers”, Journal of Materials Science, 2007;42:9267-9275.
- Kani E., Allahverdi A., Provis J., “Efflorescence control in geopolymer binders based on natural pozzolan”, Cement and Concrete Composites, 2011; 34: 25-33.
- Kolousek D., Brus J., Urbanova M., Andertova J., Hulinsky V., Vorel J., “Preparation, structure and hydrothermal stability of alternative (sodium silicate free) geopolymers”, Journal of Materials Science. 2007; 42, 9267-9275. <http://dx.doi.org/10.1007/s10853-007-1910-5>
- Ke, X., Bernal S., Ye, N., Provis J., Yang J., “One-part geopolymers based on thermally treated red mud/NaOH blends”, Journal of American Ceramic Society, 2015; 98: 5-11.
- Kong D., Sanjayan J., Sagoe-Cretensil K., “Factors affecting the performance of metakaolin geopolymers exposed to elevated temperatures”, Journal of Material Science, 2008; 43:824–31.
- Krivenko P., Guziy S., “Fire resistant alkaline Portland cements”, In: Alkali activated materials – research, production and utilization 3rd conference, Prague, Czech Republic, 2007; 333–47.
- Khunthongkeaw K., Tangtermsirikul S., Leelawat T., A study on carbonation depth prediction for fly ash concrete, Journal of Construction and Building Materials. 1996; 20: 744–753.

- Laldji S., Tagnit-Hamou A., “Glass frit for concrete structures: a new alternative cementitious material”, *Canadian Journal of Civil Engineering*, 2007; 34:793–802.
- Lampris C., Lupo R., Cheeseman C., “Geopolymerization of silt generated from construction and demolition waste washing plants”, *Waste Management*, 2009; 29:368–73.
- Lancellotti I., Kamseu E., Michelazzi M., Barbieri B., Corradi A., Leonelli C., “Chemical stability of geopolymers containing municipal solid waste incinerator fly ash”, *Waste management*, 2010; 30: 673-679.
- Li C., Sun H., Li L., “A review: The comparison between alkali-activated slag (Si+Ca) and metakaolin (Si+Al) cements”, *Cement and Concrete Research*. 2010; 40:1341-1349. [http:// dx.doi.org/10.1016/j.cemconres.2010.03.020](http://dx.doi.org/10.1016/j.cemconres.2010.03.020)
- Lloyd R., Provis J., Van Deventer S.J.S., “Pore solution composition and alkali diffusion in inorganic polymer cement”, *Cement and Concrete Research*, 2010; 40: 1386–92.
- Lloyd R., “Accelerated ageing of geopolymers. In Provis and Van Deventer (Ed.) *Geopolymers: Structure, processing, properties and industrial applications*”, CRC Press, 2009; 139–166.
- LNEC E 463 - Concrete: Calculation of the chloride coefficient by migration test under nonstationary conditions (in Portuguese), LNEC, Lisboa; 2004.
- Macphee D.E., “Solubility and aging of calcium silicate hydrates in alkaline solutions at 25° C”, *Journal of American Ceramic Society*.1989; 72: 646-654.
- MacKenzie K.J. D., Brew D., Fletcher R., Nicholson C.L., Vagana R., Schmucker Masi G., Rickard W., Vickers I., Bignozzi M., Van Riessen A., “A comparison between different foaming methods for the synthesis of light weight geopolymers”, *Ceramics International* 40, 2014; 13891-13902.
- Material Safety Data Sheet, Solid sodium hydroxide, Link address: <http://www.certified-lye.com/> access date (6/9/2015)
- McLellan B., Williams R., Lay J., Van Riessen A., Corder G., “Costs and carbon emissions for geopolymer pastes in comparison to ordinary Portland cement”, *Journal of Cleaner Production*, 2011; 19:1080–90.
- Metso J., “The Alkali Reaction of Alkali-activated Finnish Blast Furnace Slag. *Silicates industriels*”, 1982; 4-5: 123–127.
- Miranda J.M., Fernandez-Jimenez A., Gonzalez A., Palomo A., “Corrosion resistance in activated fly ash mortars”, *Cement and Concrete Research*, 2005; 35:1210–7.
- Moore F., Diaz D., “Temperature impacts on economic growth warrant stringent mitigation policy”, *Nature Climate Change*, 2015; 5: 127-131.
- Toward M., “An understanding of the synthesis mechanisms of geopolymer materials”, *Proceedings of the World Geopolymer, Geopolymer Green Chemistry and Sustainable Development Solutions*. 2005; 41-44.

Norman G., Earnshaw A., “Chemistry of the Elements” (2nd ed.), Butterworth-Heinemann, 1997. [ISBN 0080379419].

NP EN 450-1, Fly ash for concrete – Part 1: Definition, specifications and conformity criteria, 2005.

NP EN 206-1: 2007, Concrete: Part 1. Specification, performance, production and conformity, 2007.

OCDE Environmental sustainable building—challenges and policies, 2003; Paris.

Patent US7691198 B2, Jan Stephanus Jakob Van Deventer, Dingwu Feng, Peter Duxson, “Dry mix cement composition, methods and systems involving same”, 2010.

Pacheco-Torgal, F., Introduction. In Handbook of Alkali-Activated Cements, Mortars and Concretes, 1-16 (Eds) Pacheco-Torgal, F.; Labrincha, J.; Palomo, A.; Leonelli, C.; Chindaprasirt, P., Woodhead Publishing, Cambridge, UK, 2014.

Pacheco-Torgal, F., “Eco-efficient construction and building materials research under the EU Framework Programme Horizon 2020”, Construction and Building Materials. 2014; 51: 151-162.

Pacheco-Torgal, F., Cabeza, L., Mistretta, M., Kaklauskas, A., Granqvist, G., “Nearly zero energy building refurbishment. A multidisciplinary approach”, Springer Verlag, London, UK, 2013.

Pacheco-Torgal F, Fucic A., Jalali S., “Toxicity of Building Materials”, Woodhead Publishing Limited Abington Hall, Cambridge, UK, 2012a

Pacheco -Torgal, F., Abdollahnejad Z., Camões A.F., Jamshidi, M., Ding Y., “Durability of alkali-activated binders. A clear advantage over Portland cement or an unproven issue”, Construction and Building Materials. 2012b; 30: 400-405.

Pacheco-Torgal, F., Jalali, S., “Eco-efficient construction and building materials”, Springer Verlag, London, UK. 2011.

Pacheco-Torgal F., Gomes J., Jalali S., “Durability and environmental performance of alkali-activated tungsten mine waste mud mortars”, Journal of Materials in Civil Engineering, 2010; 22:897–904.

Pacheco-Torgal F., Gomes J., Jalali S., “Adhesion characterization of tungsten mine waste geopolymeric binder. Influence of OPC concrete substrate surface treatment”, Construction and Building Materials, 2008a; 22:154–61.

Pacheco-Torgal F., Gomes J., Jalali S., “Alkali – activated binders: a review Part 2: About materials and binders manufacture”, Construction and Building Materials, 2008b; 22:1315–22.

Pacheco-Torgal F., Gomes J.P., Jalali S., “Properties of tungsten mine waste geopolymeric binder”, Construction and Building Materials, 2008c; 22:1201–11.

Pacheco-Torgal F., Gomes J.P., Jalali S., “Investigations on mix design of tungsten mine waste geopolymeric binders”, Construction and Building Materials, 2008d; 22:1939–49.

Pacheco-Torgal F., Castro-Gomes J.P., Jalali S., “Investigations about the effect of aggregates on strength and microstructure of geopolymeric mine waste mud binders”, Cement and Concrete Research, 2007; 37: 933-941.

Palomo A., Blanco-Varela M.T., Granizo M.L., Puertas F., Vasquez T., Grutzeck M.W., “Chemical stability of cementitious materials based on metakaolin”, *Cement and Concrete Research*, 1999a; 29:997–1004.

Palomo A., Grutzeck M.W., Blanco M.T., “Alkali-activated fly ashes. A cement for the future”, *Cement and Concrete Research*, 1999b; 29(8): 1323-1329.

Peng M.X., Wan Z.H., Shen S.H., Xiao Q.G., “Synthesis, characterization and mechanisms of one-part geopolymeric cement by calcining low-quality kaolin with alkali”, *Materials and Structures*, 2014; 48: 699-708.

Provis J.L., Van Deventer J.S.J., “Alkali-activated materials”, *State-of-the-Art Report*, RILEM TC 224-AAM. Springer/RILEM, Berlin, 2014.

Provis, J.L., “Geopolymers and other alkali activated materials: why, how, and what?”, *Materials and Structures*. 2014; 47: 11-25.

Provis J, Van Deventer J., editor. “Geopolymers, structure, processing, properties and applications”, Woodhead Publishing Limited Abington Hall, Cambridge, UK; 2009: 194–210.

Provis, J. “Immobilisation of toxic wastes in geopolymers. In *Geopolymers, Structure, Processing, Properties and Applications*”, ISBN -13: 978 1 84569 449 4, Ed. J. Provis & J. Van Deventer, Woodhead Publishing Limited Abington Hall, Cambridge, UK, 2009; 421-440.

Provis, J.L., Muntingh, Y., Lloyd R.R., Xu H., Keyte L.M., Lorenzen L., Krivenko P.V., Van Deventer J.S.J. “Will geopolymers stand the test of time?”, *Ceramic Engineering and Science Proceedings*, 2008; 28: 235-248.

Pawlasova S., Skavara F., “High-temperature properties of geopolymer materials. In: *Alkali activated materials – research, production and utilization*”, 3rd conference, Prague, Czech Republic, 2007; 523–4.

Perná I, Hanzlicek T, Straka P, Steinerova M. “Utilization of fluidized bed ashes in thermal resistance applications. In: *Alkali activated materials – research, production and utilization*”, 3rd conference, Prague, Czech Republic, 2007; 527–37.

Prud’homme E., Michaud P., Joussein E., Peyratout C., Smith A., Arrii-Clacens S., Clacén J.M., Rossignol S., “Silica fume as porogen agent in geo-materials at low temperature”, *Journal of the European Ceramic Society*, 2010; 30: 1641-1648.

Puertas F., “Cementos de escórias activadas alcalinamente”, *Situación actual y perspectivas de futuro*. *Materials Construction*, 1995; 45:53–64.

Puertas F., Palacios M., Gil-Maroto A., Vázquez T., “Alkali-aggregate behavior of alkali-activated slag mortars: effect of aggregate type”, *Cement and Concrete Composition*, 2009; 31:277–284.

Beddoe R.E., Schmidt K., “Acid attack on concrete – effect of concrete composition. Part 1”, *Centrum Baustoffe und Materialprüfung*, 2009; 7:88–94.

Regulation (EU) 305/2011- Construction Products Regulation

- Richardson I.G., “The nature of the hydration products in hardened cement pastes”, *Cement and Concrete Composites*. 2000; 22: 97-113.
- Roy D.M., Jiang W., Silsbee M.R., “Chloride diffusion in ordinary blended and alkali-activated cement pastes”, *Cement and Concret Research*, 2000; 30:1879–84.
- Saraswathy V., Muralidharan S., Thangavel K., Srinivasan S., “Influence of activated fly ash on corrosion resistance and strength of concrete”, *Cement and Concret Research*. 2003; 25:673–80.
- Shi D., Shi L., Zhang J., Cheng J., “Preparation and properties of a novel non-flammable thermal insulation material”, *Advanced Materials Research*, 2012, 1504-1512
- Shi C., Fernández Jiménez A., Palomo A., “New cements for the 21st century: the pursuit of an alternative to Portland cement”, *Cement and Concret Research*. 2011; 41:750–63.
- Shi C., Krivenko P.V., Roy D.M., “Alkali-activated cements and concretes”, Taylor and Francis, Abingdon, 2006.
- Shi C., Stegmann J.A., “Acid corrosion resistance of different cementing materials”, *Cement and Concret Research*, 2000; 30:803–8.
- Sims I., Brown B., “Concrete aggregates. In: Hewlett PC, editor. *Lea’s chemistry of cement and concrete*”, 4th ed. London; 1998: 903–89.
- Skvara F., Kopecky L., Smilauer V., Alberovska L., Vinsova L., “Aluminosilicate polymers – influence of elevated temperatures, efflorescence”, *Ceramics – Silikaty*, 2009; 53:276–82.
- Skvara F., Kopecky L., Smilauer V., Alberovska L., Bittner Z., “Material and structural characterization of alkali activated low-calcium brown coal fly ash”, *Journal of Hazardous Material*, 2008; 168:711–20.
- Slavik R., Bednarik V., Vondruska M., Nemecek A., “Preparation of geopolymer from fluidized bed combustion bottom ash”, *Journal of Material Processing Technology*, 2008; 200:265–70.
- Stern N., “Stern review on economics of climate change”, Cambridge University Press; 2006.
- Stanford Report Estimated social cost of climate change not accurate, Stanford scientists say. <http://news.stanford.edu/news/2015/january/emissions-social-costs-011215.html>
- Stanton T.E., “Influence of cement and aggregate on concrete expansion”, *EngNews Record* 1940; 1:50–61.
- Temuujin J., Rickard W., Lee M., Van Riessen A., “Preparation and thermal properties of fire resistant metakaolin-based geopolymer-type coatings”, *Journal of Non-Cryst Solids*, 2011; 357:1399–404.
- Temuujin J., Van Riessen A., Williams R., “Influence of calcium compounds on the mechanical properties of fly ash geopolymer pastes”, *Journal of Hazardous Material*, 2009; 167:82–8.
- UN Energy for a sustainable future. The Secretary-General’s Advisory Group on energy and climate change, 2010; New York

Van Deventer J.S.J., Provis J., Duxson P., “Technical and commercial progress in the adoption of geopolymer” cement. *Miner Eng.* 2012; 29: 89–104.

Van Deventer J.S.J., Feng D., Duxson P., “Dry mix cement composition, methods and systems involving same”, US Patent 7691,198 B2; 2010.

Vance e., Perera D., “Geopolymers for nuclear waste immobilisation. In *Geopolymers, Structure, Processing, Properties and Applications*”, Ed. J. Provis & J. Van Deventer, Woodhead Publishing Limited Abington Hall, Cambridge, UK. 2009; 401-420.

Vinsova H., Jedinakova K., Gric L., Sussmilch J., “Immobilization of toxic contaminants into aluminosilicate matrixes. In: *Proceedings of the 2007 – alkali activated materials – research, production and utilization 3rd conference*. Prague: Czech Republic, 2007; 735–6.

Vijaya R., “Low-Calcium Fly-Ash-Based Geopolymer Concrete. Faculty of Engineering”, Curtin University of Technology, Perth, Australia, 2008; Chapter 26:1-19.

Wang S., “Review of recent research on alkali-activated concrete in china”, *Magazine of Concret Research* 1991; 5154:29–35.

Weng L., Sagoe-Crentsil K., Brown, T., Song S., “Effects of aluminates on the formation of geopolymers”, *Materials Science & Engineering*, 2005; 117: 163-168.

Wang Q., Ding Z.Y., Li L., Zhang C.Y., Sui Z.T., “Effect of Alkali-Activator on Alkali-Aggregate Reaction of Slag-Based Geopolymer.”, *First International Conference on Advances in Chemically-activated Marterials*, 2010; 131–138.

WHO (2014) Urban population growth. Global health observatory. http://www.who.int/gho/urban_health/situation_trends/urban_population_growth_text/en/

Wood J.G., Johnson R.A., “The appraisal and maintenance of structures with alkali–silica reaction”, *Journal of Structural Engineering*, 1993; 71(2).

Hwai-Chung W., Sun P., “New building materials from fly ash-based lightweight inorganic polymer”, *Construction and Building Materials*, 2005; 21: 211-217.

Xu H., Van Deventer S.J., “The geopolymerisation of alumino-silicate minerals”, *International Journal of Mineral Processing*, 2000; 59: 247-266.

Xu H., “The geopolymerisation of alumino-silicate minerals”, PhD Thesis, University of Melbourne. 2002.

Yang K.-H., Lee K.-H., “Tests on alkali-activated slag foamed concrete with various water-binder ratios and substitution levels of fly ash”, *Building Construction and Planning Research*: 1, 8–14.

Yang, K.H., Lee J.K., Song M.H., “Properties and sustainability of alkali-activated slag foamed concrete”, *Journal of Cleaner Production*, 2014; 68: 226-233.

Yip C.K., Van Deventer S.J.S., “Microanalysis of calcium silicate hydrate gel formed within a geopolymeric binder”, *Journal of Materials Science* 38, 2003; 3851-3860.

Yip C.K., Lukey G.C., Van Deventer S.J.S., “The coexistence of geopolymeric gel and calcium silicate hydrate gel at the early stage of alkaline activation’, *Cement and Concrete Research*, 2005;35: 1688-1697.

Yunsheng Z., Wei S., “Fly ash based geopolymer concrete”, *Indian Concrete Journal*, 2006; 80:20–4.

Zhang, Z., Provis J., Reid A., Wang H., “Geopolymer foam concrete: An emerging material for sustainable construction”, *Construction and Building Materials*, 2014;56: 113-127.

Zhang L., Ahmari S., Zhang J., “Synthesis and characterization of fly ash modified mine tailings-based geopolymers”, *Construction and Building Materials*, 2011; 25:3773–81.

Zhang M., Wruck B.A., Graeme – Barber E., Salje M., Carpenter, “Phonon-spectroscopy on alkali-feldspar: phase transitions and solid solutions”, *American Mineralogist* 81; 1996: 92-104.

Zhao R., Sanjayan J.G., “Geopolymer and Portland cement concretes in simulated fire”, *Magazine Concrete Research*, 2011; 63(3):163–73.

Zheng D., Van Deventer J.S.J., Duxson P., “The dry mix cement composition, methods and systems involving same”, *International Patent WO 2007/109862 A1*, 2007.